Politecnico di Torino

Master of Science

IN PETROLEUM AND MINING ENGINEERING

By:

Daniel Hanna

Wellbore stability analysis in transversely isotropic rock

Student:

Daniel Hanna

Supervisors:

Prof. Chiara Deangeli

Dr. Wenjie Liu

Acknowledgements

I express my gratitude to all the professors who followed me closely especially my supervisor ***Professor Chiara Deangeli*** *for her support and for the valuable knowledge that she shared during my formation. A special thanks to* ***Dr. Wenjie Liu,*** *co-supervisor of my MSc thesis.*

Finally, we express my feelings to my parents and friends who gave me moral support and the right atmosphere and who sacrificed all of them so that I could finish my formation.

Abstract

The presence of lamination planes in shales poses significant challenges to borehole stability. The stability during drilling operations is closely related to the features of the weakness planes, such as strength properties and inclination of the wellbore axis. The mud pressure to avoid failure is affected by the induced state of stress, pore fluid pressure, coupled with the mechanical characteristics of the rock matrix and weak planes.

The thesis focuses on the comparison between the mud pressures calculated with the Weakness Plane Model and the Hoek and Brown criterion adapted for the transversely isotropic rocks. To this end, the interpretation of laboratory tests, carried out on Tournemire shale specimens was carried out. The difficulty of the data regression was investigated by excluding some confinements in triaxial tests.

In general, the data fitting carried out with the Hoek and Brown criterion can capture in a more appropriate way the transversely isotropic behavior of the shale. However, the Weakness Plane Model needs a lower number of triaxial tests.

The study uses the Kirsch solution, Mohr Coulomb criterion, Hoek and Brown criterion to calculate the limit mud pressure establish the drilling instability equation, and analyzes the influence of the weak planes dip angle, far field stresses on the mud pressure. The results reveal limitations of the weakness plane model in capturing shale behavior across all inclination angles. Furthermore, it is observed that mud pressure decreases with increasing the degree of anisotropy, and a critical inclination of the weak planes is identified, which depends on the location of the minimum strength.

Table of Contents

List of figures

List of Tables

List of symbols

σ'_1	Maximum principal effective stress
σ'_3	Minimum principal effective stress
σ'_r	Effective radial stress
σ'_θ	Effective tangential stress
σ'_{axis}	Effective axial stress
σ_{Max}	Maximum principal stress
σ_{min}	Minimum principal stress
Co or σ_c	Uniaxial compressive strength of the intact rock
To	Uniaxial tensile strength
m	The empirical dimensionless constant
m_c	m in the compression zone
m_t	m in the tension zone
$m_{\beta w}$	Instantaneous empirical dimensionless constant with βw
$C_{o\beta w}$	Instantaneous uniaxial compressive strength of the rock with βw
ϕ'_w	Friction angle of the weakness planes
ϕ'	Friction angle
C'_w	Cohesion of the weakness planes
C'	Cohesion
β_w	Inclination of the failure plane
P_o	Support pressure
S	Induced state of stress
u	Pore water pressure
α	Biot coefficient
δ_{ij}	Kronecker delta
∂	Poisson ratio
Pw	Pressure in borehole

K	In situ stress anisotropy
R_w	Borehole radius
r	Radial direction
P_w	Pressure in the wellbore
τ	Shear stress acting on the plane,

Introduction

The oil and gas industry remains concerned about preserving stability in a wellbore during drilling operations, as any instability can lead to heightened drilling expenses. [1]

Wellbores that are drilled to reach reservoirs encounter various types of rocks that may contain structural discontinuities, ranging from large-scale faults to finely layered planes. Specifically, when drilling through shale formations, wellbores are prone to encountering significant instabilities caused by sliding along the bedding planes. [2]

Several studies have examined wellbore failure in different fields. Last and McLean [3], Twynam et al. [4], and Willson et al. [5] conducted analyses on the Cusiana Field in Colombia and the Pedernales Field in Venezuela. They observed instability during drilling operations in the intra-reservoir shales, which are characterized by fissility and natural fractures. The researchers found that stability was enhanced by increasing mud pressure [6] and maintaining a wellbore axis that was nearly perpendicular to the bedding planes (up-dip). Conversely, drilling in a down-dip or cross-dip direction resulted in significant instability.

Oakland and Cook [7] investigated wellbore instabilities in the Osenberg Field in the North Sea. They encountered instability issues while drilling in the Draupne formation, which is a fissile shale. Based on their field experience, they concluded that stability was improved when the wellbore trajectory was perpendicular to the bedding planes, while severe instability occurred when the hole axis was parallel to the bedding planes.

In their study (Brehm et al., [8], it was documented that the Shenzi Field in the Gulf of Mexico experienced wellbore instabilities due to weakly bedded rocks. They observed that drilling down-dip at low attack angles resulted in increased instability, while drilling up-dip (almost perpendicular to the bedding planes) showed minimal instability [9-10-11]. To mitigate instability while drilling down-dip, the mud pressures were raised, but this led to lost circulation issues.

In a separate study by Wu and Tan [12] in Bohai Bay, China, significant instability problems were encountered, particularly when drilling at high angles (exceeding 60 degrees) and drilling horizontal wells in shales with nearly horizontal bedding planes. Vertical or sub-vertical wellbores experienced fewer drilling problems.

Narayanasamy et al. [13] also reported wellbore instabilities in the Clair Oilfield, located west of Shetlands, UK. The instabilities were observed in cretaceous mudstones with bedding planes. They found that wellbores drilled with the axis nearly parallel to the weakness planes experienced severe problems. Although a successful wellbore was drilled by increasing the mud pressure, it was noted that the required mud pressure to prevent slip was close to the tensile fracturing pressure of the mudstones. This field evidence revealed the relationship between wellbore stability and the angle between the wellbore axis and the weakness planes. Wellbores drilled parallel to the weakness planes required the highest mud pressures to prevent slip, but these high mud pressures could result in mud leakage or even lost circulation.

Software based on the weakness plane model [14] was utilized for stability analyses of wellbores drilled in these fields. This model is commonly used in the oil and gas industry to predict mud pressures necessary to prevent slip [4–5, 7-8, 12-13, 15–25].

The limitations of the weakness plane model [25] in accurately matching experimental strength data, especially within the inclination range represented by the constant strength plateau, are widely acknowledged. Transversely isotropic rocks may demonstrate strength patterns that deviate from the predicted constant strength. To ensure accurate prediction of mud pressures, it becomes necessary to conduct a comparative analysis between the weakness plane model and an alternative criterion, considering how well each approach aligns with the experimental data. In some cases, the mud pressures calculated with the Hoek and Brown criterion yielded different results from those calculated with the weakness plane model.

The cost of drilling operation is strongly affected by anisotropy. Transversely isotropic rocks are common in many oil and gas reservoirs, and their anisotropic behavior can significantly impact the wellbore stability. When a well is drilled, the borehole is typically stabilized by drilling mud or other fluids that exert hydrostatic pressure on the wellbore walls. This pressure counteracts the stresses imposed by the surrounding rock formations, maintaining the integrity of the wellbore. However, when there is a change in the confining stress, such as during drilling, production, or changes in reservoir conditions, the balance between the wellbore pressure and the surrounding rock stress can be disrupted, leading to wellbore instability. Wellbore instability is the most common and immediate effect of inducing a change in confinement stress is the potential for wellbore instability and it can lead to mechanical failure or collapse of the wellbore walls. This can result in lost circulation, stuck pipe, wellbore collapse, and difficulties in drilling or completing the well.

It can lead also to borehole breakout: When the wellbore pressure is lower than the pore pressure and the minimum horizontal stress in the surrounding rock, it can induce tensile stresses in the wellbore walls. This can cause the formation of borehole breakout, which refers to the extension or enlargement of the wellbore in the direction of the least horizontal stress [26]. Borehole breakout can negatively impact well stability, as it weakens the wellbore walls and can lead to further instability and pipe sticking [27].

Conversely, if the wellbore pressure exceeds the maximum horizontal stress in the rock, it can induce compressive stresses in the wellbore walls and borehole collapse occur. This can result in borehole collapse, where the wellbore walls deform inward and potentially close off the wellbore [28]. Borehole collapse can impede drilling progress, hinder production, and require remedial actions to reopen the wellbore.

Changes in confinement stress can also affect fluid flow and the potential for lost circulation. If the wellbore pressure is too high or if the stresses induce fractures or pathways in the rock, drilling fluids can escape into the formation, leading to lost circulation [29]. Lost circulation can reduce drilling efficiency, increase costs, and necessitate the use of specialized techniques and materials to regain fluid circulation.

A fitting between the experimental data with Mohr coulomb and Hoek and Brown is done as a first step in this thesis in order to obtain strength parameters. These parameters should be obtained very carefully in order to obtain good results.

The mud pressure is then calculated using the weakness plane model and Hoek and Brown modified for different degree of anisotropy, for different authors (Niandou and Abdi) and for different inclination angle δ.

The report is composed of three chapters:

- Chapter 1 Methods

Presentation and discussion of the methods used in this thesis as well, i will fit the experimental data with Hoek and brown and with Mohr Coulomb for two different authors Niandou and Abdi.

- Chapter 2 Calculation of mud pressure using Hoek and Brown and the weakness plane model
  Calculation of the mud pressure using Hoek and brown and the weakness plane model for both authors with and without fitting the data and with different degree of anisotropy.

- Chapter 3 Conclusion
  Analyzing and interpreting the results in order to conclude the report

Chapter 1 – Methods

A. Theoretical

1.1 Terzaghi principle

Terzaghi principle assumes that the stress is opposed by the fluid that fill the pores in the material. Sedimentary rocks possess porosity and can experience a notable reduction in strength when subjected to increased pore water pressure caused by changes in loading. Consequently, it becomes imperative to consider the influence of pore water pressure in such situations. The deformation of the rock is directly related to the effective stress, a concept initially introduced by Terzaghi (1923, 1936) in the context of soils. The theory of poroelasticity states that the deformation of a porous medium is proportionate to the effective stress (Detournay and Cheng, 1993) [30].

$$\sigma'ij = \sigma ij - \alpha pf\, \delta ij \quad (1)$$

Where pf is the pore pressure and it is equal in all directions on a certain point for a continuous medium; σ′ij and σij are the effective and the total stress tensor. The wellbore stability must be studied using effective stress approach. [31]

Terzaghi's principle rely on several important assumptions: [32, 33]

1. The soil is homogenous and isotropic.
2. The soil is fully saturated, which means there is no air.
3. The solid particles are incompressible.
4. Compression and flow are one-dimensional (vertical axis being the one of interest).
5. Strains in the soil are relatively small.

1.2 Weakness plane model

The transversely isotropic rock is classified with two types: discontinuous and continuous models. In case of discontinuous model, we have to distinguish between the failure along the weakness plane and the failure in the rock matrix, the strength is constant when failure occur in the rock matrix, but when it fails along weakness plane, the strength changes with the orientation angle, while for the continuous model, the strength is changing with the inclination angle. [34]

The weakness plane model is a discontinuous model and is based on a constant cohesion and friction angle, and a constant value of strength for the rock matrix. Equation (30) has a minimum at $\beta w = 45^\circ + \phi'w/2$. Slip cannot occur for the values of βw less than ϕ'_w and close to 90° [35].

The failure occurs over several modes: axial splitting, shearing, or a combination between splitting and shearing [36]. The mode of failure depends also on the confining pressure [37] and the loading orientation θ [38, 39]. For θ between 0 and 15° we have an axial splitting behavior of the "tournemire shale" for low confinement, while it fails by shear in the same inclination for high confining pressure. For any θ between 30 and 60° the failure generally takes place because of the sliding of bedding planes and thus the fracture orientation is nearly equal to θ for both high and low confinement. For θ between 60 and 90°, we have a combination between splitting and shearing for low confinement, for which it starts with splitting on the top of the rock and become shearing in the lower half of the specimen. But for high confinement

"tournemire shale" will experience an increasing in shear stress along the bedding plane, causing it to deform and potentially slip.

1.3 Hoek and Brown modified

Hoek and brown criterion [40] is a continuous model, because the strength is varying continuously with the orientation of the weakness plane, but this criterion require a huge number of tensile test in order to determine $C_{o\beta w}$ and $m_{\beta w}$ within the range βw=0-90°. Hoek and Brown criterion is a non-linear criterion and is strongly recommended in case of transversely isotropic rock, which m and s are varying with the inclination of the weakness plane. Tien and Kuo [41] and Colak & Unlu [42] assumed s=1 and is instantaneously isotropic for each inclination of weakness plane, so we will have the following formula:

$$(\sigma 1 - \sigma 3)\,\beta w = (m\beta w C o\beta w \sigma' 3 + C\,2o\beta w)^{0.5} \quad (2)$$

Where $C_{o\beta w}$ and $m_{\beta w}$ are the instantaneous uniaxial compressive strength of the rock and the empirical dimensionless constant respectively, which change with the inclination βw of the weakness planes.

1.4 Mohr Coulomb

Mohr coulomb criterion is a linear and it is widely used. This criterion states that failure occurs when the shear stress (τ) on a plane exceeds the shear strength of the material at that plane. Failure occur at $45+\frac{\phi'}{2}$. The shear strength of the material is determined by two parameters: the cohesion (c') and the angle of internal friction (ϕ').The equation for the Mohr-Coulomb criterion is [43-47]:

$$\tau = c' + \sigma' * tan(\phi') \quad (3)$$

Where:

τ is the shear stress acting on the plane,

c' is the cohesion, which represents the shear strength of the material at zero normal stress,

σ' is the normal stress acting perpendicular to the plane, and

ϕ'is the angle of internal friction, which represents the slope of the shear strength envelope.

However, σ'1 vs. σ'3 is a very important plot because it allow us to calculate the uniaxial compressive stress and Nϕ which are respectively the intersection of the line with σ'1 and the slope of the line, and from these two parameters, c' and ϕ'could be calculated using the following formulas:

$$N\phi = \frac{1+sin\phi'}{1-sin\phi'} \quad (4)$$

$$C0 = \frac{2c'cos\phi'}{1-sin\phi'} \quad (5)$$

Mohr coulomb criterion is widely used because it is a simple and linear criterion. However, it does not take into account the transition from shear to ductile in the compression zone and the occurrence of the intermediate principle stress in the compression zone [48]. It has some limitations because it is not in accord with lab test since it overestimates the tension zone [49]. So we fix a cutoff $\frac{Co}{To} = 10$. For that reason, Hoek and Brown criterion is introduced. It is consistent with the experimental data and take the transition into account. However, the value of m depends on the confinement pressure and on the compression and the tension zone [50-51-52]. The experimental data shows that Hoek and brown is conservative for analyzing wellbore stability in the tension zone. The Hoek and brown criterion is not widely used because of the uncertainties in the determination of the main parameters.

After selecting the strength criterion, it is important to determine the strength properties of the rock. So a uniaxial compressive test is made in order to determine the uniaxial compressive strength. This test is not enough because we will have at failure the same Mohr circle, so we cannot determine the frictional component of the strength which are ϕ' and m, for that reason a triaxial test is made. However, we still have to find the uniaxial tensile strength, so the Brazilian test is made and it is widely used because it is easy to prepare the specimen, but it usually overestimates the uniaxial tensile strength [53]. We normally need a reduction factor for the uniaxial tensile strength for the Brazilian test which is equal to 0.7[54]. If the tension zone is lower than the compression zone, it is more likely that the rock will fail in the tension zone. However, data fitting between experimental data and Hoek and brown criterion can give a good value of m in the tension zone. If the mud weight window is not narrow, using the Mohr-Coulomb criterion with a fixed cut-off value is advisable.

1.5 Kirsch solution

Kirsch solution is used for anisotropic far field stresses. It is a solution which assumes an isotropic linear elastic material and a plane strain condition [55-56-57]. The general formulas of kirsch solution are the following [58-59]:

$$\sigma r = \frac{1}{2}(\sigma min + \sigma \max)\left(1 - \frac{Rw^2}{r^2}\right) + \frac{1}{2}(\sigma max - \sigma \min)\left(1 + \frac{3Rw^4}{r^2} - \frac{4Rw^2}{r^2}\right) cos2\theta + pw\frac{Rw^2}{r^2} \quad (6)$$

$$\sigma\theta = \frac{1}{2}(\sigma min + \sigma \max)\left(1 + \frac{Rw^2}{r^2}\right) - \frac{1}{2}(\sigma max - \sigma \min)\left(1 + \frac{3Rw^4}{r^2}\right) cos2\theta - pw\frac{Rw^2}{r^2} \quad (7)$$

$$\sigma axis = \sigma 11 - 2\nu(\sigma max - \sigma \min)\frac{Rw^2}{r^2} cos2\theta \quad (8)$$

$$\tau r\theta = -\frac{1}{2}(\sigma max - \sigma \min)\left(1 - \frac{3Rw^4}{r^2} + \frac{2Rw^2}{r^2}\right) sin2\theta \quad (9)$$

$$\tau z\theta = \tau rz = 0 \quad (10)$$

Where:

σ_{Max} is the maximum principal stress

σ_{min} is the minimum principal stress

R_w is the borehole radius

r is the radial direction

P_w is the pressure in the wellbore

σr is the radial stress

σ_θ is the tangential stress

At the borehole wall, we have r=R_w, and the formulas (6), (7), (8), (90 and (10) become:

$$\sigma r = pw \tag{11}$$

$$\sigma\theta = \sigma min + \sigma\max - 2(\sigma max - \sigma\min)cos2\theta - pw \tag{12}$$

$$\sigma z = \sigma v - 2\nu(\sigma max - \sigma\min)\, cos2\theta \tag{13}$$

$$\tau r\theta = \tau z\theta = \tau rz = 0 \tag{14}$$

Our aim now is to provide the failure limit on the boundary of an excavation. The first step is to calculate the induced state of stress (S). At θ=0°, the induced state of stress is minimum, but at θ=90°, the induced state of stress is maximum [57]. Using kirsh solution in plane strain condition, and after applying pf, the formulas of the effective stresses are the following [60]:

$$\sigma' r \;=\; Pw - pf \tag{15}$$

$$\sigma' \vartheta \;=\; S \;-\; Pw - pf \tag{16}$$

$$\sigma' axis \;=\; Sz - pf \tag{17}$$

Where S is the induced state of the stress with the following formula:

$$S = \; [\sigma max + \sigma min \; - 2(\sigma max \; - \sigma min)\, cos\,(2\theta)] \tag{18}$$

(16) Shows that for a low value of S, that's means for θ=0°, we may have σ'_ϑ<0 in case Pw and Pf are high. But for θ=90°, σ′ϑ is always positive since S is maximum.

Mud pressure is more or less the only adjustable factor for wellbore stability. If for example the reason for the instability is hole collapse, then the standard solution is to increase the mud weight. If there are mud loss the solution is to reduce the mud weight.

We have three types of conditions: Drilling in overbalance (OBD), drilling in balance, and drilling in underbalance (UBD). In case the wellbore pressure is higher than the formation pore pressure, we are drilling in overbalance [61]. In case they are equal, we are drilling in balance. But if case the wellbore pressure is lower than the formation pore pressure, we are drilling in underbalance [62]. In an overpressure reservoir, we may have an unexpected high pore pressure and UBD may occur. OBD means that σ'_r >0, while it is <0 for UBD and null for drilling in balance. An unexpected overpressure will lead to a decrease in the strength of a material and also the effective stress, so the analysis will move to the tension zone since the effective stress can become negative. However, drilling in balance is not a satisfied condition because it is not safe enough and it is controlled by the uniaxial compressive strength.

A high frictional component of strength in the tension zone underestimate the tension zone so we can say that it is conservative and is better especially in case of overpressured basin. It is the opposite for the compression zone, for which it is recommended to take low value of the frictional component of strength. So we suggest in case of overpressured basin to take two different values of the frictional component.

We define the mud pressure window: the range of mud pressure necessary in order to keep the wellbore stable during drilling operations, and it is the mud pressure to avoid tensile fracturing and slip for all the inclinations δ of the weakness planes [63]. This criterion fit well the Brazilian test and the results of the tensile test.

The experimental data shows a good agreement with the Hoek and brown criterion for all the inclination angle while this matching didn't occur with the weakness plane model because the plateau with constant strength cannot describe properly the behavior of the rock, it's because the weakness plane model does not take into account for failure both along the weakness planes and in the rock matrix. If the uniaxial tensile strength at βw=90° is higher than that at βw=0°, so we will have the tensile strength at βw=90° is higher than that at βw=0°.

For an inclination δ of the weakness plane, beta change with theta using the following formulas:

$$\beta w = |\vartheta - \delta| \; 0 \circ \leq \vartheta \leq \delta + 90 \circ \tag{19}$$

$$\beta w = 180 \circ - |\vartheta - \delta| \leq \delta + 90 \circ \leq \vartheta \leq 180 \circ \tag{20}$$

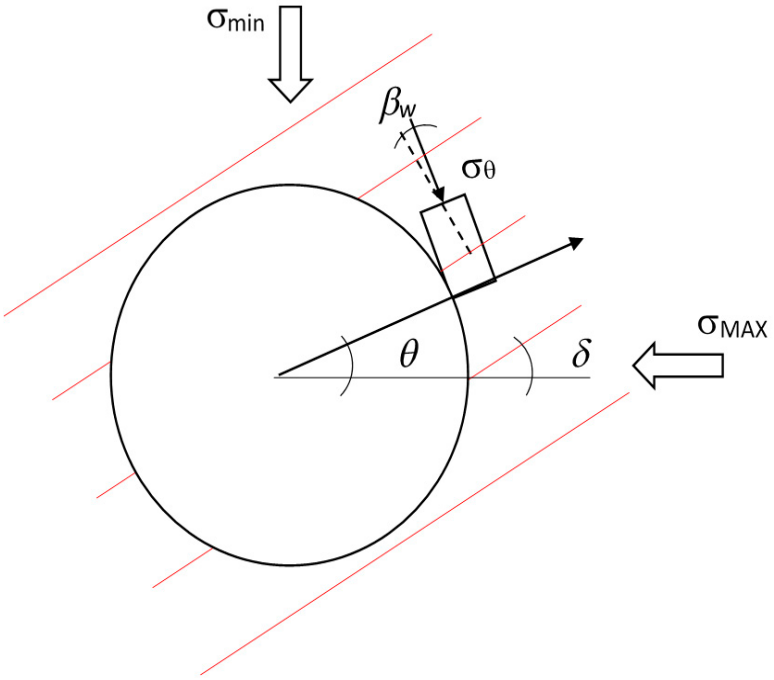

Figure 1 Definition of the angles δ, ϑ and βw around the wellbore for the analysis of slip. The red lines represent the weakness planes. The dotted line represents the normal to the planes.

The strength changes with βw and ϑ. We use Hoek and brown criterion and the weakness plane model in order to study this strength variation along the weakness plane.

Zhang [64] uses only the formula (19) but it was seldom valid for the inclination $\vartheta > \delta + 90^\circ$ because we will have βw greater than 90°, from here the need of the equation (20).

From the formulas (19) and (20) we can notice that for $\vartheta=0$ and 180° we have $\beta w= \delta$. However, it is very important to determine the highest mud pressure so we set $\delta= \delta_{crit}$. After coupling kirsh solution and the weakness plane model, we will have the minimum mud pressure to avoid slip:

$$Pslip = AS - B + C \tag{21}$$

$$S = [\sigma max + \sigma min - 2(\sigma max - \sigma min)\cos(2\theta)] \tag{22}$$

$$A = (1 - \frac{\tan \phi' w}{\tan \beta w}) * \frac{\sin 2\beta w}{2D} \tag{23}$$

$$B = \frac{C' w}{D} \tag{24}$$

$$C = \frac{\tan \phi' w * Pf}{D} \tag{25}$$

$$D = (\tan \phi' w + (1 - \frac{\tan \phi' w}{\tan \beta w})\sin 2\beta w] \tag{26}$$

From equation (23), we have two maximums which are equal, independently from the value of δ at $\phi'w$ and occur at $\beta w = 45^\circ + \frac{\phi' w}{2}$.. However, the extremum has not the same positions and locations, they change with δ. The slip condition does not occur in the case when $\vartheta = 0^\circ$ and $\delta \leq \phi'_w$, the angle $\beta w \leq \phi'_w$, in this condition, slip occur starting from $\vartheta > \delta + \phi'_w$. While, when $\delta = 90^\circ$ at $\vartheta = 0^\circ$, the angle $\beta w = 90^\circ$ and the slip condition always start for a theta higher than 0 degree, regardless of the friction angle ϕ'_w. Equations (24) and (25) does not affect the results and show always a minimum at $\beta_{wcrit} = 45^\circ + \phi'_w/2$, so we can consider these 2 equations as 0. So we will have simply:

$$Pslip = AS \tag{27}$$

After calculations, we obtain:

$$\delta crit = 45 - \frac{\phi' w}{2} \tag{28}$$

Replacing (27) in (22) we obtain:

$$PW\ slip = AS = \frac{[1 - \tan \phi' w / \tan[\vartheta - (45^\circ - \phi' w/2)]] \sin 2[\vartheta - (45^\circ - \phi' w/2)]]}{2[\tan \phi' w + [1 - \tan \phi' w / \tan[\vartheta - (45^\circ - \phi' w/2)]] * \sin 2[\vartheta - (45^\circ - \phi' w/2)]]} * [\sigma MAX + \sigma min - 2(\sigma MAX - \sigma min)\cos 2\vartheta] \tag{29}$$

The first derivative of (29) gives us a maximum at $\vartheta=90^\circ$, from here we can have the highest P_{mud} to avoid slip which depend on $\delta= \delta_{crit}$ and it is function of ϕ'_w. The weakness plane model is not able to predict properly the behavior of the rock near $\beta w=90^\circ$ or for βw less than ϕ'_w.

(19) And (20) show the existence of a critical inclination of the weakness plane which a function of $\phi'w$.

In all cases, at $\theta=90^\circ$ we require the lowest mud pressure. The weakness plane model coupled with Mohr coulomb criterion cannot predict some aspects and some phenomena, but it can predict local failure. The mud pressure to avoid slip is a function of δ, so we should study the minimum mud pressure to avoid slip with more than one inclination of the weakness plane. [65-66].With the weakness plane model the critical

condition occur at $\delta crit = 45 \circ + \frac{\phi'w}{2}$. Choosing the critical mud pressure, may help us to save time when drilling and to avoid unexpected drilling problems. In case k=1, the mud pressure is independent of δ, and the peak of the mud pressure is lower than the case when k>1. When δ = 90°, we have the lowest mud pressure. We have a decrease in the difference of mud pressure in case of decrease in the strength anisotropy. For a wide range of δ, the mud pressure to avoid slip is high, so tensile failure can occur. The mud pressure window is strongly dependent on the strength anisotropy of the tensile strength. Nova and Zaninetti criterion helped us to know that the lowest fracturing pressure occur for δ between 0 and 30°.

When δ = 0◦ and δ = 90◦, the mud pressures show two equal maximum values. This behavior is due to the variation of both the tangential stress S and the inclination of the weak planes βw in the elements with the wellbore azimuth ϑ.

In general, the trend of $P_{w\ H\&B}$, corresponding to different δ is very similar to the trend of P_w slip. The locations of the mud pressure peaks for a given δ, calculated with the two criteria, agree with and confirm the validity of the results obtained in the first set of analyses. When $\delta = \delta_{crit}$, the mud pressures are highest, and occur at a wellbore azimuth ϑ = 90◦

1.6 Mud pressure

Our objective is to study the stability of the wellbore using the weakness plane model and Hoek and brown modified. We consider the condition where the stress in theta direction is higher than that in the axial direction and radial direction. However, we encountered a contradiction between kirsch solution and the selected criteria since kirsh assume an elastic, isotropic, linear and homogeneous material [67], while the weakness plane model or Hoek and brown modified are drilled in transverse isotropic material. The result of the numerical simulation show that the variation of strength is negligible, so the anisotropy is also negligible and so we can use kirsh solution for the tournemire shale. Our purpose is to determine the failure at the wellbore of the borehole drilled for the tournemire shale.

We have two mode of failure for the weakness plane model: failure along the intact rock material and failure along the discontinuity. For the values of β_w close to 90° and between 0 and ϕ'_w we define a plateau with a continuous strength which is not always in agreement with the experimental data. Coupling kirsh equation with the weakness plane equation:

$$(\sigma 1 - \sigma 3)\ \text{slip} = \frac{2(c'w+\sigma'3\ \tan\phi'w)}{[(1-\frac{\tan\phi'w}{\tan\beta w})\sin 2\beta w]} \tag{30}$$

We will have:

$$PWPM = \frac{S(1-\tan\phi'w/\tan\beta w)*\sin 2\ \beta w - 2c'w + 2\tan\phi'w * Pf}{2[\tan\phi' w + (1-\tan\phi'w/\tan\beta w)\sin 2\ \beta w\ ]} \tag{31}$$

For the Hoek and brown modified, $C_{o\beta w}$ and $m_{\beta w}$ are used in order to calculate the value of strength for each value of inclination of the weakness plane and it is considered isotropic instantaneously [68-69]. Coupling kirsh solution with H&B criterion $(\sigma 1 - \sigma 3)\ \beta w = (m\beta w Co\beta w\sigma'3 + C\ 2o\beta w)^{0.5}$ (32), we obtain: [70]

$$PH\&B = \frac{4S+m\beta w\ co\beta w-[(4S+\ m\beta w\ co\beta w)2-16(S2+\ m\beta w\ co\beta wPf - co\beta w2)]0.5}{8} \tag{33}$$

We use these 2 equations of P in order to compare the wellbore stability using two different criterions.

With H&B criterion we found that $m_{\beta w}$ range between 3.6 and 5MPa for the different inclination angle, and we obtain maximum values of $C_{o\beta w}$ at β_w=0 and 90° and a minimum close to β_w=45°, but for the WPM we have a constraint location of the minimum strength at $\beta_w = 45+\phi_w'/2$. After comparison of experimental data with H&B we find a very good matching while we don't observe this agreement between the experimental data and the WPM.

B. Analytical

This part aims to fit the experimental data for both authors (Niandou and Abdi) with both Hoek and brown and Mohr Coulomb.

1.7 Working procedure in calculation for the first author

We are working only on the compression zone

1.7.1 for Hoek and Brown

1. Plot $(\sigma_1-\sigma_3)^2$ vs. σ_3 in order to find m , C_0
2. Using the values of m and Co already found, we calculate the values of σ1 with Hoek and Brown
3. We plot σ_1 vs. σ_3 and we see if Hoek and Brown fit the experimental data
4. In case they didn't fit, we repeat the procedure already mentioned (1-2-3) with removing the highest value of stress

1.7.2 for Mohr Coulomb

1. We plot σ_1 vs. σ_3 that contain the values of experimental data , and from the equation of the line, we find C0 and N_ϕ
2. Using the values of C0 and N_ϕ already found, we calculate the value of σ_1 with Mohr Coulomb Criterion
3. We plot σ_1 vs. σ_3 and we see if Mohr Coulomb fit the experimental data
4. In case they didn't fit, we repeat the procedure already mentioned (1-2-3) with removing the highest value of stress

1.8 Working procedure in calculation for the second author

1.8.1 for Hoek and Brown

1. Plot $(\sigma_1-\sigma_3)^2$ vs. σ_3 in order to find m , C_0
2. Using the values of m and Co already found, we calculate the values of σ_1 with Hoek and Brown
3. We plot σ_1 vs. σ_3 and we see if Hoek and Brown fit the experimental data
4. In case they didn't fit, we change the straight line equation so we can repeat the first three steps already mentioned
5. If 4 was not enough, that's mean that the value of m is not the same value for both compression and tension zone and we need to work on the zone that is not matching by repeating the first three steps

1.8.2 for Mohr Coulomb

We work only on the compression zone. We have only three confinements so we can't do any correction

1. We plot σ_1 vs. σ_3 that contain the values of experimental data , and from the equation of the line, we find C0 and N_ϕ
2. Using the values of C0 and N_ϕ already found, we calculate the value of σ_1 with Mohr Coulomb Criterion
3. We plot σ_1 vs. σ_3 and we see how much Mohr Coulomb fit the experimental data

1.9 The experimental data

The experimental data obtained from Niandou and Abdi are the following respectively:

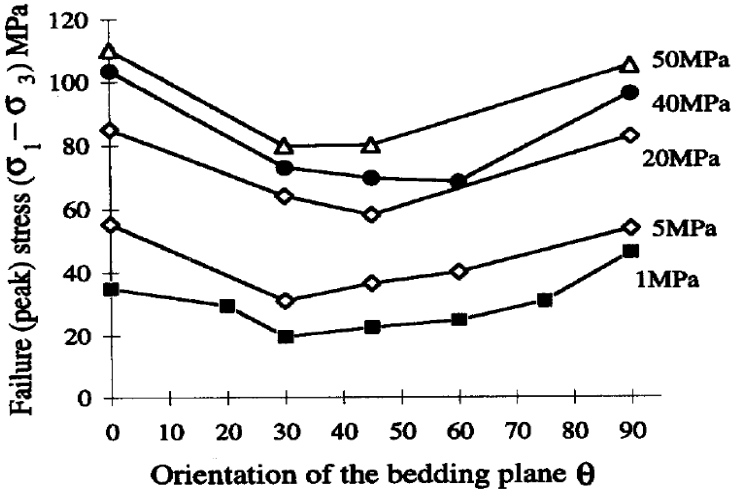

Fig. 18. Variation of failure stress vs loading orientation for various confining pressure.

Figure 2 Variation of failure stress vs. loading orientation for various confining pressure (Niandou)

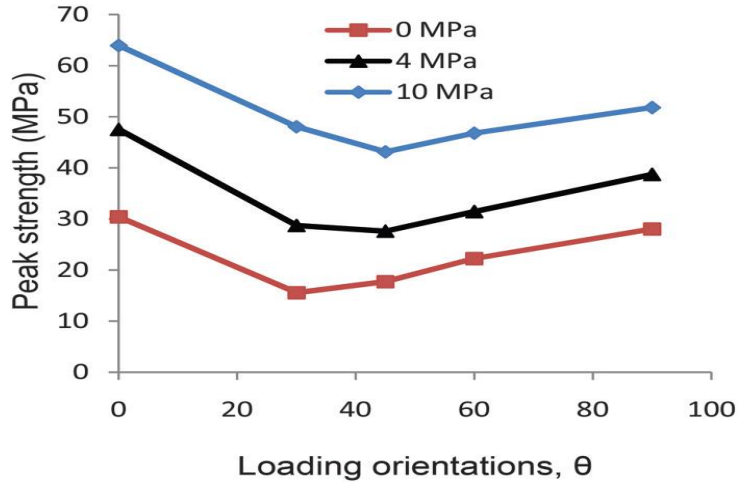

Figure 3 Variation of peak strength with theta at different confining pressure (0, 4 and 10 MPa) (Abdi)

1.10 First author (Niandou)

1.10.1 Hoek and Brown

Figure 2 represents different values of σ_1-σ_3 function of theta (orientation of bedding plane) when applying different values of σ_3.

Using figure (2), we can calculate different values of σ_1 for different orientation angle:

σ_3(MPa)	0	30	45	60	90
1	45.45	24.17	21.96	19.77	35.64
5	56.22	43.42	41.16	34.75	61.61
20	100.77		79.00	85.24	104.50
40	138.51	107.00	109.96	112.85	144.70
50	154.42		128.43	130.46	159.87

Table 1 experimental data values

For θ=90°:

Using the values of experimental data with theta=90°, we have:

σ_3 (MPa)	σ_1 (MPa)	$(\sigma_1-\sigma_3)^2$
1	35.64	1199.93
5	61.61	3204.692
20	104.50	7140.25
40	144.70	10962.09
50	159.87	12071.42

Now we can plot $(\sigma_1-\sigma_3)^2$ vs. σ_3 in order to find m, C_0:

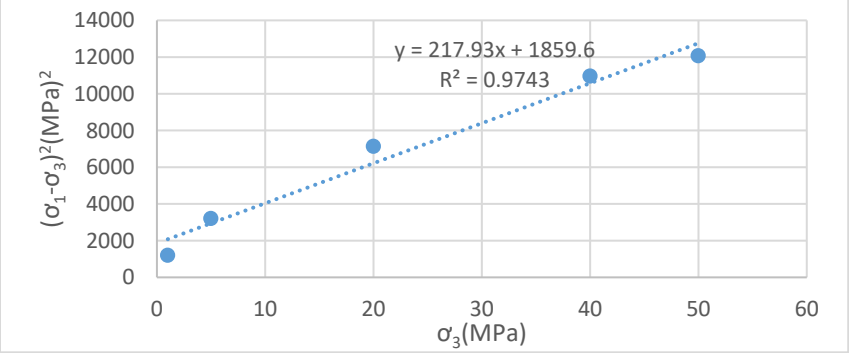

Figure 4 $(\sigma 1-\sigma 3)^2$ vs. $\sigma 3$, theta=90°, first fitting

From the equation of the line: y = 217.93x + 1859.6 we can find $m_{\beta w}$ and $C_{o\beta w}$

$m_{\beta w}\, C_{o\beta w}$=a =217.93 and b= $C_{o\beta w}^{2}$=1859.6

$C_{o\beta w}$=43.12307967MPa and $m_{\beta w}=\frac{a}{Co\beta w}=\frac{217.93}{43.12307967}$=5.054369996MPa

Now, we try to fit the experimental data with Hoek and Brown criterion using equation 5.

We recalculate the values of σ'_1 using this formula and using the previous values of m and C0 respectively (5.054369996MPa and 43.12307967MPa), the formula became:

$$\sigma'_1 = \sigma'_3 + (217.93\ \sigma'_3 + 1859.6)^{0.5}$$

We replace the different values of σ'_3: 1, 5, 20, 40,50MPa in the formula, we got:

σ_3(MPa)	σ_1(MPa)
1	46.58025888
5	59.30837873
20	98.8593685
40	142.8494045
50	162.9495463

Now we check if Hoek and brown fit with the experimental data by drawing σ_1 vs. σ_3

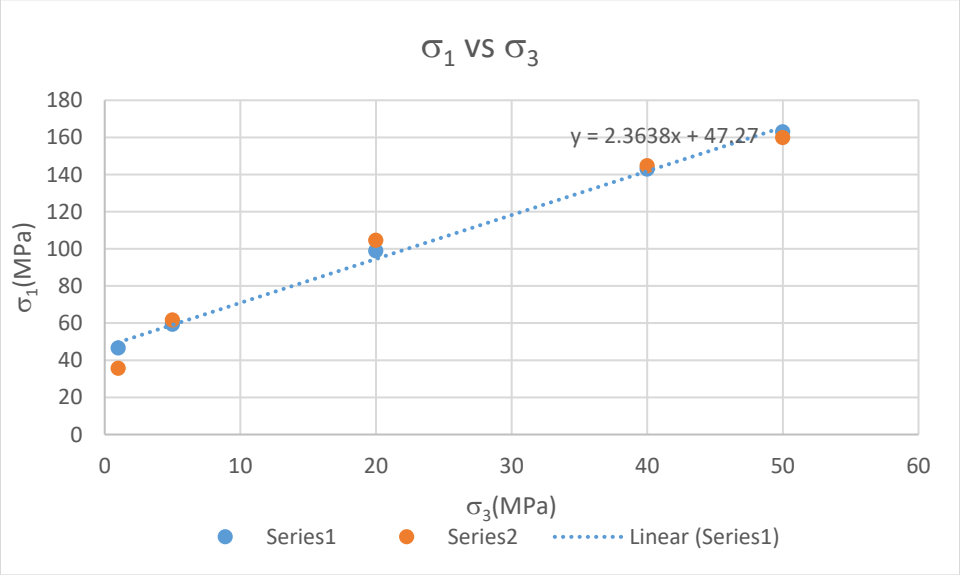

Figure 5 σ1 vs σ3, first fitting

The one in orange are the experimental data, it is show that they are close but not everywhere, so we need a correction.

Now we will work only on the first four points:

σ_3(MPa)	σ_1(MPa)
1	35.64
5	61.61
20	104.50
40	144.70

We can plot $(\sigma_1-\sigma_3)^2$ vs. σ3 in order to find a corrected value of m, C_0:

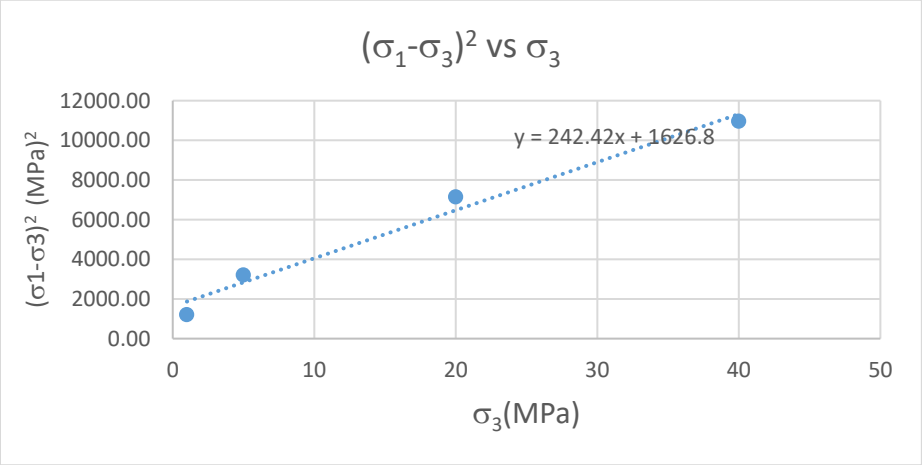

Figure 6 $(\sigma 1-\sigma 3)^2$ vs. σ3, theta=90°, second fitting

From the equation of the line: y = 242.42x + 1626.8 we can find $m_{\beta w}$ and $C_{o\beta w}$

$m_{\beta w}C_{o\beta w}$=a =242.42 and b= $C_{o\beta w}^2$=1626.8

$C_{o\beta w}$=40.333MPa and $m_{\beta w}=\frac{a}{Co\beta w}=\frac{242.42}{40.333}$=6.01MPa

Now, we try to fit the experimental data with Hoek and Brown criterion using equation 5.

We recalculate the values of σ'_1 using this formula and using the previous values of m and c0 respectively (6.01MPa and 40.33MPa), the formula became:

$$\sigma'_1 = \sigma'_3 + (242.42\sigma'_3 + 1626.8)^{0.5}$$

We replace the different values of σ'_3: 1, 5, 20,40MPa in the formula, we got:

σ_3(MPa)	σ_1(MPa)
1	44.233
5	58.28
20	100.46
40	146.41

Finally, we want to check if Hoek and brown fit with the experimental data by drawing σ1 vs. σ3

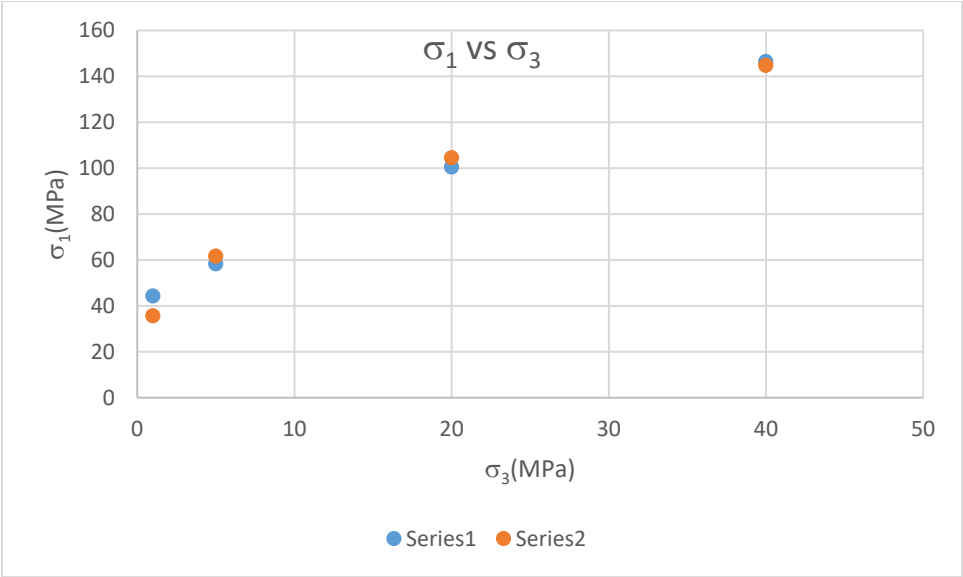

Figure 7 σ1 vs σ3, second fitting

It is clear that the fitting between the experimental data and Hoek and brown values are getting better, however it is better to do a further correction:

So now we will work on the first 3 points:

σ_3(MPa)	σ_1(MPa)
1	35.64
5	61.61
20	104.5

Now we plot $(\sigma1-\sigma3)^2$ vs. σ3 to find m and co:

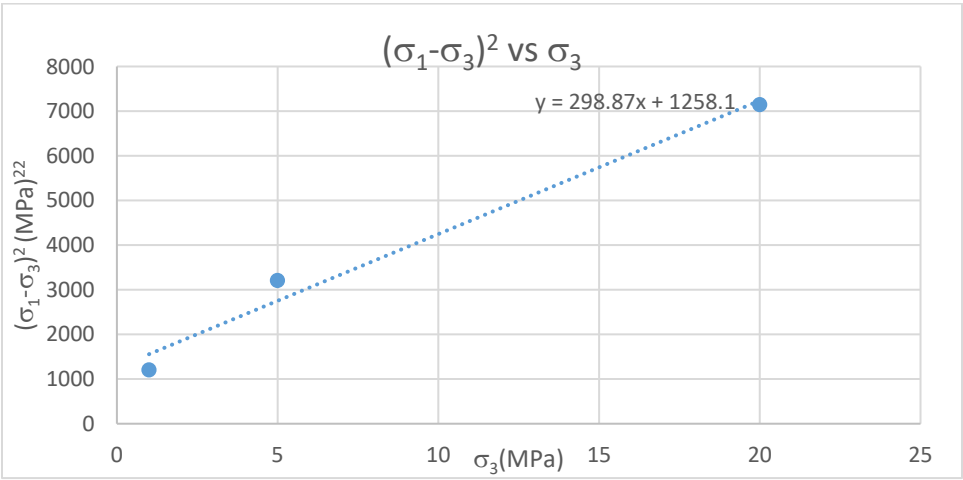

Figure 8 $(\sigma1-\sigma3)^2$ vs. σ3, theta=90°, third fitting

From the equation of the line: y = 298.87x + 1258.1we can find $m_{\beta w}$ and $C_{o\beta w}$

$m_{\beta w}Co_{\beta w}$=a =298.87 and b= $C_{o\beta w}^2$=1258.1

$C_{o\beta w}$=35.47MPa and $m_{\beta w}=\frac{a}{Co\beta w}=\frac{298.87}{35.47}$=8.426MPa

Now, we try to fit the experimental data with Hoek and Brown criterion using equation 5.

We recalculate the values of σ'_1 using this formula and using the previous values of m and C0 respectively (8.426MPa and 35.47MPa), the formula became:

$$\sigma'_1 = \sigma'_3 + (298.87\ \sigma'_3 + 1258.1)^{0.5}$$

We replace the different values of σ'_3: 1, 5,20MPa in the formula, we got respectively:

σ'1=40.45, 57.463 and 105.06MPa

They are quite similar to the experimental data, so we have Co=35.47MPa and m=8.426MPa

Doing the same procedure with the same author and same criterion but with different values of theta we obtain the following values of m and co corrected:

Theta(degree)	m	Co (MPa)
90	8.428	35.47
60	5.775	22.738
45	4.33	25.98
30	3.59	26.55
0	6.156	39.8

Table 1 m and co values for different theta, with correction, Hoek and Brown, first author

Now we are able to plot m and Co vs. theta:

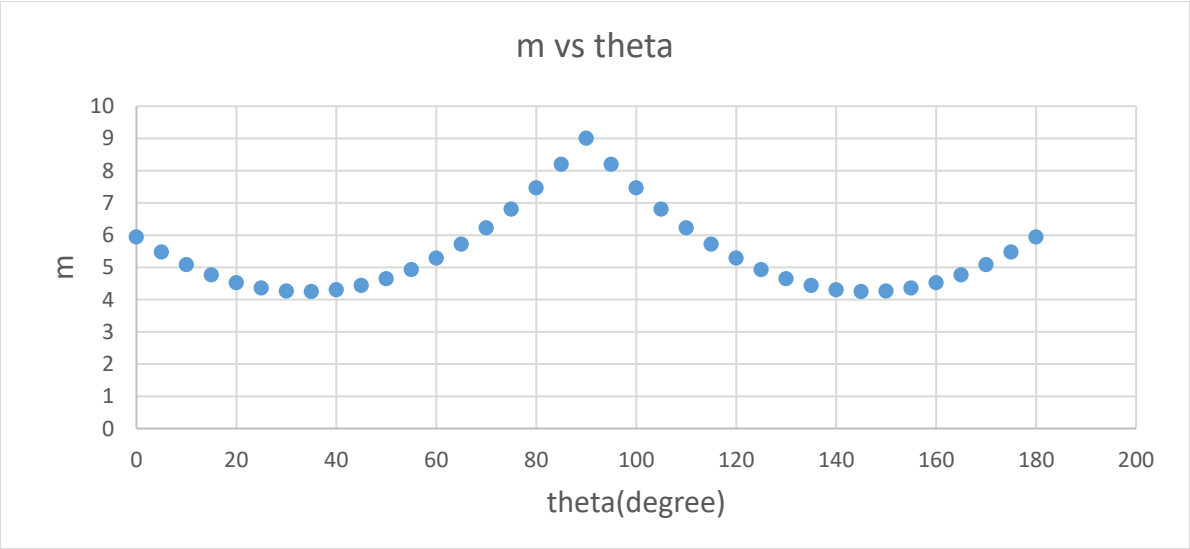

Figure 9 m vs. theta, δ=0, Niandou with correction

m has highest value at θ=0 and θ=90 in the range [0-90°], while it has the lowest value around 45. For δ=0°, theta has the highest value around beta=90 or 0 and the lowest around 45°. From this analysis, we can understand the trend of the plot, which start with a high value, then start to decrease till beta=45°, increase again to reach a peak at 90°, then decrease till theta= 135°, finally increase until theta=180°.

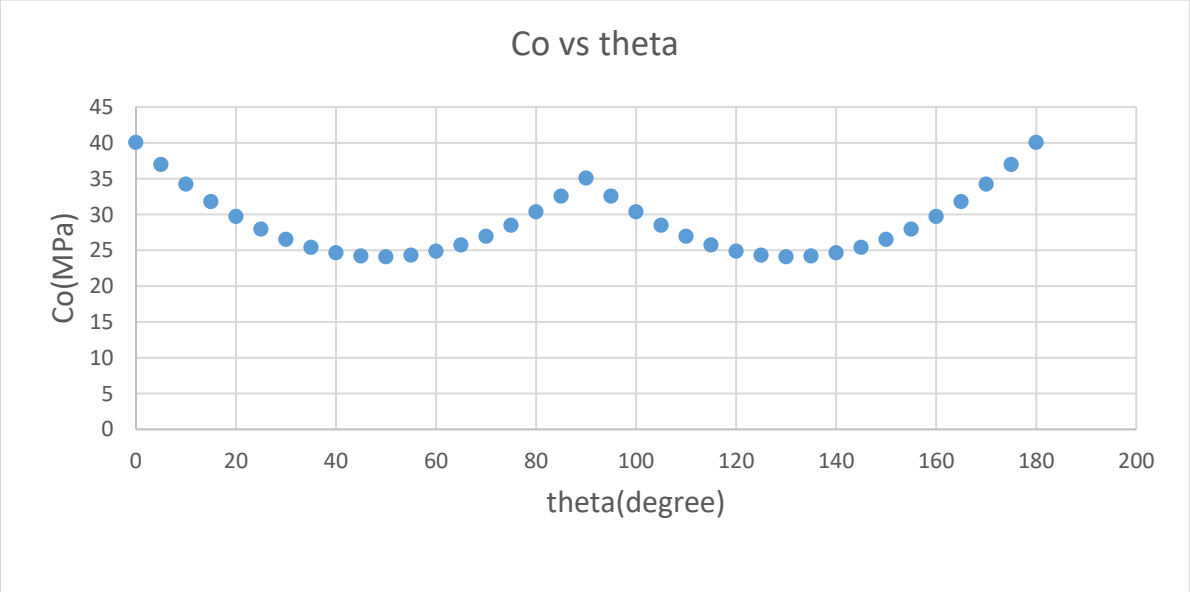

Figure 10 Co vs. theta, δ=0, Niandou with correction

Co has highest value at θ=0 and θ=90 in the range [0-90°], while it has the lowest value around 45 or 60°. For δ=0°, theta has the highest value around beta=90 or 0 and the lowest around theta=30 or 45°. From this analysis, we can understand the trend of the plot, which start with the highest value, then start to

decrease till beta=45°, increase again to reach a peak at 90°, then decrease till theta= 135°, finally increase se again to a maximum at beta=180°.

Neglecting the fitting between the experimental data and Hoek and brown, we will have the following values of m and co:

Theta(degree)	m	Co (MPa)
90	5.054	43.123
60	4.973	24.66
45	4.182	26.374
30	3.59	26.55
0	4.1645	44.857

Table 2 m and co values for different theta, without correction, Hoek and Brown, first author

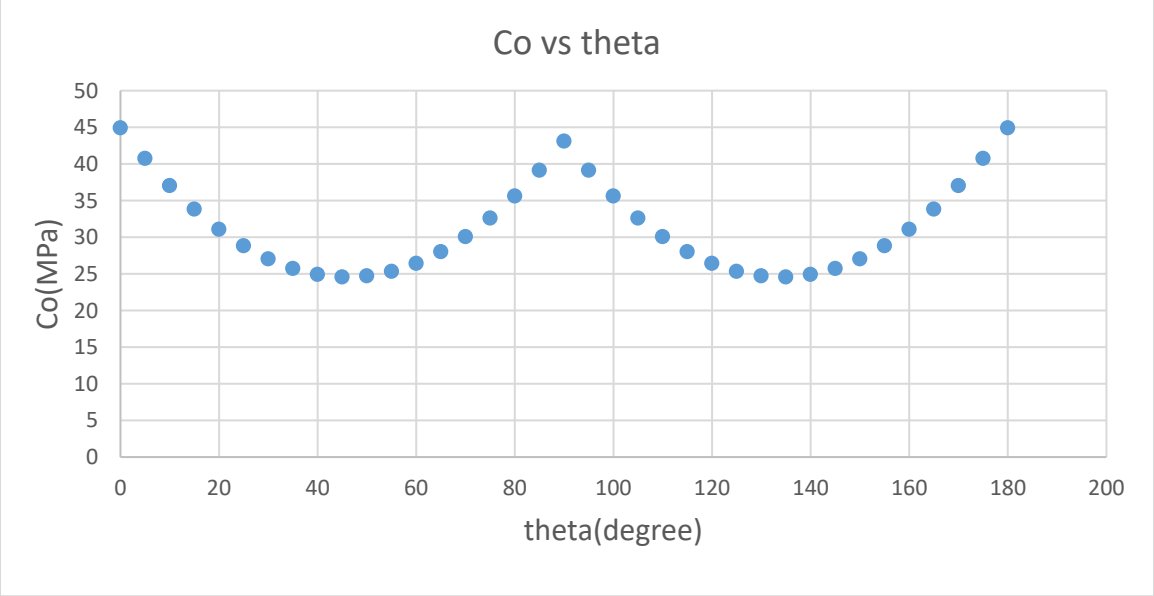

Figure 11 Co vs. theta, δ=0, Niandou without correction

Co has highest value at θ=0 and θ=90 in the range [0-90°], while it has the lowest value around 45. For δ=0°, theta has the highest value around beta=90 or 0 and the lowest around theta=30 or 45°. From this analysis, we can understand the trend of the plot, which start with the highest value, then start to decrease until theta=45°, increase again to reach a peak at 90°, then decrease till theta= 135°, finally increase se again to a maximum at theta=180°.

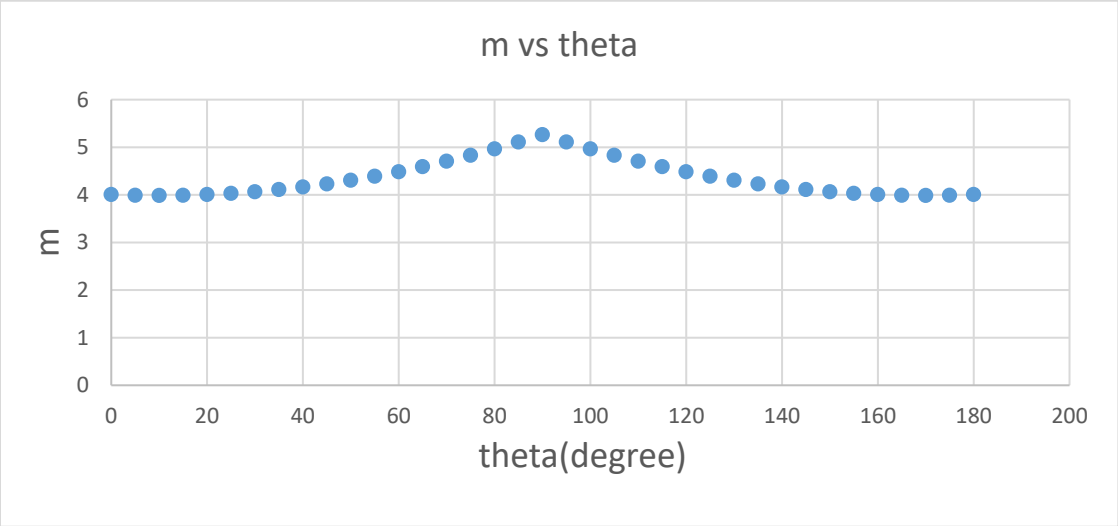

Figure 12 m vs. theta, δ=0, Niandou without correction

Without a well-fitting of the data with Hoek and Brown, the plot shows a small change in the range of m along the inclination theta, which start with a minimum at theta=0, increase slowly to reach a peak at theta=90°, then decrease to a minimum at theta=0°.

2.10.2 Mohr Coulomb

It's time to fit Jaeger's linear regression (Mohr coulomb criterion) with fit the experimental data:

Mohr Coulomb Criterion equation:

$$\sigma' 1s = C0 + \sigma' 3N\phi \tag{34}$$

Co is b and N_ϕ is the slope a of the linear equation of line y=ax+b of the plot σ'_1 vs. σ'_3

We will start working on all the values found from the experimental data:

σ'_3(MPa)	σ'_1(MPa)
1	35.64
5	61.61
20	104.50
40	144.70
50	159.87

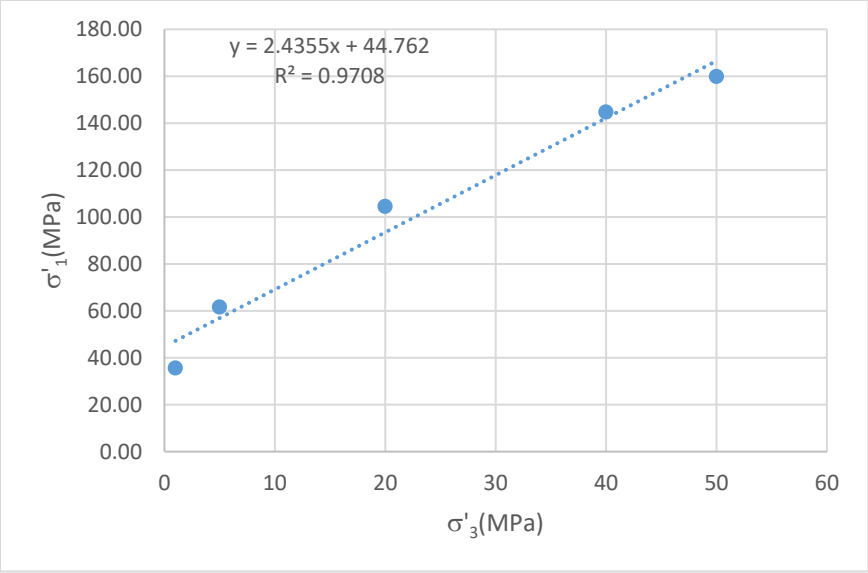

Figure 13 σ'1 vs σ'3, first author, first fitting, mohr coulomb

We found that C0=44.76MPa and N_ϕ=2.4355

So now we calculate the values of σ'_{1s}:

σ'_{1s} =44.76+2.4355 σ'_3

We Calculate σ'_{1s} for different values of σ'_3 (1, 5, 20, 40,50MPa) we will have the following values of σ'_{1s}: 47.1975, 56.9395, 93.472, 142.182, 166.537MPa

Now we plot σ'_1 vs. σ'_3 in order to see how well the fitting is.

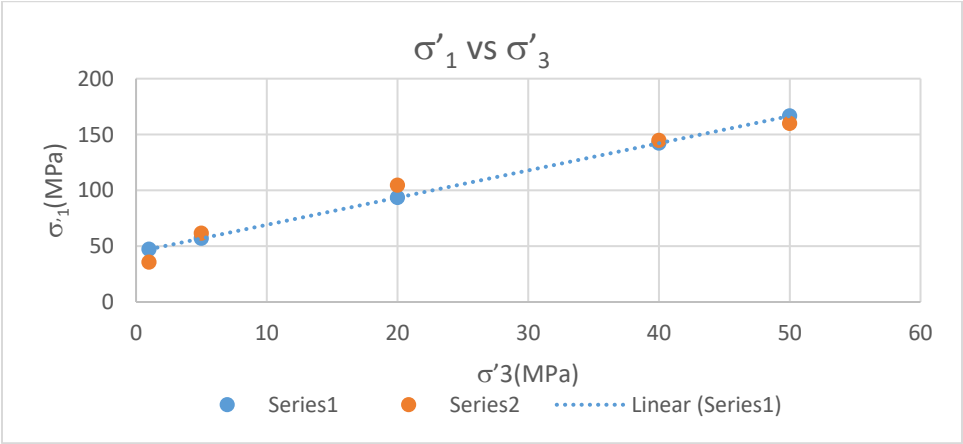

Figure 14 σ'1 vs σ'3, first author, fitting comparaison, mohr coulomb

The orange point are the experimental data. It is shown that we have a poor fitting in some points, so it is better to ameliorate the fitting

Now I will work on the first four points:

σ'_3(MPa)	σ'_1(MPa)
1	47.1975
5	56.9395
20	93.472
40	142.182

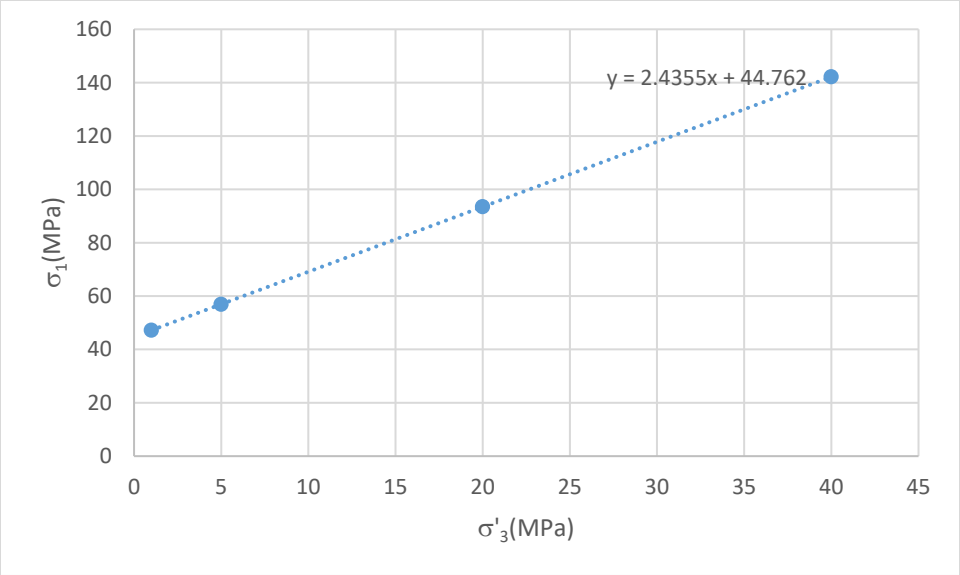

Figure 15 σ'1 vs σ'3, first author, second fitting, mohr coulomb

The equation of line y=ax+b of the plot σ'1 vs. σ'3 is the same, a and b are the same, so N_ϕ and C0 are the same, so we will obtain the same values of σ'_{1s}. However, we will go for a further correction

We will work now on the first three values of σ_3:

σ_3(MPa)	σ_1(MPa)
1	35.64
5	61.61
20	104.5

From the plot σ_1 vs. σ_3 we got:

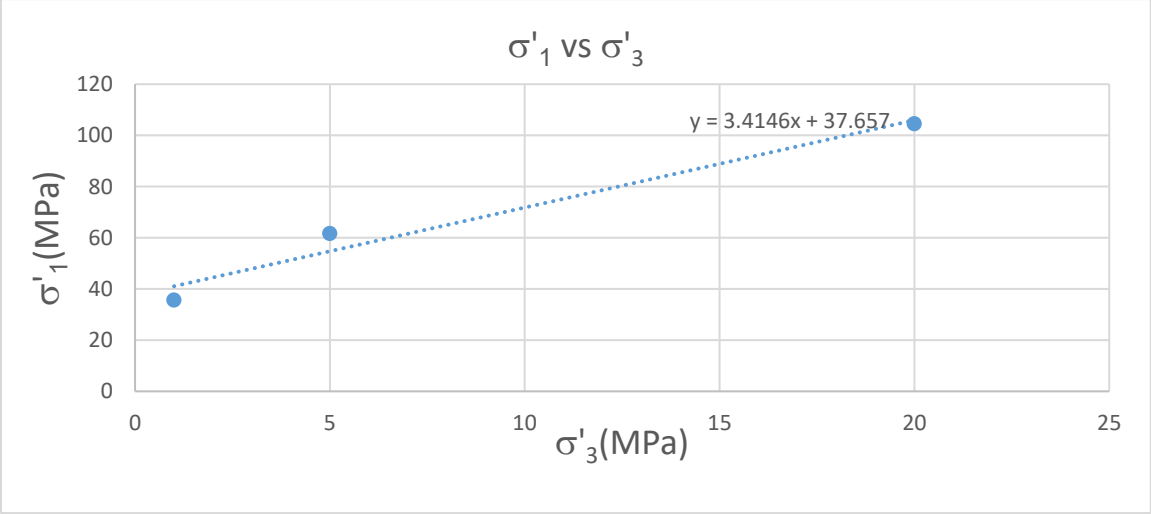

Figure 16 σ'1 vs σ'3, first author, second fitting comparaison, mohr coulomb

The equation of the line is: y = 3.4146x + 37.657, so co=37.657 and Nϕ=3.4146MPa

Now we calculate the values of σ'_{1s} for different values of σ'_3 (1, 5,20MPa) and using the following formula:

$$\sigma'_{1s} = 37.657 + 3.4146\ \sigma'_3$$

We obtain respectively: σ'_{1s}= 41.0716, 54.73, and 105.95 MPa.

They are in agreement with the experimental data.

Doing the same procedure with the same author and same criterion but with different values of theta we obtain the following values of Nϕ and co corrected:

Theta(degree)	Nϕ	Co (MPa)
90	3.4146	37.657
60	3.4239	16.913
45	2.9707	22.494
30	2.0031	27,482
0	2.9276	42.108

Table 3 Co and Nϕ values for different theta, with correction, Mohr Coulomb

Neglecting the fitting between the experimental data and Hoek and brown, we will have the following values of Nϕ and co:

Theta(degree)	Nϕ	Co (MPa)
90	2.4355	44.76
60	2.21	25.428
45	2.071	28.055
30	2.0031	27,482
0	2.24	47.096

Table 4 Co and Nϕ values for different theta, without correction, Mohr Coulomb

1.11 Second author

1.11.1 Hoek and Brown

For θ=0°:

From the experimental data, we have:

σ_3 (MPa)	σ_1 (MPa)
-4.64	0.00
0	28.13
4	40.38
10	49.01

We plot $(\sigma 1- \sigma 3)^2$ vs. σ3 in order to get m and co:

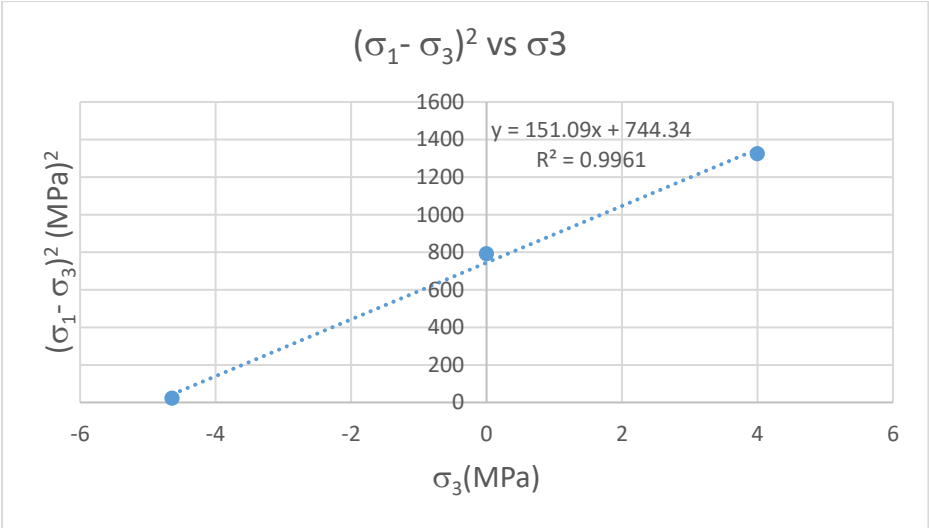

Figure 17 $(\sigma 1-\sigma 3)^2$ vs. σ3, theta=0°, first fitting, second author

From the equation of the line: y = 151.09x + 744.34 we can find $m_{\beta w}$ and $C_{o\beta w}$

From equation 1 and 2, we have:

$m_{\beta w}C_{o\beta w}$=a =151.09 and b= $C_{o\beta w}^2$=744.34

$C_{o\beta w}$=27.286and $m_{\beta w}=\frac{a}{Co\beta w}=\frac{151.09}{27.286}$=5.537963MPa

Finally, we can calculate T_0

$T_0= -\frac{C0}{2}((m^2+4)^{0.5}-m) = -\frac{27.286}{2}((5.537963)^2+4)^{0.5}-5.537963) =$- 4.77553MPa

We use the formula of H-B in order to calculate σ1:

$$\sigma_1' = \sigma_3' + \left(mC_o\sigma_3' + sC_o^2\right)^{0,5}$$

We will have:

σ_3(MPa)	σ_1(MPa)
-4.775526797	-3.19744E-14
-4.225526797	6.06549629
-3.675526797	10.07236963
-3.125526797	13.3700531
-2.575526797	16.27132058
-2.025526797	18.91016417
-1.475526797	21.35871626

-0.925526797	23.66109876
-0.375526797	25.84663284
0.174473203	27.93597814
0.724473203	29.94434069
1.274473203	31.88329801
1.824473203	33.76190667
4	40.72465112
10	57.48936723

Now we plot $\sigma 1$ vs. $\sigma 3$ with $m_c=m_t=5.5MPa$ in order to see If Hoek and brown criterion fit the experimental data:

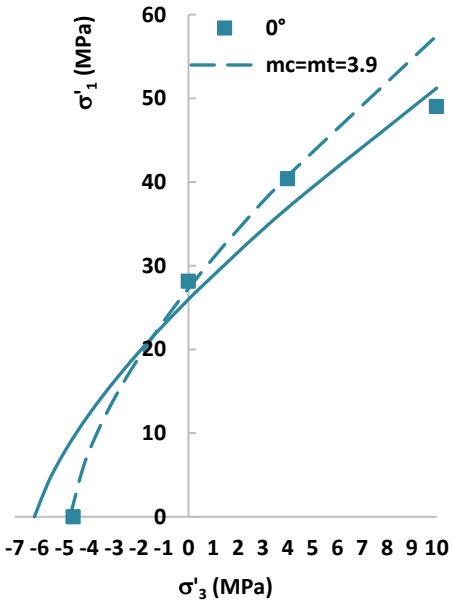

Figure 18 σ'1 vs σ'3, second author, first fitting, θ=0

We don't see a good fitting between the experimental data and Hoek and brown criterion for mc=mt=5.5MPa in both compression and tension zone so we have to do some correction.

We plot $(\sigma_1 - \sigma_3)^2$ vs. σ_3 in order to get m and co with another line.

So now we can plot $(\sigma_1 - \sigma_3)^2$ vs. σ_3:

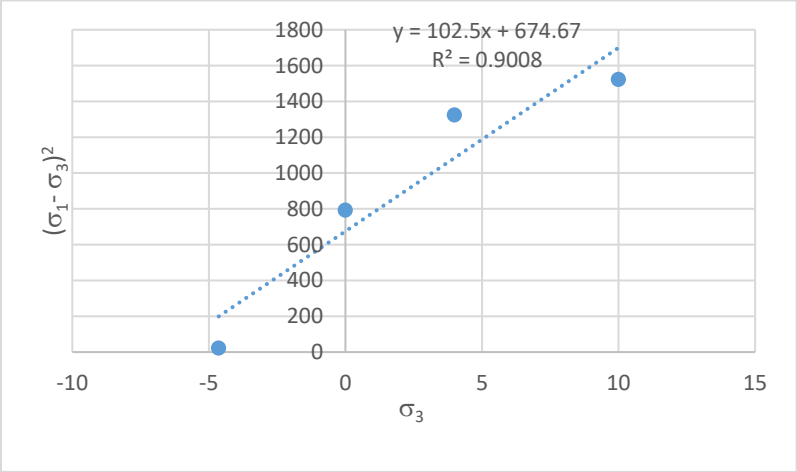

Figure 19 $(\sigma 1-\sigma 3)^2$ vs. σ3, theta=0°, second fitting, second author

From the equation of the line: y = 102.5x + 674.67 we can find $m_{\beta w}$ and $C_{o\beta w}$

From equation 1 and 2, we have:

$m_{\beta w}C_{o\beta w}$=a =102.5 and b= $C_{o\beta w}^2$=674.47

$C_{o\beta w}$=25.97441048MPa and $m_{\beta w}=\frac{a}{Co\beta w}=\frac{102.5}{25.97441048}$=3.946191582MPa

Finally, we can calculate T_0

$T_0 = -\frac{C0}{2}((m^2+4)^{0.5}-m) = -\frac{25.97441048}{2}((3.946191582)^2+4)^{0.5}-3.946191582) =$- 6.20635MPa

We use the formula of H-B in order to calculate σ1:

$$\sigma_1' = \sigma_3' + \left(mC_o\sigma_3' + sC_o^2\right)^{0,5}$$

σ3(MPa)	σ1(MPa)
-6.206352999	3.4639E-14
-5.656352999	4.084992778
-5.106352999	7.192785895
-4.556352999	9.853498407
-4.006352999	12.24230287
-3.456352999	14.44319497
-2.906352999	16.50418068
-2.356352999	18.45575448
-1.806352999	20.31871915
-1.256352999	22.10801769
-0.706352999	23.83481277
-0.156352999	25.50770392
0.393647001	27.13348278
4	36.93432859
10	51.22705422

Now we plot σ1 vs. σ3 with $m_c=m_t$=3.9MPa in order to see If Hoek and brown criterion fit the experimental data:
We obtain the dotted line:

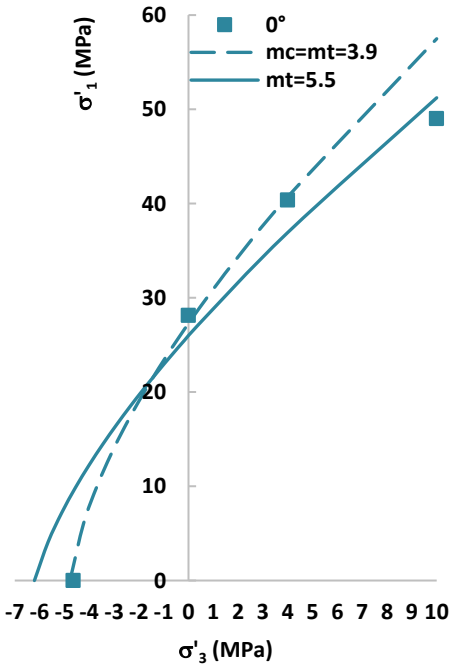

Figure 20 σ'1 vs σ'3, theta=0°, second fitting, second author

So we can see, that for $m_c=m_t=3.9$MPa, Hoek and brown criterion fit the data in the tension zone but not for the compression zone, so we have to change the value of $m_c=3.9$MPa.

We try another trend of line for only the compression zone, we will have:

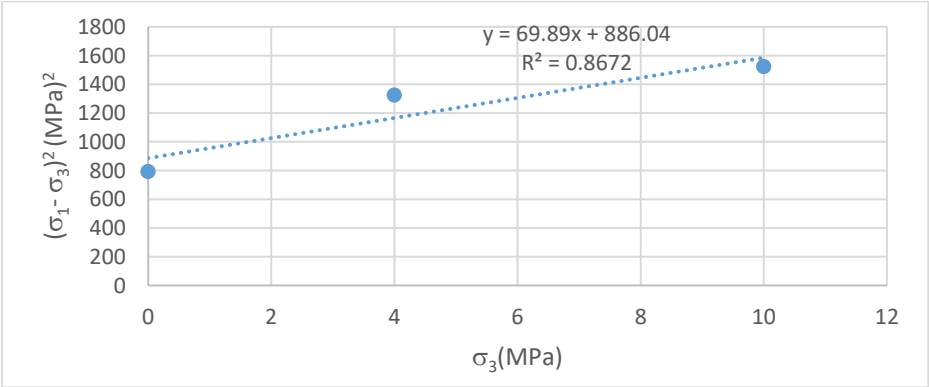

Figure 21 $(\sigma 1-\sigma 3)^2$ vs. σ3, theta=0°, third fitting, second author

From the equation of the line: y = 68.89x + 886.04 we can find $m_{\beta w}$ and $C_{o\beta w}$

From equation 1 and 2, we have:

$m_{\beta w}C_{o\beta w}$=a =69.89 and b= $C_{o\beta w}^2$=886.04

$C_{o\beta w}$=29.42855756MPa and $m_{\beta w}=\frac{a}{Co\beta w}=\frac{68.89}{29.42855756}$=2.374904032MPa

Finally, we can calculate T_0 which is equal to -10.7408077MPa

We use the formula of H-B in order to calculate σ1:

$$\sigma_1' = \sigma_3' + \left(mC_o\sigma_3' + sC_o^2\right)^{0,5}$$

σ_3(MPa)	σ_1(MPa)
-10.7408077	0
-10.1908077	2.210984511
-9.640807698	4.224398756
-9.090807698	6.097459155
-8.540807698	7.864159538
-7.990807698	9.546650784
-7.440807698	11.16031996
-6.890807698	12.71637083
-6.340807698	14.2232617
-5.790807698	15.68756398
-5.240807698	17.11450375
-4.690807698	18.50831836
-4.140807698	19.87250007
0	29.42855756
4	37.84671328
10	49.55932254

Now we plot σ1 vs. σ3 with m_t=3.9MPa and m_c=2.374MPa in order to see If Hoek and brown criterion fit the experimental data:

We obtain:

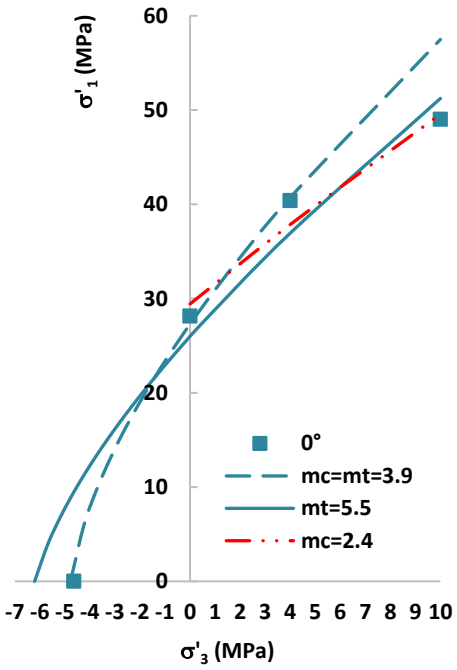

Figure 22 σ'1 vs σ'3, second author, best fitting, θ=0

As it is shown, this graph with trend in red in compression zone, is the best fit for theta=0°.

Doing the same procedure with the same author and same criterion but with different values of theta we obtain the following values of m and co corrected:

Theta(degree)	m	Co (MPa)
90	7.16	29.6
60	8.88	13.79
45	4.39	17.399
30	4.6	20.026
0	2.374	29.428

Table 5 m and co values for different theta, Hoek and Brown, second author

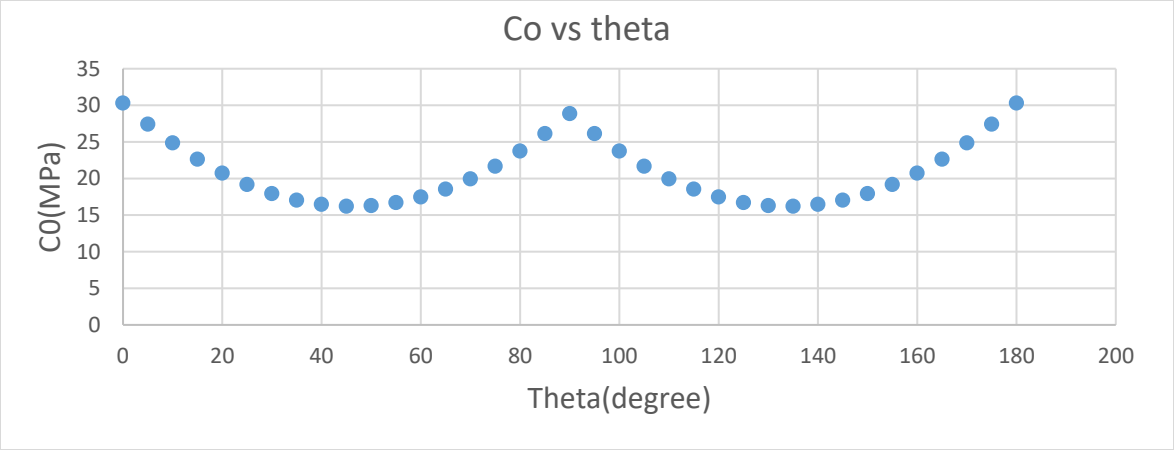

Figure 23 Co vs. theta, δ=0, Abdi

Co has the highest value at θ=0 and θ=90 in the range [0-90°], while it has the lowest value around 45. For δ=0°, theta has the highest value around beta=90 or 0 and the lowest around theta=30 or 45°. From this analysis, we can understand the trend of the plot, which start with the highest value, then start to decrease till beta=45°, increase again to reach a peak at 90°, then decrease till theta= 135°, finally increase se again to a maximum at theta=180°.

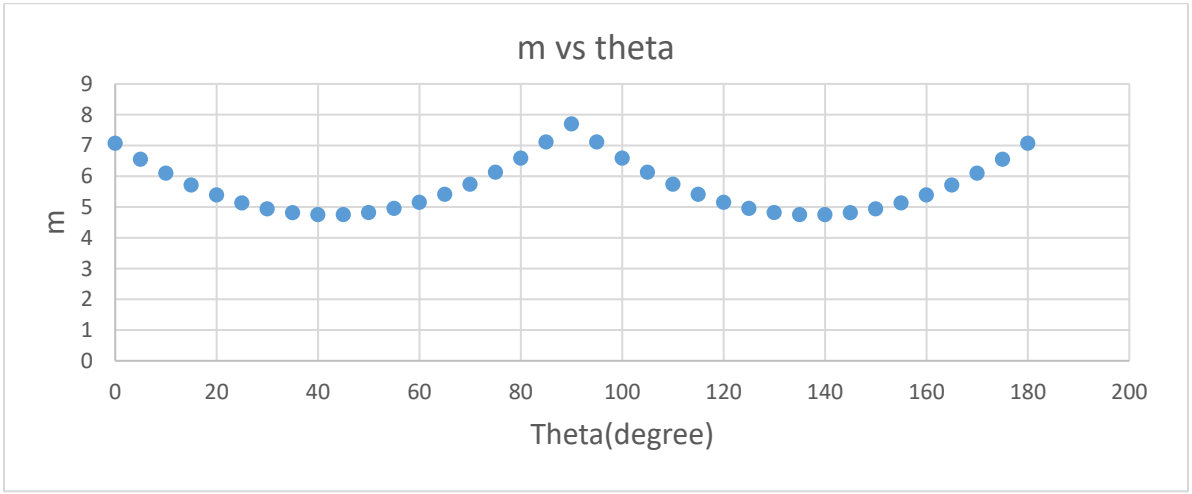

Figure 24 m vs. theta, δ=0, Abdi

m has the highest value at θ=0 and θ=90 in the range [0-90°], while it has the lowest value around 45. For δ=0°, theta has the highest value around beta=90 or 0 and the lowest around theta=30 or 45°. From this analysis, we can understand the trend of the plot, which start with the highest value, then start to decrease till beta=45°, increase again to reach a peak at 90°, then decrease till theta= 135°, finally increase se again to a maximum at beta=180°.

1.11.2 Mohr Coulomb

For θ=0°:

It's time to match Jaeger's linear regression (Mohr coulomb criterion) with the experimental data:

Mohr Coulomb Criterion equation:

$$\sigma'_{1s}=C0+\sigma'_3 N_\phi$$

Co is b and N_ϕ is the slope a of the linear equation of line y=ax+b of the plot σ'_1 vs. σ'_3

σ_3(MPa)	σ_1(MPa)
0	28.13
4	40.38
10	49.01

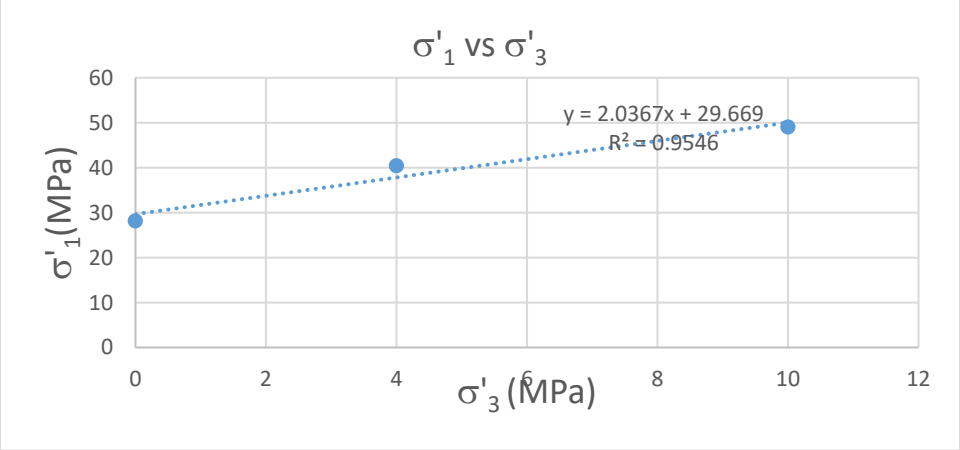

Figure 25 σ'1 vs σ'3, second author, first fitting, θ=0

From the equation of the line: y = 2.0367x + 29.669 we found C0=29.669MPa and Nϕ=2.0367.

Now Calculating σ'_{1s} for different values of σ'_3 (0, 4 and 10MPa) we will have the following values of σ'_{1s}:

σ_3(MPa)	σ_1(MPa)
0	29.669
4	37.82
10	50.03

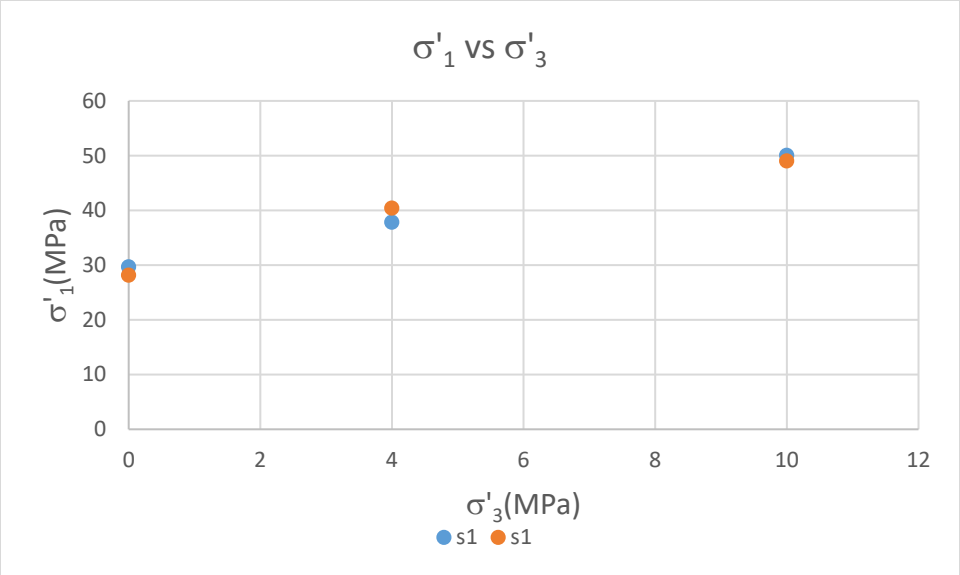

Figure 26 σ'1 vs σ'3, second author, second fitting, θ=0

We have a very good fitting between the experimental data and Mohr coulomb data

Doing the same procedure with the same author and same criterion but with different values of theta we obtain the following values of Nϕ and co corrected:

Theta(degree)	Nϕ	Co (MPa)
90	3.4142	30.934
60	3.2689	15.392
45	2.5888	17.246
30	2.5891	20.948
0	2.0367	29.669

Table 6 Co and Nϕ values for different theta, second author, Mohr Coulomb

Chapter 2: Mud pressure calculation

A. Mud pressure using Hoek and Brown modified

2.1 Procedure

My aim in the following calculations is to calculate the mud pressure using Hoek and Brown. After coupling kirsh solution with Hoek and Brown, we obtain the following formula:

$$PH\&B = \frac{4S + m\beta w\, co\beta w - [(4S + m\beta w\, co\beta w)2 - 16(S2 + m\beta w\, co\beta wPf - co\beta w2)]0.5}{8}$$

In order to study the variation of $P_{H\&B}$ with theta we will proceed the following steps:

1. We start by studying the variation of Co and m with beta using the relationships between δ, βw and ϑ:

$$\beta_w = |\vartheta - \delta| \; 0^\circ \leq \vartheta \leq \delta + 90^\circ$$

$$\beta_w = 180^\circ - |\vartheta - \delta| \; \delta + 90^\circ \leq \vartheta \leq 180^\circ$$

a) For δ=0,45,90° we have different values of βw, so different values of m and co, consequently, different values of $P_{H\&B}$

b) After calculating β_w, we start in the calculation of m and co for all the range of βw using the previous values of m and co found from the fitting of the experimental data with Hoek and Brown. Since we have the value of m and co for some values of θ, we can plot co and m vs. βw for each δ. We obtain a plot with an equation of a parabola, and we use it by substituting x by βw to obtain m and co along all the interval.

2. Finally, we calculate the state of stress using the following formula:

$$S = [\sigma max + \sigma min - 2(\sigma max - \sigma min)\, cos\,(2\theta)]$$

All this procedure is done for both author Niandou and Abdi, for different values of σ_{max} (36, 23 and 20MPa) with a constant σ_{min}=20MPa and pf=8MPa, with the values of m and co corrected after fitting the experimental data and removing some increment and without the fitting. However, the correction for the second author is not done since we have only three values of increments, so no room for any correction.

2.2 For the first author (Niandou)

With and without correction comparison

We start with a detailed calculation as an example with the first author without correcting the data, and after that we put directly in each plot for the same author and same δ with and without correction in order to do the comparison.

2.2.1For σ_{max} =36MPa, σ_{min}=20MPa, k=1.8

For δ=0°:

Using equation (19) and (20), we obtain:

We can find βw for δ=0◦ and for different values of ϑ.

From the values of Co already found for different theta, we can plot Co vs. beta:

Beta(degree)	C0(MPa)
0	44.857
30	26.55
45	26.374
60	24.668
90	43.123

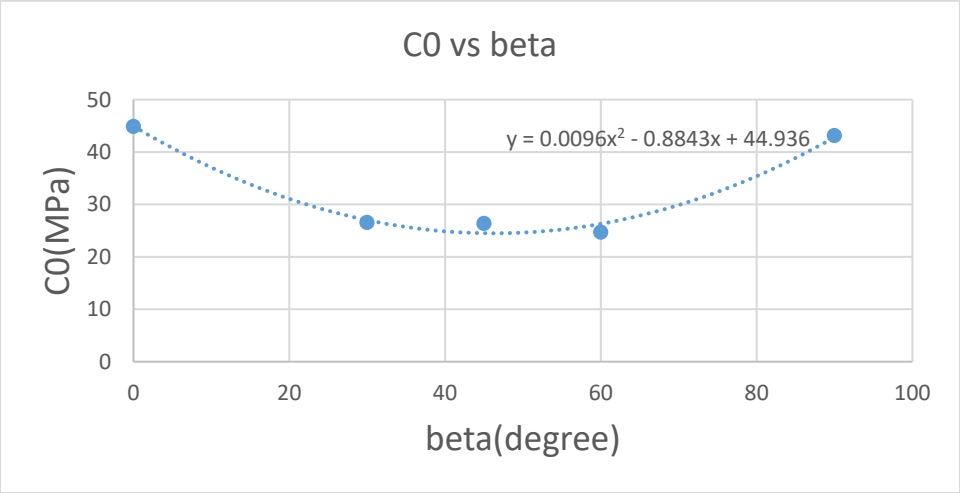

Figure 27 Co vs beta, δ=0, Niandou without correction

Using the equation of parabola from the plot, I can calculate all the possible values of c0

From the values of m already found for different theta, we can plot m vs. beta to calculate co for all the possible values of beta:

theta(degree)	Beta(degree)	m
0	0	4.1645
30	30	3.58984
45	45	4.182
60	60	4.9734

90	90	5.054

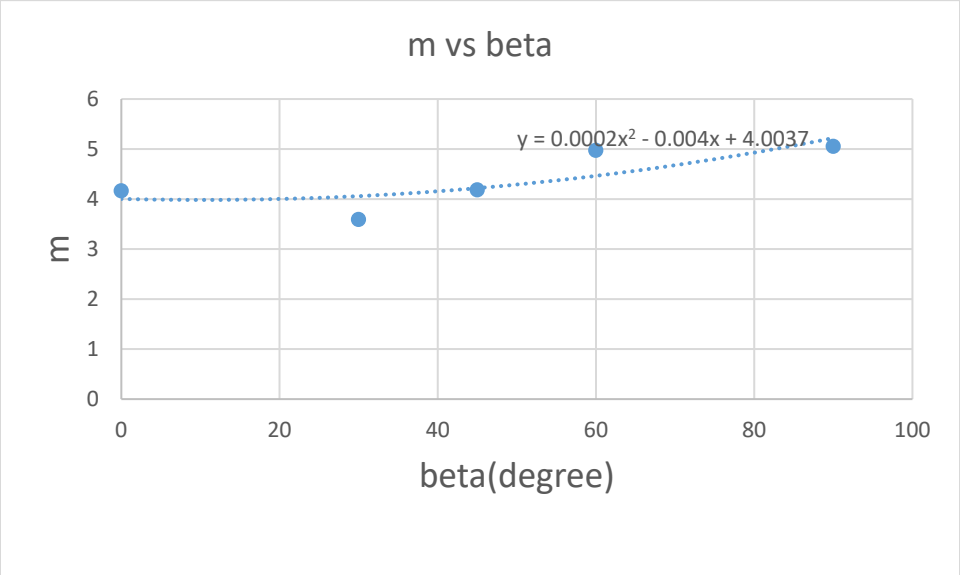

Figure 28 m vs beta, δ=0, Niandou without correction

Using the equation of parabola from the plot, I can calculate all the possible values of m along all the interval:

Now we calculate the state of stress S using equation (18)

For σ_{max} =36MPa and σ_{min} =20MPa, we calculate Pw H&B using the formula (33)

Theta(degree)	Beta(degree)	Co(MPa)	m	mc0(MPa)	S(MPa)	$P_{wH\&B}$ WITHOUT CORRECTION
0	90	44.936	4.0037	179.9103	24	-0.01436
5	85	40.7545	3.9887	162.5575	24.48615	0.931165
10	80	37.053	3.9837	147.608	25.92984	1.972991
15	75	33.8315	3.9887	134.9437	28.28719	3.120149
20	70	31.09	4.0037	124.475	31.48658	4.382363
25	65	28.8285	4.0287	116.1414	35.4308	5.76378

30	60	27.047	4.0637	109.9109	40	7.255394
35	55	25.7455	4.1087	105.7805	45.05536	8.829428
40	50	24.924	4.1637	103.7761	50.44326	10.43805
45	45	24.5825	4.2287	103.952	56	12.01679
50	40	24.721	4.3037	106.3918	61.55674	13.49136
55	35	25.3395	4.3887	111.2075	66.94464	14.78589
60	30	26.438	4.4837	118.5401	72	15.83064
65	25	28.0165	4.5887	128.5593	76.5692	16.56808
70	20	30.075	4.7037	141.4638	80.51342	16.95672
75	15	32.6135	4.8287	157.4808	83.71281	16.97306
80	10	35.632	4.9637	176.8666	86.07016	16.61175
85	5	39.1305	5.1087	199.906	87.51385	15.88482
90	0	43.109	5.2637	226.9128	88	14.81991
95	5	39.1305	5.1087	199.906	87.51385	15.88482
100	10	35.632	4.9637	176.8666	86.07016	16.61175
105	15	32.6135	4.8287	157.4808	83.71281	16.97306
110	20	30.075	4.7037	141.4638	80.51342	16.95672
115	25	28.0165	4.5887	128.5593	76.5692	16.56808
120	30	26.438	4.4837	118.5401	72	15.83064
125	35	25.3395	4.3887	111.2075	66.94464	14.78589
130	40	24.721	4.3037	106.3918	61.55674	13.49136
135	45	24.5825	4.2287	103.952	56	12.01679
140	50	24.924	4.1637	103.7761	50.44326	10.43805
145	55	25.7455	4.1087	105.7805	45.05536	8.829428
150	60	27.047	4.0637	109.9109	40	7.255394
155	65	28.8285	4.0287	116.1414	35.4308	5.76378
160	70	31.09	4.0037	124.475	31.48658	4.382363
165	75	33.8315	3.9887	134.9437	28.28719	3.120149
170	80	37.053	3.9837	147.608	25.92984	1.972991

175	85	40.7545	3.9887	162.5575	24.48615	0.931165
180	90	44.936	4.0037	179.9103	24	-0.01436
185	85	40.7545	3.9887	162.5575	24.48615	0.931165
190	80	37.053	3.9837	147.608	25.92984	1.972991
195	75	33.8315	3.9887	134.9437	28.28719	3.120149
200	70	31.09	4.0037	124.475	31.48658	4.382363
205	65	28.8285	4.0287	116.1414	35.4308	5.76378
210	60	27.047	4.0637	109.9109	40	7.255394
215	55	25.7455	4.1087	105.7805	45.05536	8.829428
220	50	24.924	4.1637	103.7761	50.44326	10.43805
225	45	24.5825	4.2287	103.952	56	12.01679
230	40	24.721	4.3037	106.3918	61.55674	13.49136
235	35	25.3395	4.3887	111.2075	66.94464	14.78589
240	30	26.438	4.4837	118.5401	72	15.83064
245	25	28.0165	4.5887	128.5593	76.5692	16.56808
250	20	30.075	4.7037	141.4638	80.51342	16.95672
255	15	32.6135	4.8287	157.4808	83.71281	16.97306
260	10	35.632	4.9637	176.8666	86.07016	16.61175
265	5	39.1305	5.1087	199.906	87.51385	15.88482
270	0	43.109	5.2637	226.9128	88	14.81991
275	5	39.1305	5.1087	199.906	87.51385	15.88482
280	10	35.632	4.9637	176.8666	86.07016	16.61175
285	15	32.6135	4.8287	157.4808	83.71281	16.97306
290	20	30.075	4.7037	141.4638	80.51342	16.95672
295	25	28.0165	4.5887	128.5593	76.5692	16.56808
300	30	26.438	4.4837	118.5401	72	15.83064
305	35	25.3395	4.3887	111.2075	66.94464	14.78589
310	40	24.721	4.3037	106.3918	61.55674	13.49136
315	45	24.5825	4.2287	103.952	56	12.01679

320	50	24.924	4.1637	103.7761	50.44326	10.43805
325	55	25.7455	4.1087	105.7805	45.05536	8.829428
330	60	27.047	4.0637	109.9109	40	7.255394
335	65	28.8285	4.0287	116.1414	35.4308	5.76378
340	70	31.09	4.0037	124.475	31.48658	4.382363
345	75	33.8315	3.9887	134.9437	28.28719	3.120149
350	80	37.053	3.9837	147.608	25.92984	1.972991
355	85	40.7545	3.9887	162.5575	24.48615	0.931165
360	90	44.936	4.0037	179.9103	24	-0.01436

Table 7 PwH&B without correction detailed calculation

Now we will plot $P_{wH\&B}$ vs. theta:

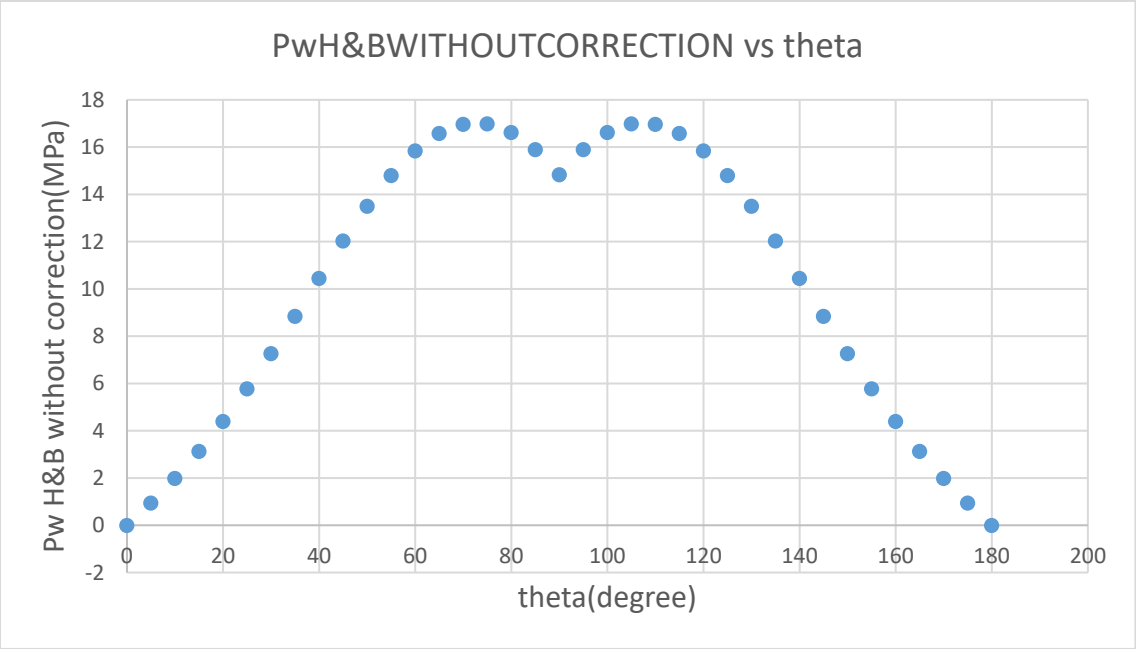

Figure 29 PwH&B vs theta without correction, δ=0, σ_{max} =36MPa

The mud pressure for θ =0 is 0 and then starts to increase significantly with the increase of θ to reach a peak of 17MPa at θ=70°. We have than a small decrease in mud pressure and it is followed by another peak at θ=110°. A significantly decrease in mud pressure is shown after θ=110° to reach 0MPa at θ=180°. The highest mud pressure is around 17MPa.The risk region is around the peak so around θ=70 and θ=110°, because the highest mud pressure exists, so the closer we are to the pressure to avoid the tensile fracturing and the narrower is the mud weight window.

With correction:

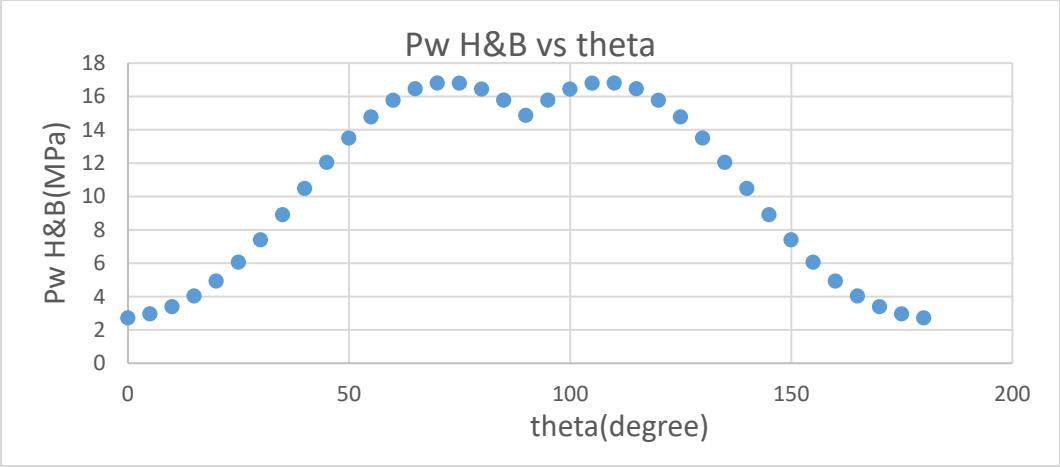

Figure 30 PwH&B vs theta with correction, δ=0, σ_{max} =36MPa

The mud pressure for θ =0 is 2.7MPa and then starts to increase significantly with the increase of θ to reach a peak of 16.7MPa at θ=70°. We have than a small decrease in mud pressure and it is followed by another peak at θ=110°. A significantly decrease in mud pressure is shown after θ=110° to reach 2.71MPa at θ=180°. The highest mud pressure is around 17MPa.The risk region is around the peak so around θ=70 and θ=110°, because the highest mud pressure exists, so the closer we are to the pressure to avoid the tensile fracturing and the narrower is the mud weight window.

For δ=45°:

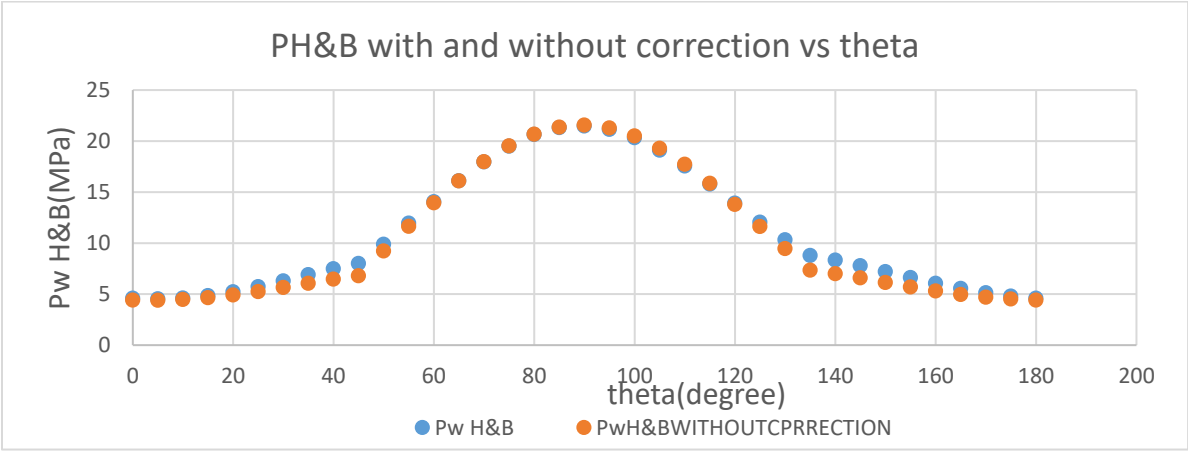

Figure 31 PwH&B vs theta, δ=45, σ_{max} =36MPa

The mud pressure for Hoek and Brown modified with the corrected values of m and Co for θ =0 is 4.5MPa, and then it started to increase significantly with the increase of θ to reach a peak of 21.5MPa at θ=90°. A significantly decrease in mud pressure is shown after that peak to reach 4.5MPa at θ=180°. The highest mud pressure is around 21.5MPa. Both trend of pressure agrees in general for this degree of anisotropy and for this inclination angle. The risk region is around the peak so around θ=90°, because the highest mud pressure exists, so the closer we are to the pressure to avoid the tensile fracturing and the narrower is the mud weight window.

At theta=0, the mud pressure is relatively low. This is because the rock mass is weakest in these directions, because the applied stress aligns with the preferred orientation of strength. The mud pressure increase with

theta, because the stress applied to the shale is moving away from the preferred orientation of strength. The mud pressure after theta=90° starts to decrease because the stress applied to the shale is approaching again to a direction which is parallel to the preferred orientation of strength.

Both trend of mud pressure agrees in general for this case.

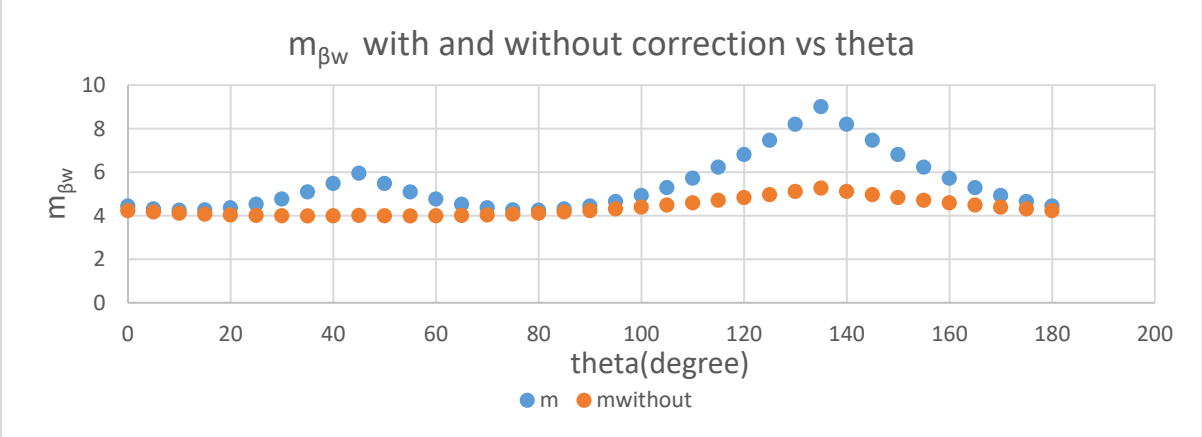

Figure 32 $m_{\beta w}$ vs. theta, δ=45, Niandou

The plot starts with a low value, then start to increase till theta=45°, decrease again to a minimum at 90°, and increase to reach a peak at theta= 135°and finally decrease again to a minimum at theta=180°.

m vs. theta shows different trend in two cases: The first one with bleu trend in which the value of m is corrected, and the second one in orange in which the value of m is not corrected. The second case show a very small variation of m with theta because m is not corrected, and after each correction, the value of m normally increases and the range of m increase.

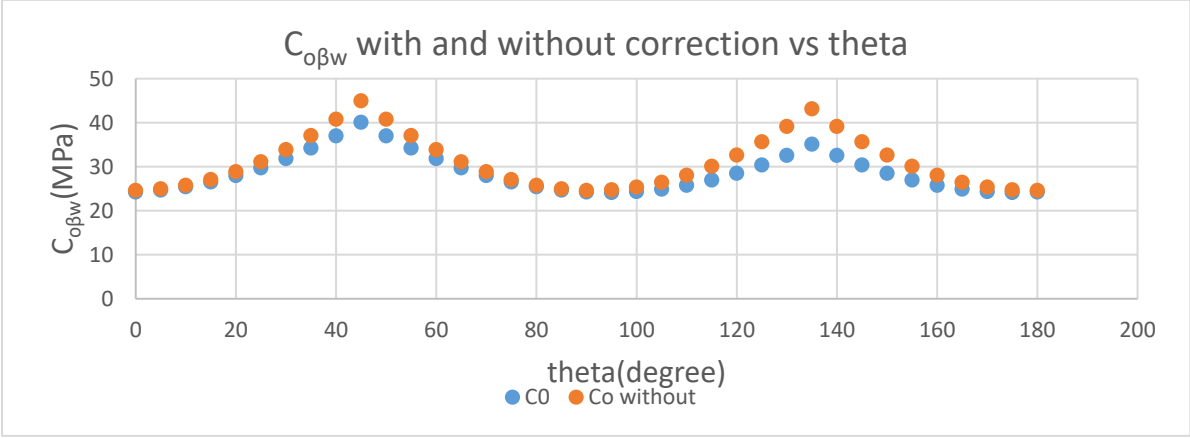

Figure 33 $C_{o\beta w}$ vs. theta, δ=45, Niandou

The two plots start with a low value, then start to increase until theta=45°, decrease to a minimum at 90°, and increase to reach a peak at theta= 135° and finally decrease again to a minimum at theta=180°.

Co show very close trend in both cases, with and without correction in this case.

For δ=90°:

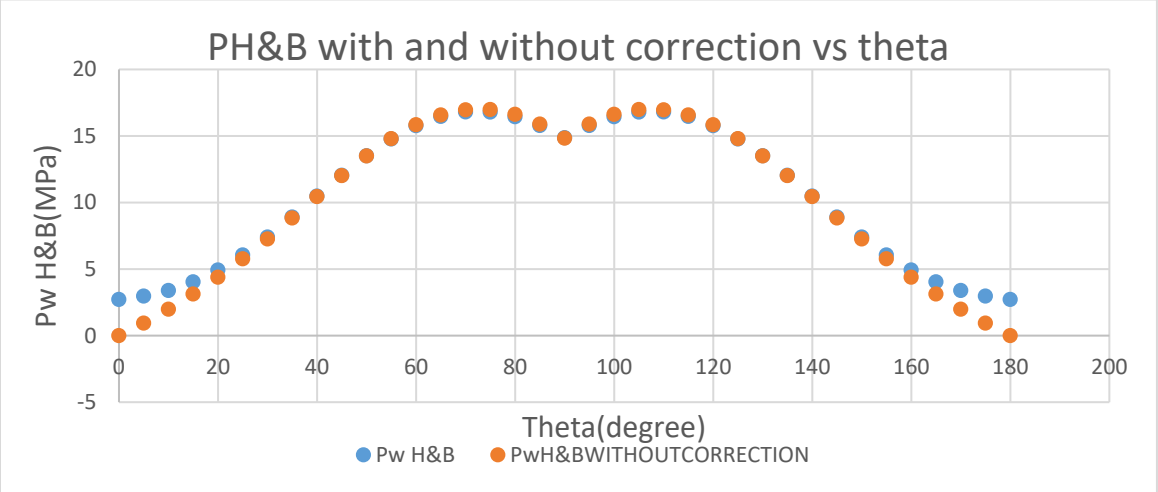

Figure 34 PwH&B vs theta, δ=90, σ_{max} =36MPa

The mud pressure for Hoek and Brown modified with the corrected values of m and Co is 5MPa at θ =0, and then starts to increase significantly with the increase of θ to reach a peak of 17.3MPa at θ=70°. We have than a small decrease in mud pressure and it is followed by another peak at θ=110°. A significantly decrease in mud pressure is shown after θ=110° to reach 5MPa at θ=180°. The highest mud pressure is around 17.3 MPa. The risk region is around the peak so around θ=70 and θ=110°, because the highest mud pressure exists, so the closer we are to the pressure to avoid the tensile fracturing and the narrower is the mud weight window.

For δ=90°, at theta=0, the mud pressure is relatively low. The rock is weak in these directions, because the applied stress aligns with the preferred orientation of strength. The mud pressure increase with theta, because the stress applied to the shale is moving away from the preferred orientation of strength to reach a peak at theta=45° and at 135°. The mud pressure is decreasing again after the second peak because the stress applied to the shale is approaching again to a direction which is parallel to the preferred orientation of strength.

The highest mud pressure is decreasing with the decrease of the degree of anisotropy.

The two plots of pressure match for a wide range of inclination angle theta, but shows different trend at the beginning and at the end of the plot.

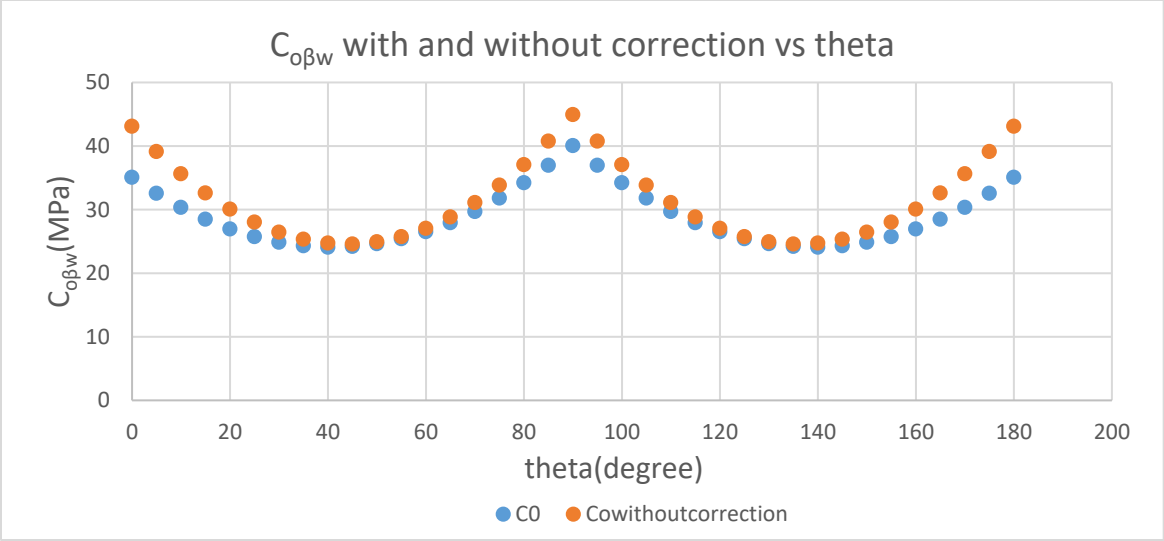

Figure 35 $C_{o\beta w}$ vs. theta, δ=90, Niandou

The two plots start with the highest value, then start to decrease until theta=45°, increase to a maximum at 90°, decrease to reach a minimum at beta= 135° and finally increase again to a maximum at beta=180°.

Co show very close trend in both cases, with and without correction in this case.

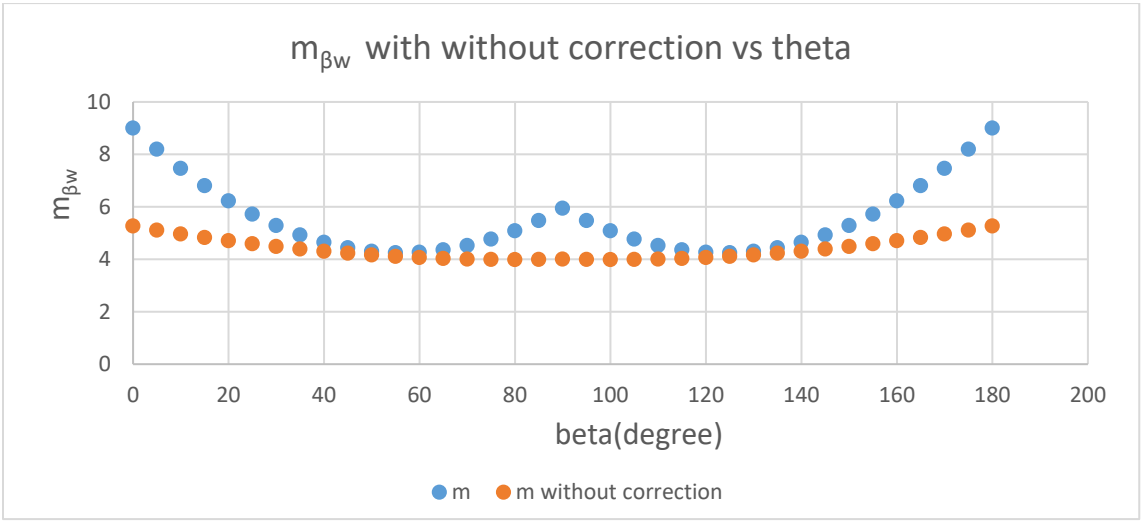

Figure 36 $m_{\beta w}$ vs. theta, δ=90, Niandou

The two plots start with a maximum value, then start to decrease till beta=45°, increase to a maximum at 90°, decrease to reach a minimum at beta= 135° and finally increase again to a maximum at beta=180°.

m vs. beta shows different trend in two cases: The first one with bleu trend in which the value of m is corrected, and the second one in orange in which the value of m is not corrected. The second case show a very small variation of m with beta because m is not corrected, and after each correction, the value of m normally increases and the range of m increase.

2.2.2 For σ_{max} =23MPa, σ_{min}=20MPa, k=1.15

For δ=90°:

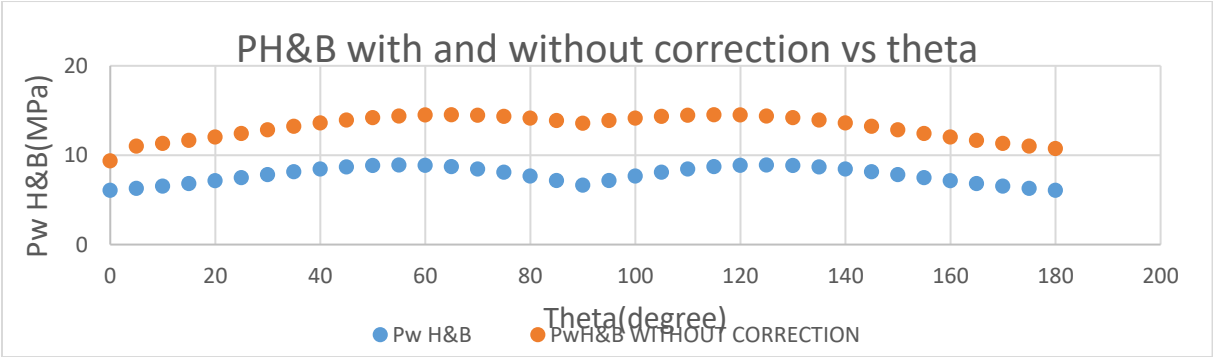

Figure 37 PwH&B vs theta, δ=90, σ_{max} =23MPa

The mud pressure for Hoek and Brown modified with the corrected values of m and Co for θ =0 is 6MPa, and then starts to increase significantly with the increase of θ to reach a peak of 8.9MPa at θ=60°. We have than a small decrease in mud pressure and it is followed by another peak at θ=120°. A significantly decrease in mud pressure is shown after θ=120°. The highest mud pressure is around 9MPa.The risk region is around the peak so around θ=60 and θ=120°, because the highest mud pressure exists, so the closer we are to the pressure to avoid the tensile fracturing and the narrower is the mud weight window.

For δ=90°, at theta=0, the mud pressure is relatively low. The rock is weak in these directions, because the applied stress aligns with the preferred orientation of strength. The mud pressure increase with theta, because the stress applied to the shale is moving away from the preferred orientation of strength to reach a peak at theta=45° and at 135°. The mud pressure is decreasing again after the second peak because the stress applied to the shale is approaching again to a direction which is parallel to the preferred orientation of strength.

The highest mud pressure is decreasing with the decrease of the degree of anisotropy.

There is no matching at all between the two trends of mud pressure, with and without correction of the m and Co for δ=90° and k=1.15, and the mud pressure without correcting the data has higher trend comparing to the other mud pressure.

For δ=45°:

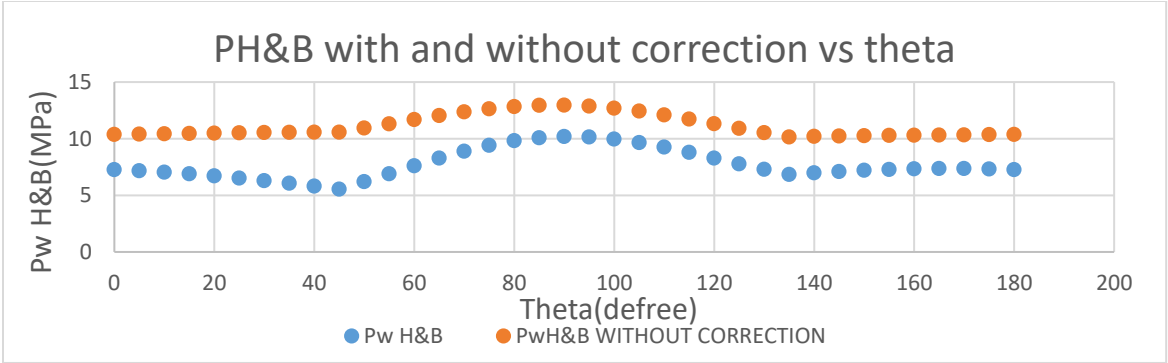

Figure 38 PwH&B vs theta, δ=45, σ_{max} =23MPa

We have a decrease in mud pressure from 7.25 to 5.5MPa in the range θ=0 to θ=45°. Then, the mud pressure increase to peak at=90° for P=10MPa and decrease again to reach 6.8MPsat θ=140°. A small increase in mud pressure is showed again for higher values of θ. The risk region is around the peak so around θ=90°, because the highest mud pressure exists, so the closer we are to the pressure to avoid the tensile fracturing and the narrower is the mud weight window.

The mud pressure increase with theta, because the stress applied to the shale is moving away from the preferred orientation of strength. The mud pressure after theta=90° starts to decrease because the stress applied to the shale is approaching again to a direction which is parallel to the preferred orientation of strength. The peak of mud pressure decrease, the margin between the mud pressures for different angle theta decrease, we can deduce that with decrease the degree of anisotropy, the mud pressure decrease.

There is no matching at all between the two trends of mud pressure, with and without correction of the m and Co for δ=45° and k=1.15 and the mud pressure without correcting the data has higher trend comparing to the other mud pressure.

For δ=0°:

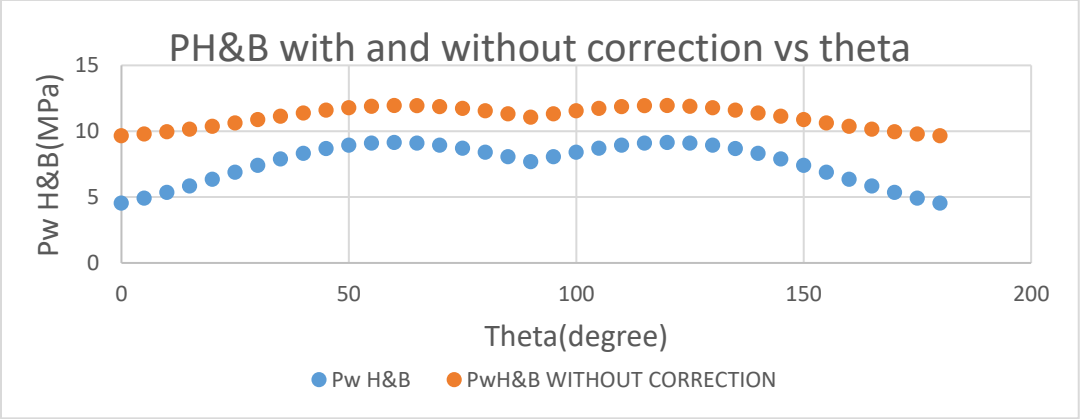

Figure 39 PwH&B vs theta, δ=0, σ_{max} =23MPa

The mud pressure for θ =0 is 4.5MPaand then starts to increase significantly with the increase of θ to reach a peak of 9.2MPa at θ=60°. We have than a small decrease in mud pressure and it is followed by another peak at θ=120°. A decrease in mud pressure is shown after θ=120° to reach 4.5MPa. The highest mud pressure is around 9.2MPa. The risk region is around the peak so around θ=60 and θ=120°, because the highest mud pressure exists, so the closer we are to the pressure to avoid the tensile fracturing and the narrower is the mud weight window.

For δ=0°, at theta=0, the mud pressure is relatively low. The rock is weak in these directions, because the applied stress aligns with the preferred orientation of strength. The mud pressure increase with theta, because the stress applied to the shale is moving away from the preferred orientation of strength to reach a peak at theta=65° and at 125°. The mud pressure is decreasing again after the second peak because the stress applied to the shale is approaching to a direction which is parallel to the preferred orientation of strength.

The highest mud pressure is decreasing with the decrease of the degree of anisotropy. There is no matching at all between the two trends of mud pressure, with and without correction of the m and Co for δ=0° and k=1.15 and the mud pressure without correcting the data has higher trend comparing to the other mud pressure.

2.2.3For σ_{max} =σ_{min}=20MPa, k=1

For δ=90°:

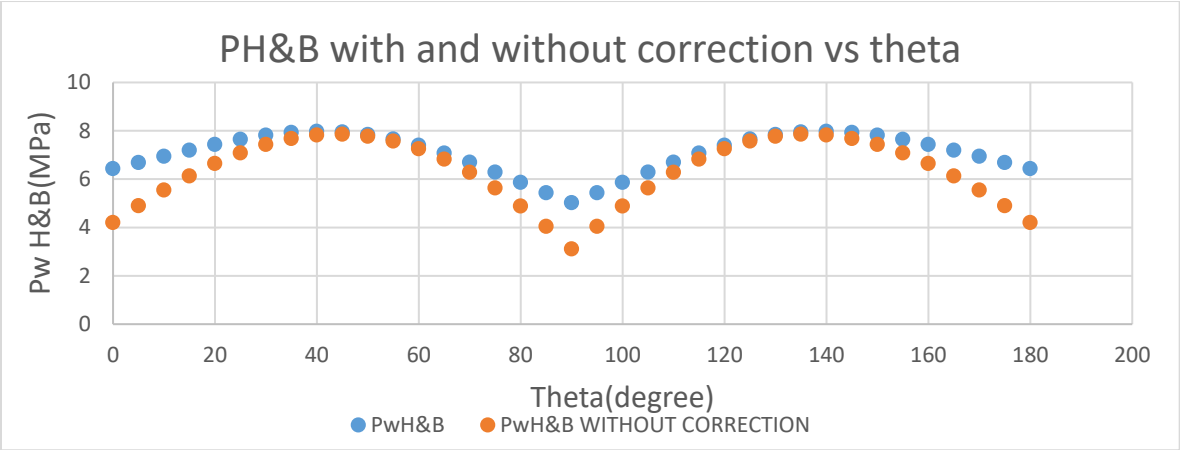

Figure 40 PwH&B vs theta, δ=90, σ_{max} =20MPa

The mud pressure for θ =0 is 6MPa and starts to increase significantly with the increase of θ to reach a peak of 8MP around θ=40°. We have than a small decrease in mud pressure and it is followed by another peak at θ=140°. A significantly decrease in mud pressure is shown after θ=140°. The highest mud pressure is around 8MPa.The risk region is around the peak so around θ=40 and θ=140°, because the highest mud pressure exists, so the closer we are to the pressure to avoid the tensile fracturing and the narrower is the mud weight window.

For δ=90°, at theta=0, the mud pressure is relatively low. The rock is weak in these directions, because the applied stress aligns with the preferred orientation of strength. The mud pressure increase with theta, because the stress applied to the shale is moving away from the preferred orientation of strength to reach a peak at theta=45° and at 135°. The mud pressure is decreasing again after the second peak because the stress applied to the shale is approaching again to a direction which is parallel to the preferred orientation of strength.

The highest mud pressure is decreasing with the decrease of the degree of anisotropy.

In general, the two trends of mud pressure don't match together, but they match for some ranges of theta.

For δ=45°:

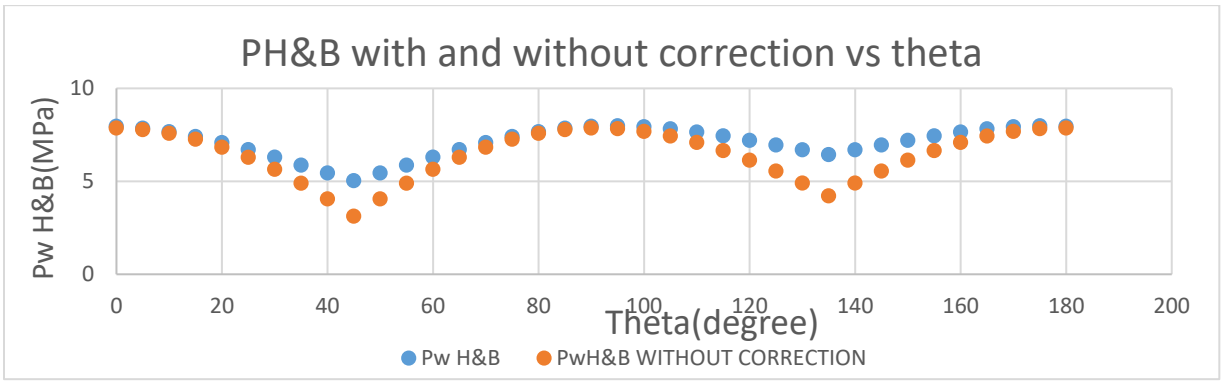

Figure 41 PwH&B vs theta, δ=45, σ_{max} =20MPa

We have a decrease in mud pressure between the range [θ=0-45°] from 8 to 5MPa. Then, the mud pressure increase to peak at=90° for P=8MPa and decrease again to reach 6.4MPa at θ=140°. A small increase in mud pressure is showed again for higher values of θ. The risk region is around the peak so around θ=90°, because the highest mud pressure exists, so the closer we are to the pressure to avoid the tensile fracturing and the narrower is the mud weight window.

The mud pressure increase with theta, because the stress applied to the shale is moving away from the preferred orientation of strength. The mud pressure after theta=90° starts to decrease because the stress applied to the shale is approaching again to a direction which is parallel to the preferred orientation of strength. The peak of mud pressure decrease, the margin between the mud pressures for different angle theta decrease, we can deduce that with decrease the degree of anisotropy, the mud pressure decrease.

In general, the two trends of mud pressure don't match together, but they match for some ranges of theta.

For δ=0°:

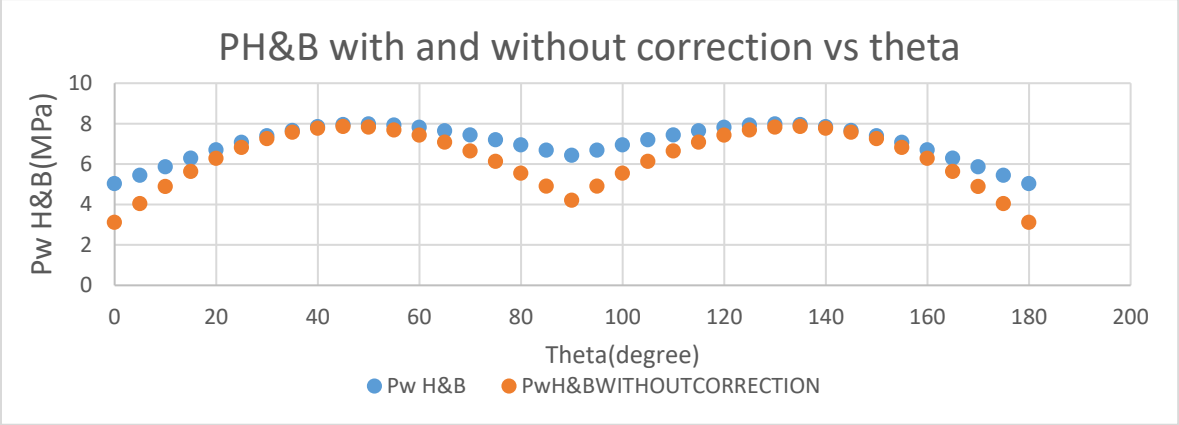

Figure 42 PwH&B vs theta, δ=0, σ_{max} =20MPa

The mud pressure for θ =0 is 5MPa and then starts to increase significantly with the increase of θ to reach a peak of 8MPa at θ=50°. We have than a small decrease in mud pressure and it is followed by another peak at θ=130°. A significantly decrease in mud pressure is shown after θ=130°. The highest mud pressure is around 8MPa.The risk region is around the peak so around θ=50 and θ=130°, because the highest mud pressure exists, so the closer we are to the pressure to avoid the tensile fracturing and the narrower is the mud weight window.

For δ=0°, at theta=0, the mud pressure is relatively low. The rock is weak in these directions, because the applied stress aligns with the preferred orientation of strength. The mud pressure increase with theta, because the stress applied to the shale is moving away from the preferred orientation of strength to reach a peak at theta=60° and at 120°. The mud pressure is decreasing again after the second peak because the stress applied to the shale is approaching to a direction which is parallel to the preferred orientation of strength.

The highest mud pressure is decreasing with the decrease of the degree of anisotropy.

In general, the two trends of mud pressure don't match together, but they match for some ranges of theta.

2.3 For the Second author (Abdi)

2.3.1For σ_{max} =36MPa, σ_{min}=20MPa, k=1.8

For δ=90°:

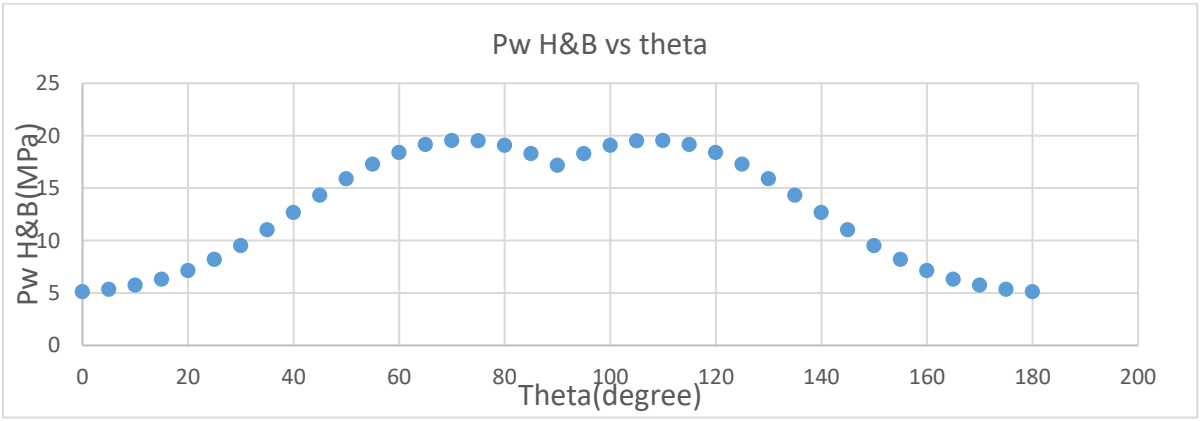

Figure 43 PwH&B vs theta second author, δ=90, σ_{max} =36MPa

The mud pressure for θ =0 starts at 5.15MPa, and starts to increase with the increase of θ to reach a peak around θ=60°. We have than a small decrease in mud pressure and it is followed by another peak at θ=110°. A decrease in mud pressure is shown after θ=110°. The highest mud pressure is around 20MPa.The risk region is around the peak so around θ=70 and θ=110°, because the highest mud pressure exists, so the closer we are to the pressure to avoid the tensile fracturing and the narrower is the mud weight window.

For δ=90°, at theta=0, the mud pressure is relatively low. The rock is weak in these directions, because the applied stress aligns with the preferred orientation of strength. The mud pressure increase with theta, because the stress applied to the shale is moving away from the preferred orientation of strength to reach a peak at theta=45° and at 135°. The mud pressure is decreasing again after the second peak because the stress applied to the shale is approaching again to a direction which is parallel to the preferred orientation of strength.

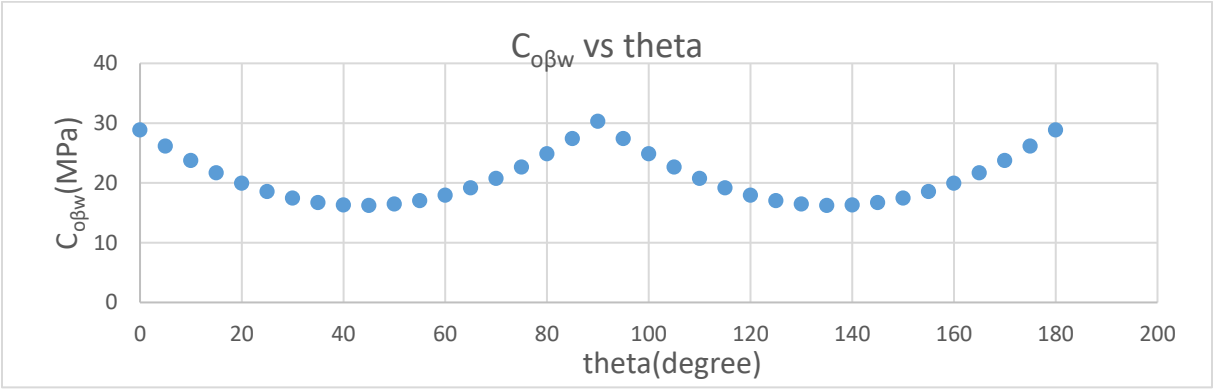

Figure 44 $C_{o\beta w}$ vs. theta, δ=90, Abdi

$C_{o\beta w}$ starts with the highest value at theta=0°, then decrease till beta=45°, increase to a maximum at beta= 90°, decrease to reach a minimum at beta= 135°, and finally increase again to a maximum at beta=180°.

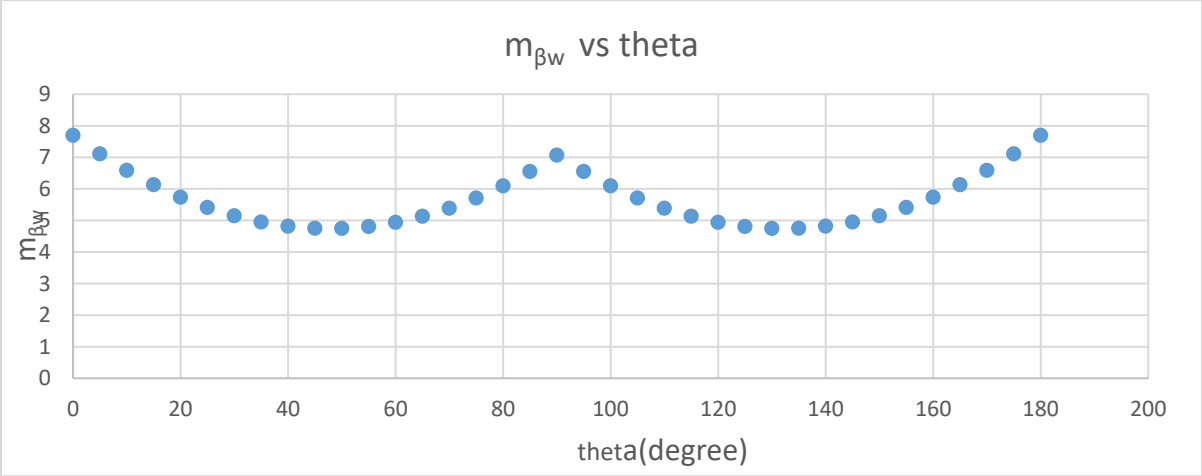

$m_{\beta w}$ starts with a maximum value at theta=0, then starts to decrease till beta=45°, increase to a maximum at 90°, decrease to a minimum at beta= 135°and finally increase again to a maximum to beta=180°.

For δ=45°:

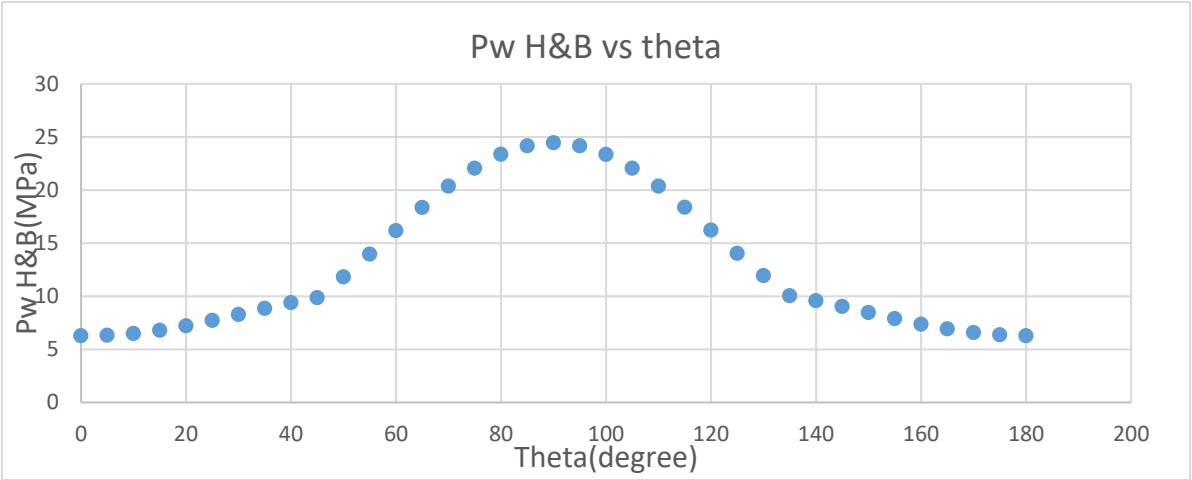

Figure 45 PwH&B vs theta second author, δ=45, σ_{max} =36MPa

The mud pressure for θ =0 is 6.2MPa, and then starts to increase significantly with the increase of θ to reach a peak at θ=90°. A significantly decrease in mud pressure is shown after that peak. The highest mud pressure is around 24.5MPa. The risk region is around the peak so around θ=90°, because the highest mud pressure exists, so the closer we are to the pressure to avoid the tensile fracturing and the narrower is the mud weight window.

At theta=0, the mud pressure is relatively low. This is because the rock mass is weakest in these directions, because the applied stress aligns with the preferred orientation of strength. The mud pressure increase with theta, because the stress applied to the shale is moving away from the preferred orientation of strength. The

mud pressure after theta=90° starts to decrease because the stress applied to the shale is approaching again to a direction which is parallel to the preferred orientation of strength.

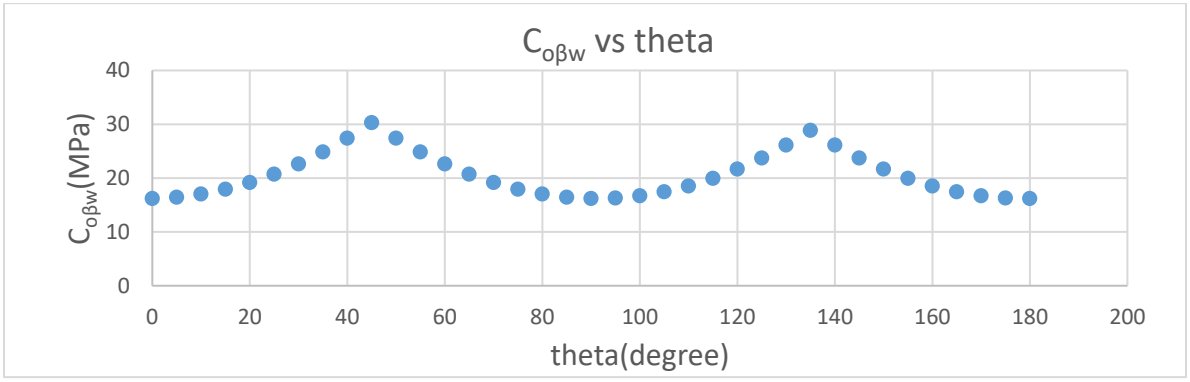

Figure 46 $C_{o\beta w}$ vs. theta, δ=45, Abdi

$C_{o\beta w}$ starts with a low value, then increase till beta=45°, decrease to a minimum at 90°, and increase to reach a peak at beta= 135°, to decrease again to a minimum at beta=180°.

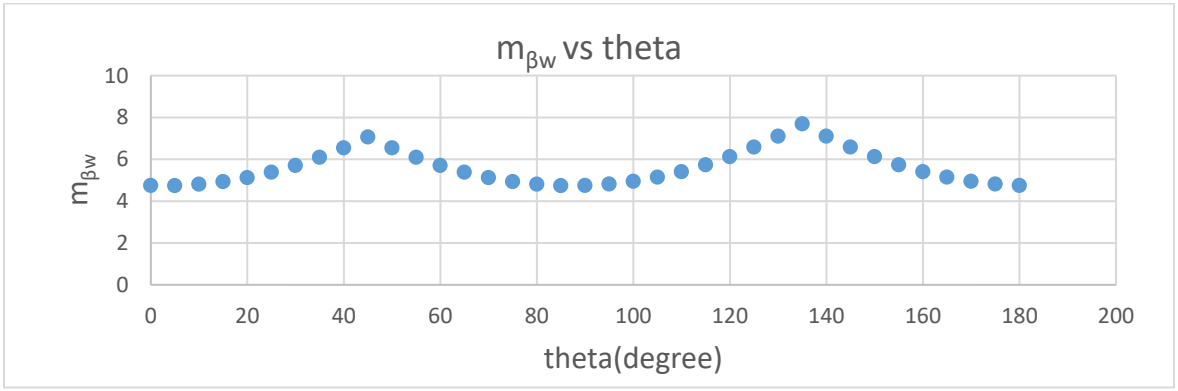

Figure 47 $m_{\beta w}$ vs. theta, δ=45, Abdi

$m_{\beta w}$ starts with a low value, then increase until beta=45°, decrease to a minimum at 90°, and increase to reach a peak at beta= 135°, to decrease again to a minimum at beta=180°.

For δ=0°:

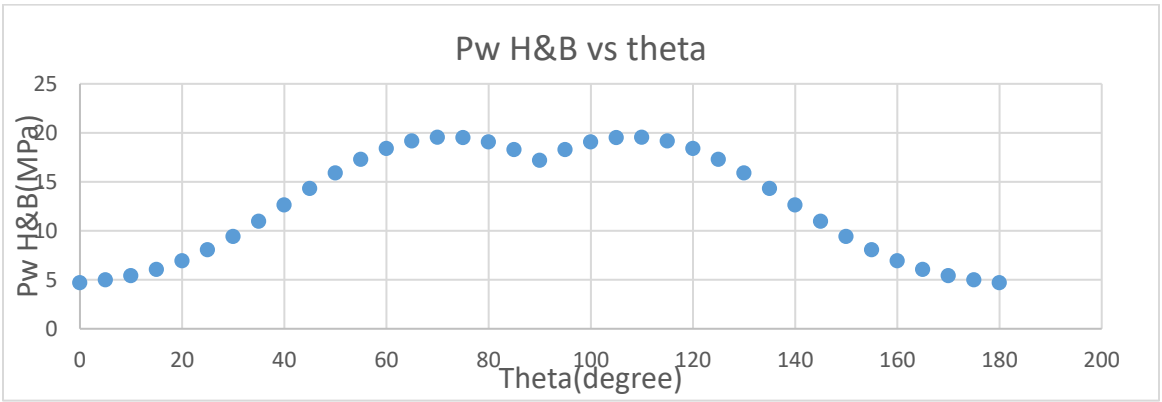

Figure 48 PwH&B vs theta second author, δ=0, σ_{max} =36MPa

The mud pressure for θ =0 starts at 4.7MPa, and starts to increase significantly with the increase of θ to reach a peak around θ=70°. We have than a small decrease in mud pressure and it is followed by another peak at θ=110°. A significantly decrease in mud pressure is shown after θ=110°. The highest mud pressure is around 20MPa.The risk region is around the peak so around θ=70 and θ=110°, because the highest mud pressure exists, so the closer we are to the pressure to avoid the tensile fracturing and the narrower is the mud weight window.

For δ=0°, at theta=0, the mud pressure is relatively low. The rock is weak in these directions, because the applied stress aligns with the preferred orientation of strength. The mud pressure increase with theta, because the stress applied to the shale is moving away from the preferred orientation of strength to reach a peak at theta=65° and at 125°. The mud pressure is decreasing again after the second peak because the stress applied to the shale is approaching to a direction which is parallel to the preferred orientation of strength.

2.3.2 for σ_{max} =23MPa, σ_{min}=20MPa, k=1.15

For δ=90°:

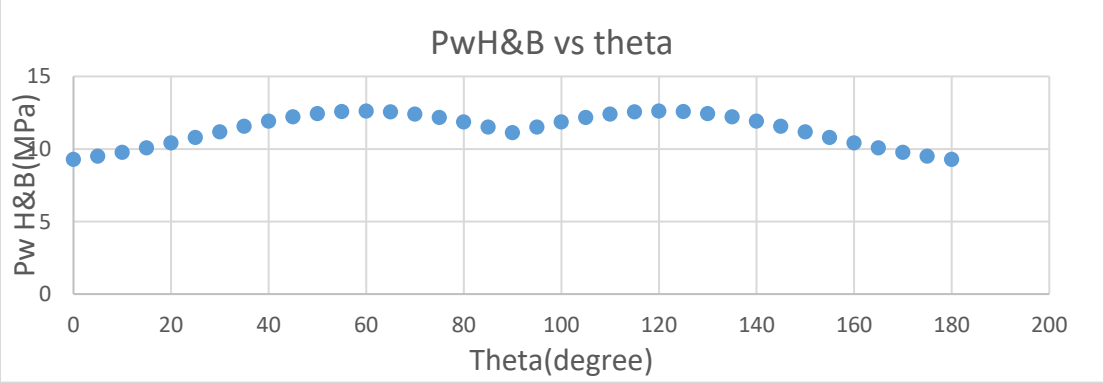

Figure 49 PwH&B vs theta second author, δ=90, σ_{max} =23MPa

The mud pressure for θ =0 starts at 9.5MPa, and starts to increase with the increase of θ to reach a peak of 12.6MPa around θ=60°. We have than a small decrease in mud pressure and it is followed by another peak at θ=120°. A decrease in mud pressure is shown after θ=120°. The highest mud pressure is around 12.6MPa. The risk region is around the peak so around θ=60 and θ=120°, because the highest mud pressure exists, so the closer we are to the pressure to avoid the tensile fracturing and the narrower is the mud weight window.

For δ=90°, at theta=0, the mud pressure is relatively low. The rock is weak in these directions, because the applied stress aligns with the preferred orientation of strength. The mud pressure increase with theta, because the stress applied to the shale is moving away from the preferred orientation of strength to reach a peak at theta=45° and at 135°. The mud pressure is decreasing again after the second peak because the stress applied to the shale is approaching again to a direction which is parallel to the preferred orientation of strength.

The highest mud pressure is decreasing with the decrease of the degree of anisotropy.

.

For δ=45°:

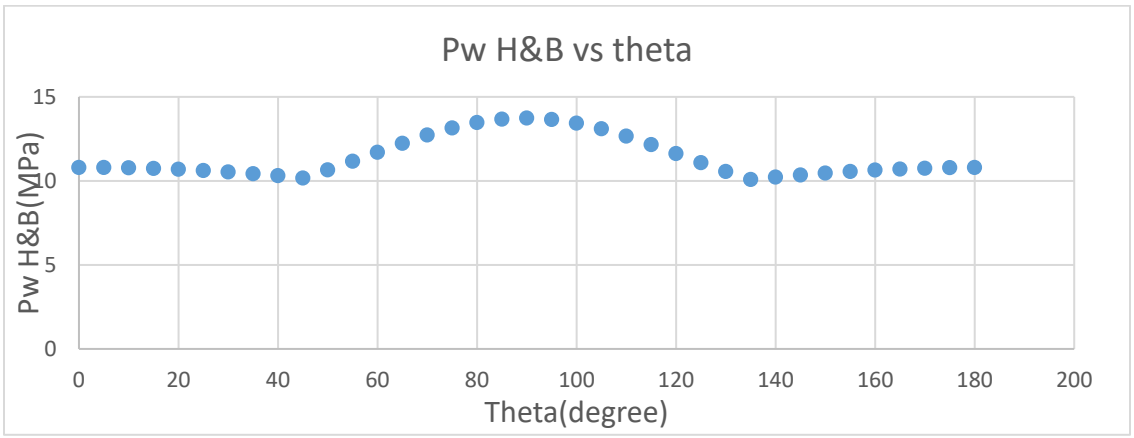

Figure 50 PwH&B vs theta second author, δ=45, σ_{max} =23MPa

We have a decrease in mud pressure from θ=0 to θ=45°.The pressure decrease from a pressure of 10.7MPa to 10MPa. Then, the mud pressure increase to peak at=90° for P=13.73MPa and decrease again to reach 10MPa at θ=135°. An increase in mud pressure is showed again for higher values of θ to reach 10.7MPa°. The risk region is around the peak so around θ=90°because the highest mud pressure exists, so the closer we are to the pressure to avoid the tensile fracturing and the narrower is the mud weight window.

The mud pressure increase with theta, because the stress applied to the shale is moving away from the preferred orientation of strength. The mud pressure after theta=90° starts to decrease because the stress applied to the shale is approaching again to a direction which is parallel to the preferred orientation of strength. The peak of mud pressure decrease, the margin between the mud pressures for different angle theta decrease, we can deduce that with decrease the degree of anisotropy, the mud pressure decrease.

For δ=0°:

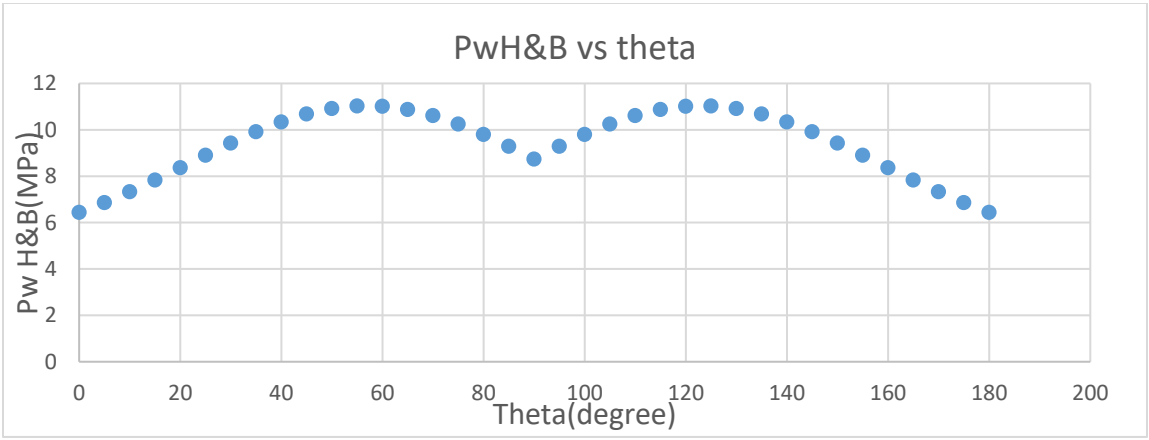

Figure 51 PwH&B vs theta second author, δ=0, σ_{max} =23MPa

The mud pressure for θ =0 starts at 6.433MPa, and starts to increase with the increase of θ to reach a peak around θ=60°. We have than a small decrease in mud pressure and it is followed by another peak at θ=120°. A significantly decrease in mud pressure is shown after θ=120°. The highest mud pressure is around

11MPa.The risk region is around the peak so around θ=60 and θ=120°, because the highest mud pressure exists, so the closer we are to the pressure to avoid the tensile fracturing and the narrower is the mud weight window.

For δ=0°, at theta=0, the mud pressure is relatively low. The rock is weak in these directions, because the applied stress aligns with the preferred orientation of strength. The mud pressure increase with theta, because the stress applied to the shale is moving away from the preferred orientation of strength to reach a peak at theta=60° and at 120°. The mud pressure is decreasing again after the second peak because the stress applied to the shale is approaching to a direction which is parallel to the preferred orientation of strength.

The highest mud pressure is decreasing with the decrease of the degree of anisotropy.

2.3.3 for σ_{max} =σmin=20MPa, k=1

For δ=90°:

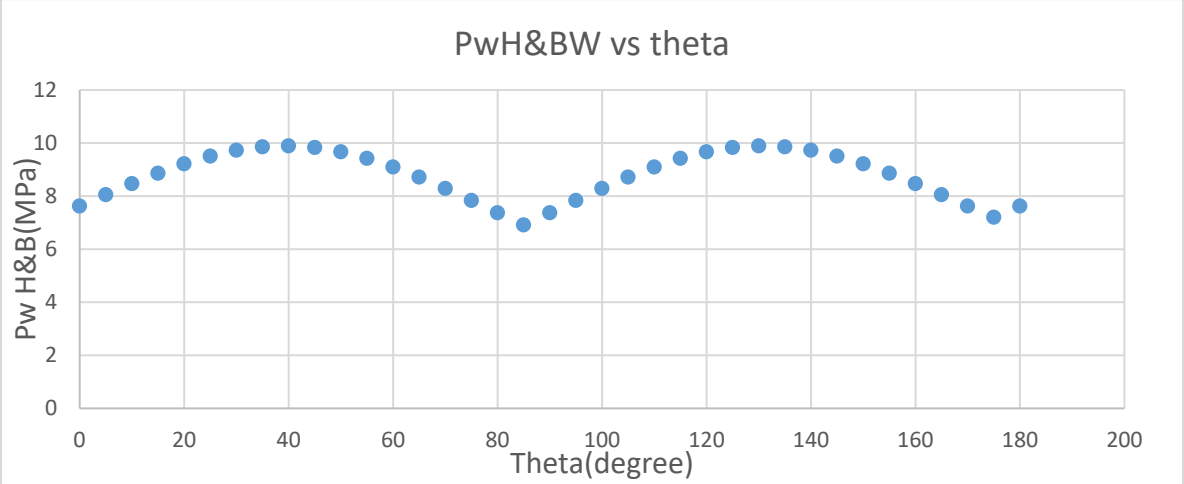

Figure 52 PwH&B vs theta second author, δ=90, σ_{max} =20MPa

The mud pressure for θ =0 starts at 7.62MPa, and starts to increase with the increase of θ to reach a peak of 10MPa around θ=40°. We have than a small decrease in mud pressure and it is followed by another peak at θ=130°. A decrease in mud pressure is shown after θ=130°. The highest mud pressure is around 10MPa.The risk region is around the peak so around θ=40 and θ=130°, because the highest mud pressure exists, so the closer we are to the pressure to avoid the tensile fracturing and the narrower is the mud weight window.

For δ=90°, at theta=0, the mud pressure is relatively low. The rock is weak in these directions, because the applied stress aligns with the preferred orientation of strength. The mud pressure increase with theta, because the stress applied to the shale is moving away from the preferred orientation of strength to reach a peak at theta=45° and at 135°. The mud pressure is decreasing again after the second peak because the stress applied to the shale is approaching again to a direction which is parallel to the preferred orientation of strength.

The highest mud pressure is decreasing with the decrease of the degree of anisotropy.

For δ=45°:

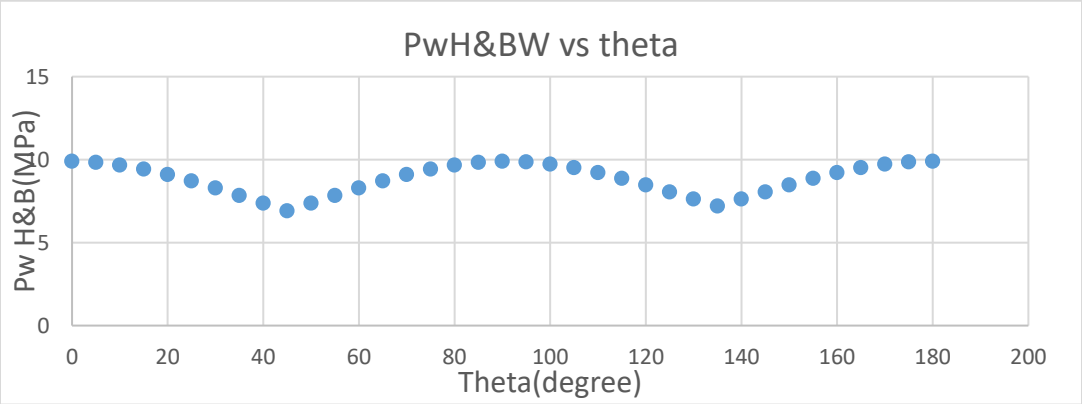

Figure 53 PwH&B vs theta second author, δ=45, σ_{max} =20MPa

We have a decrease in mud pressure from θ=0 to θ=45°.The pressure decrease from a pressure of 10MPa to 6.9MPa. Then, the mud pressure increase to peak at=90° for P=10MPa and decrease again to reach 6.9MPa at θ=135°. An increase in mud pressure is showed again for higher values of θ to reach 10MPa. The risk region is around the peak so around θ=0,90 and 180°because the highest mud pressure exists, so the closer we are to the pressure to avoid the tensile fracturing and the narrower is the mud weight window.

The mud pressure increase with theta, because the stress applied to the shale is moving away from the preferred orientation of strength. The mud pressure after theta=90° starts to decrease because the stress applied to the shale is approaching again to a direction which is parallel to the preferred orientation of strength. The peak of mud pressure decrease, the margin between the mud pressures for different angle theta decrease, we can deduce that with decrease the degree of anisotropy, the mud pressure decrease.

For δ=0°:

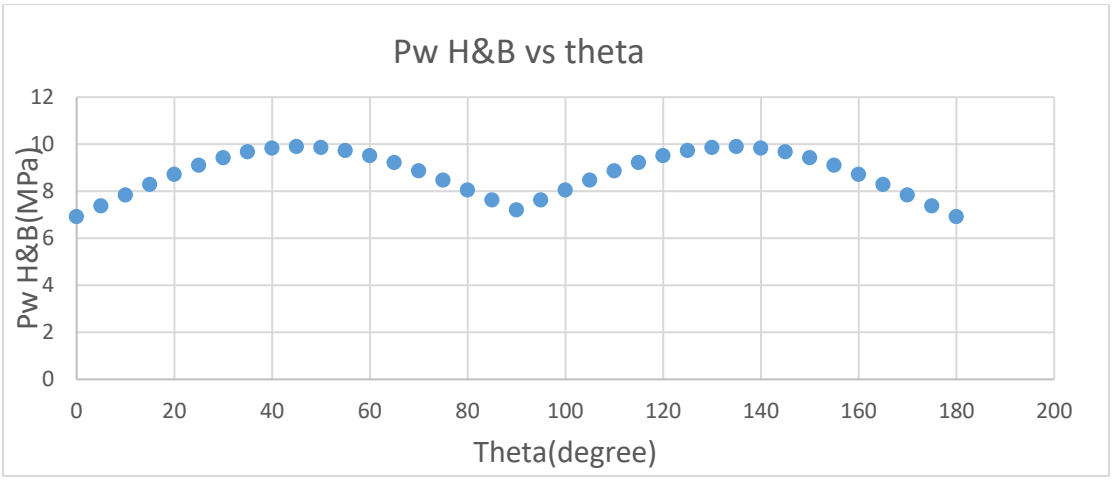

Figure 54 PwH&B vs theta second author, δ=0, σ_{max} =20MPa

The mud pressure for θ =0 starts at 6.9MPa, and starts to increase with the increase of θ to reach a peak of 10MPa around θ=50°. We have than a small decrease in mud pressure and it is followed by another peak at θ=130°. A significantly decrease in mud pressure is shown after θ=130°. The highest mud pressure is around

10MPa.The risk region is around the peak so around θ=50 and θ=130°, because the highest mud pressure exists, so the closer we are to the pressure to avoid the tensile fracturing and the narrower is the mud weight window.

For δ=0°, at theta=0, the mud pressure is relatively low. The rock is weak in these directions, because the applied stress aligns with the preferred orientation of strength. The mud pressure increase with theta, because the stress applied to the shale is moving away from the preferred orientation of strength to reach a peak at theta=60° and at 120°. The mud pressure is decreasing again after the second peak because the stress applied to the shale is approaching to a direction which is parallel to the preferred orientation of strength.

The highest mud pressure is decreasing with the decrease of the degree of anisotropy.

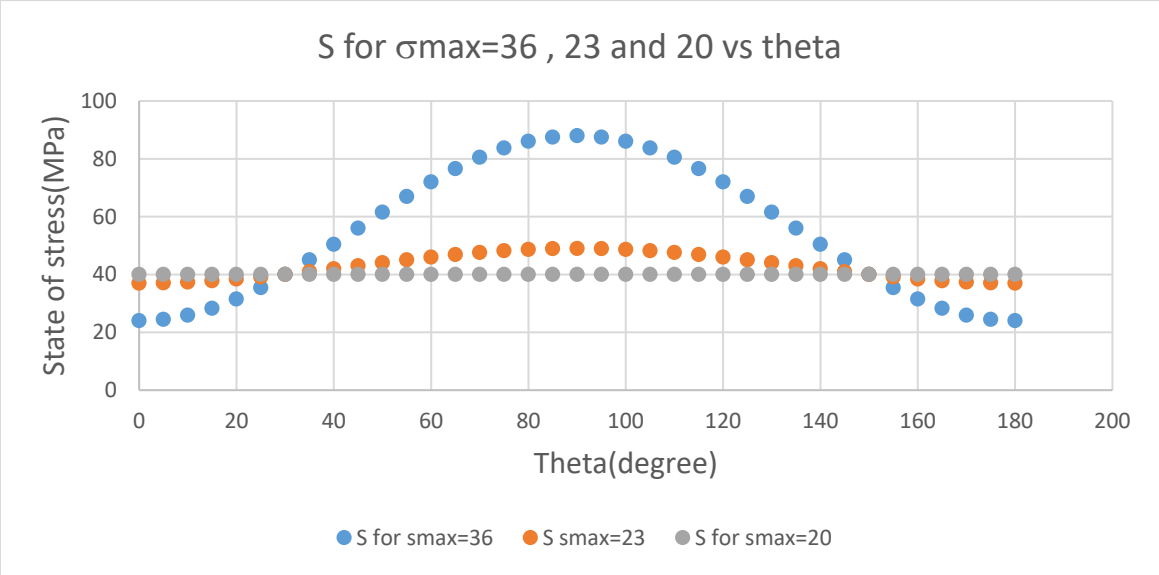

Figure 55 S vs theta

S does not depend in case if the experimental data are fitted or no with Hoek and Brown or Mohr Coulomb and does not depend on δ. So here we have the plot of S vs. theta for different values of σmax. S depends on the degree of anisotropy. The state of stress increase with increase theta for a degree of anisotropy as it is shown is fig.56. The minimum state of stress occurs at theta=0 and theta=180° and the highest is at theta=90°. This behavior is mainly because as theta increase, the shale faces less normal stress and more shear stress. At theta=90°, the normal stress becomes zero, and the shear stress is maximum, so the induced state of stress is maximum.

B. Mud pressure using the weakness plane model

2.4 Procedure

The weakness plane model divides failure between the matrix and in the plane of weakness, under the assumption a plateau with a constant strength for a range of inclination (beta). Two different formulas were used to calculate the shear mud pressure using the Mohr-Coulomb criterion, where one formula was applied along the matrix and another formula along the plane of weakness.

1. The first step is to draw σ'_1 vs. βw in order to see the intersections between the plateau and the weakness plane model.

a) The plateau can be drawn by using the equation:

$$\sigma'1 = Co + N\phi\sigma'3 \quad (34)$$

Co and N_ϕ are respectively the intersection and the slope of the plot σ'_1 vs. σ'_3 for theta=90 and theta=0 and they are fix along all the interval. For σ'_3=1MPa, we found the plateau

b) The weakness plane parabola can be obtained using the equation (20)

C_{ow} and N_ϕ are respectively the intersection and the slope of the plot σ'1 vs. σ'3 for theta=45 and theta=60 and they are fix along the interval. They are the average of the intersection of the two lines and the average of the slope.

From these two values, C'_w and ϕ'_w can be calculated using the following two formulas:

$$Cow = \frac{2c'w*cos\phi'w}{1-sin\phi'w} \quad (35) \qquad N\phi = \frac{1+sin\phi'w}{1-sin\phi'w} \quad (36)$$

Knowing that $\sigma1 - \sigma3 = \sigma'1 - \sigma'3$ we can find $\sigma'1$ for $\beta w = 45, 60$ and at βw*

For σ'_3=1MPa, we found the equation of parabola for the weakness plane

c) From the two equations already found (the equation of the horizontal line which refer to the plateau and using the equation of the parabola which belong to the weakness plane) we can find the intersection on the plot σ'_1 vs.βw, so we will have the range at which the rock fail in the weakness plane.

2. I proceeded my work by calculating P_{matrix} by coupling Mohr coulomb with kirsh solution, we obtain the following formula:

$$Pmatrix = \frac{S-C0-Pf(N\phi-1)}{(N\phi+1)} \quad (37)$$

a) S is calculated using the formula (18)

Where σ_{min} is fixed at 20MPa, but σ_{max} take three different values: 30, 23 and 20MPa.It is only function of the far field stress and theta.

Pf has a fixed value which is equal to 8MPa.

b) Co and Nϕ are already calculated from part 1.a)

So the formula of P_{matrix} change with the change of σ_{max} and the change of the author or the change of the correction and it is independent of delta.

3. Now I proceed with a detailed calculation of P_{WPM}:

After coupling the weakness plane formula and kirsh solution, we obtain the following formula:

$$PWPM = \frac{S(1 - \frac{\tan\phi'w}{\tan \beta w}) * \sin 2\beta w \ - 2c'w + 2\tan\phi'w * Pf}{2[\tan\phi'w + \left(1 - \frac{\tan\phi'w}{\tan \beta w}\right) \sin 2 \ \beta w \ ]}$$

a) S is calculated in the same way as 2.d) and Pf is constant along all the interval and in all the studied cases.
b) C_{ow} and N_ϕ are already calculated from 1.b)

From these two values, c'_w and ϕ'_w can be calculated using the formulas (5) and (4).

So the formula of P_{WPM} change with the change of σ_{max} and the change of the author or the change of the correction.

We remove the range (1.c) at which "tournemire shale" fail along the matrix from the plot of P_{WPM}

2.5 Detailed calculation

I will start by a detailed calculation in order to show how my work is done in this part.

1. The range at which the "tournemire shale "fail in the weakness plane is our first step to go.

The plateau is calculated in the first place using the equation (34)

N_ϕ is the slope of the plot σ'_1 vs. σ'_3 and Co is the interception with the axis of σ'_1.

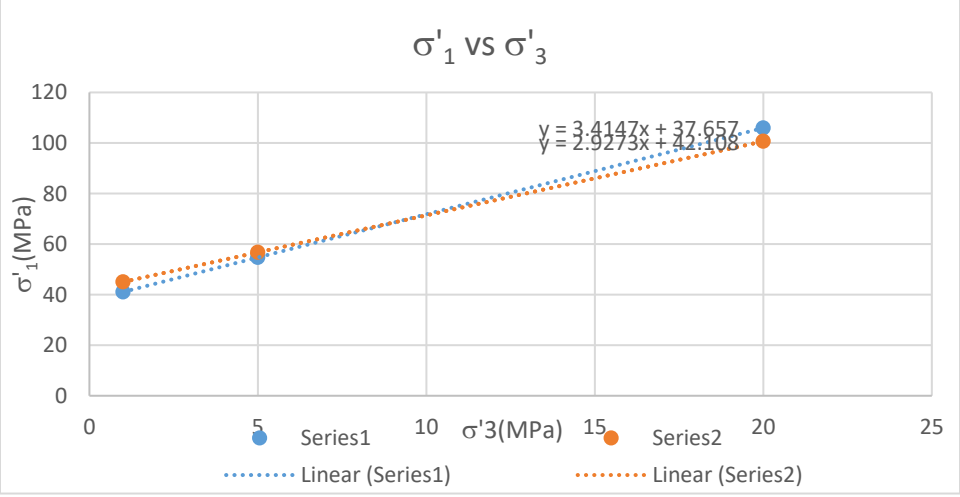

Figure 56 σ'1 vs σ'3, first author, theta=0 and 90

This is the combination of tables already found in part 3, which represent the plot σ'1 vs. σ'3.

I took an average of the slope and an average of the intercept of the two lines σ'1 vs. σ'3 at θ=0 and 90°, I got:

Co=39.8825MPa and Nϕ=3.171MPa.

For σ'_3=1MPa, we have that σ'1 at 0 and at 90° is equal to 43.0535MPa.

Using the formula (34) we are able to calculate σ'1 for the weakness plane

N_ϕ is the slope of the plot σ'_1 vs. σ'_3 and Co is the interception with the axis of σ'1.

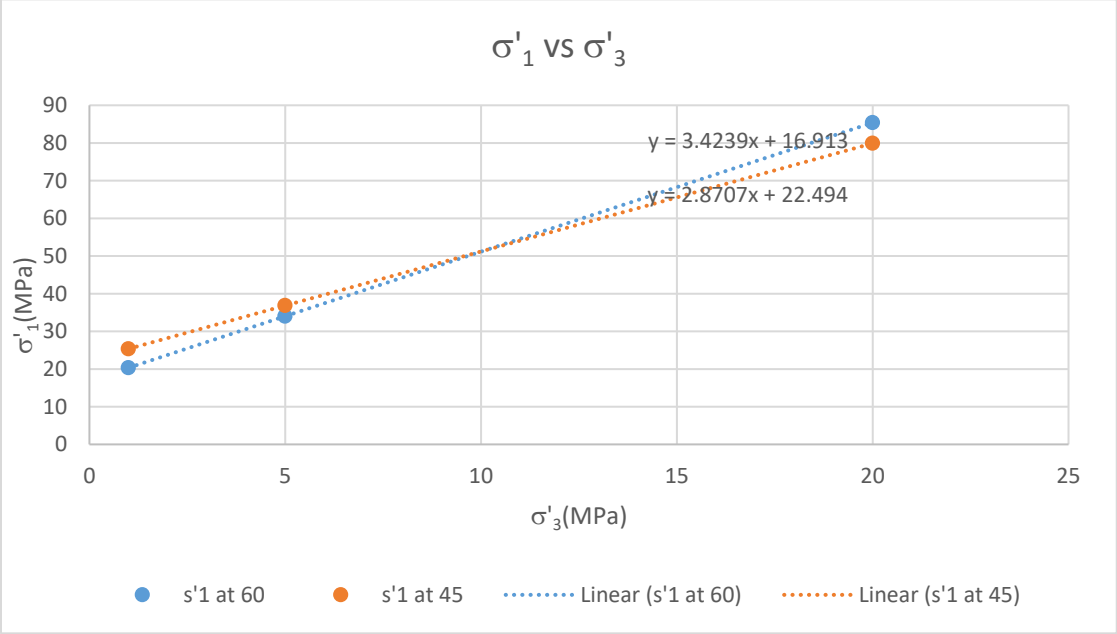

Figure 57 σ'1 vs σ'3, first author, theta=45 and 60

This is the combination of tables already found in part 3, which represent the plot σ'_1 vs. σ'_3.

I took an average of the slope and an average of the intercept and I got:

C0=19.7035(average), Nϕ=3.1473

Using equations (5) and (4), we got C_w'=5.55MPa, ϕ'_w=31.182MPa

β_w*=60.6, using the fact that the minimum strength occur at $45+\frac{\Phi'}{2}$.

σ'3 is equal to 1MPa.

3 values of βw is taken: 45, 70 and at β_w*

So we have the following values of σ'_1 respectively: 109.43MPa, 90.446MPa and 82.638MPa

We obtain the following plot:

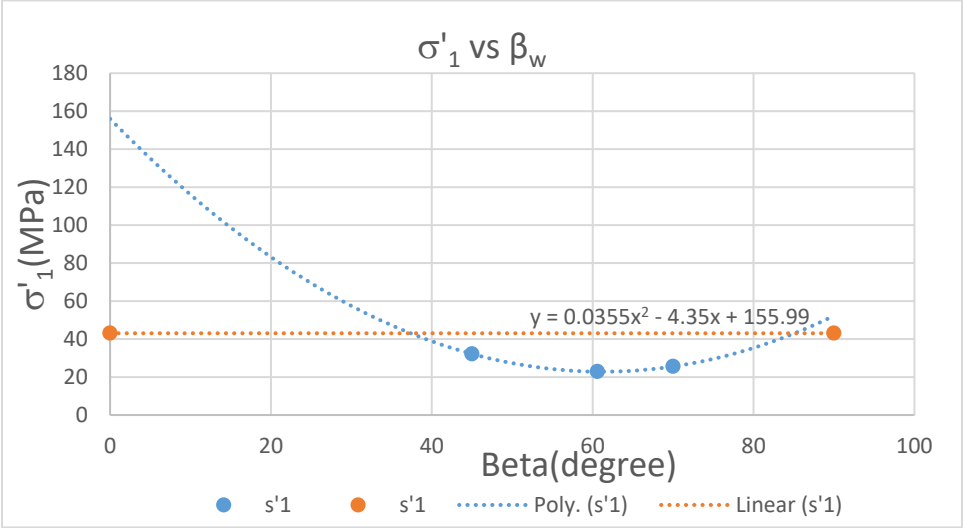

Figure 58 σ'1 vs βw

From the figure 59 we can reveal that "tournemire shale" with the first author and with correction, fail in the weakness plane between βw equal 37.34 and 85.19°

2. Now, $Pmatrix$ is calculated using equation(37)

Co and $N\phi$ are calculated from figure 58. Pf is fixed at 8MPa, and S is calculated using the following formula (18).

For the first author, with correction and for σ_{max}=36MPa, we obtain the following values of Pmatrix:

Theta	Beta	Co	Nϕ	Pf	S	Pw	2*theta	2*thetaradian
0	90	39.8825	3.171	8	24	0.35615	0	0
5	85	39.8825	3.171	8	24.48615	0.472705	10	0.174533
10	80	39.8825	3.171	8	25.92984	0.818829	20	0.349066
15	75	39.8825	3.171	8	28.28719	1.384006	30	0.523599
20	70	39.8825	3.171	8	31.48658	2.151062	40	0.698132
25	65	39.8825	3.171	8	35.4308	3.096691	50	0.872665
30	60	39.8825	3.171	8	40	4.19216	60	1.047198
35	55	39.8825	3.171	8	45.05536	5.404185	70	1.22173
40	50	39.8825	3.171	8	50.44326	6.695938	80	1.396263
45	45	39.8825	3.171	8	56	8.028171	90	1.570796
50	40	39.8825	3.171	8	61.55674	9.360403	100	1.745329
55	35	39.8825	3.171	8	66.94464	10.65216	110	1.919862
60	30	39.8825	3.171	8	72	11.86418	120	2.094395

65	25	39.8825	3.171	8	76.5692	12.95965	130	2.268928
70	20	39.8825	3.171	8	80.51342	13.90528	140	2.443461
75	15	39.8825	3.171	8	83.71281	14.67234	150	2.617994
80	10	39.8825	3.171	8	86.07016	15.23751	160	2.792527
85	5	39.8825	3.171	8	87.51385	15.58364	170	2.96706
90	0	39.8825	3.171	8	88	15.70019	180	3.141593
95	5	39.8825	3.171	8	87.51385	15.58364	190	3.316126
100	10	39.8825	3.171	8	86.07016	15.23751	200	3.490659
105	15	39.8825	3.171	8	83.71281	14.67234	210	3.665191
110	20	39.8825	3.171	8	80.51342	13.90528	220	3.839724
115	25	39.8825	3.171	8	76.5692	12.95965	230	4.014257
120	30	39.8825	3.171	8	72	11.86418	240	4.18879
125	35	39.8825	3.171	8	66.94464	10.65216	250	4.363323
130	40	39.8825	3.171	8	61.55674	9.360403	260	4.537856
135	45	39.8825	3.171	8	56	8.028171	270	4.712389
140	50	39.8825	3.171	8	50.44326	6.695938	280	4.886922
145	55	39.8825	3.171	8	45.05536	5.404185	290	5.061455
150	60	39.8825	3.171	8	40	4.19216	300	5.235988
155	65	39.8825	3.171	8	35.4308	3.096691	310	5.410521
160	70	39.8825	3.171	8	31.48658	2.151062	320	5.585054
165	75	39.8825	3.171	8	28.28719	1.384006	330	5.759587
170	80	39.8825	3.171	8	25.92984	0.818829	340	5.934119
175	85	39.8825	3.171	8	24.48615	0.472705	350	6.108652
180	90	39.8825	3.171	8	24	0.35615	360	6.283185

Table 8 Pw calculation

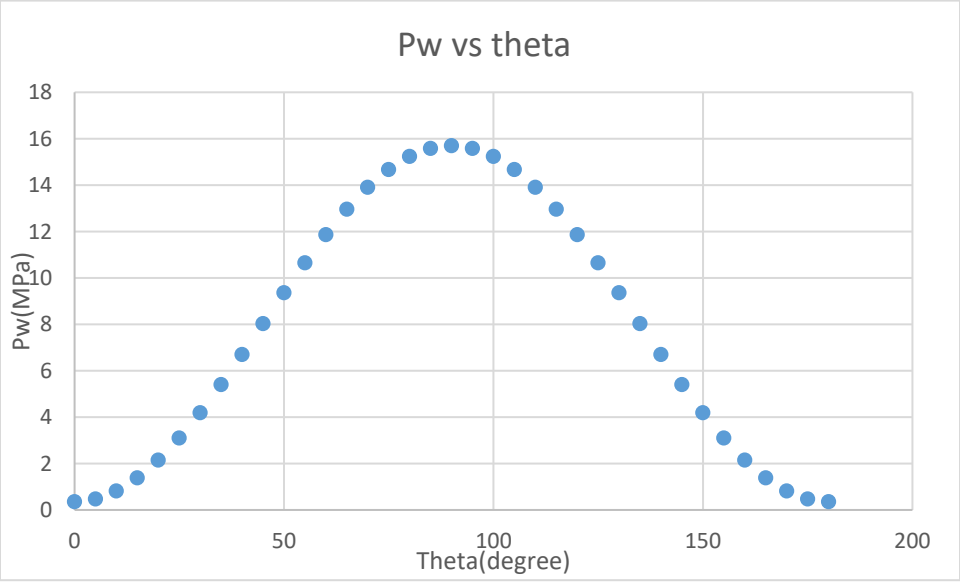

Figure 59 Pmatrix vs theta, first author, with correction, σ_{max}=36MPa

3. The mud pressure along the weakness plane is calculated with the formula (31).

Pf is fixed at 8MPa.

$\phi'w$, $c'w$ is calculated using the figure 57.

βw change with the change of δ, so we obtain for the first author, with correction, for σ_{max}=36MPa and for δ=0°, we obtain the following results:

After removing the range of beta as which the weakness plane is not able to predict the behavior of the "tournemire shale", we obtain:

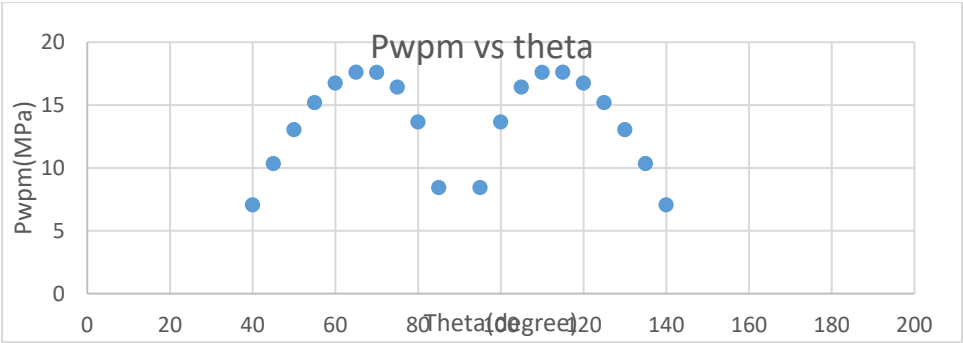

Figure 60 Pwpm vs theta, first author, with correction, σ_{max}=36MPa

2.6 For the first author

The mud pressure of the two methods are putted on the same plot vs. theta, in order to make the comparison easier and clearer:

2.6.1 for σmax =36MPa, σ_{min}=20MPa, k=1.8

2.6.1.1 with correction

For δ=0°:

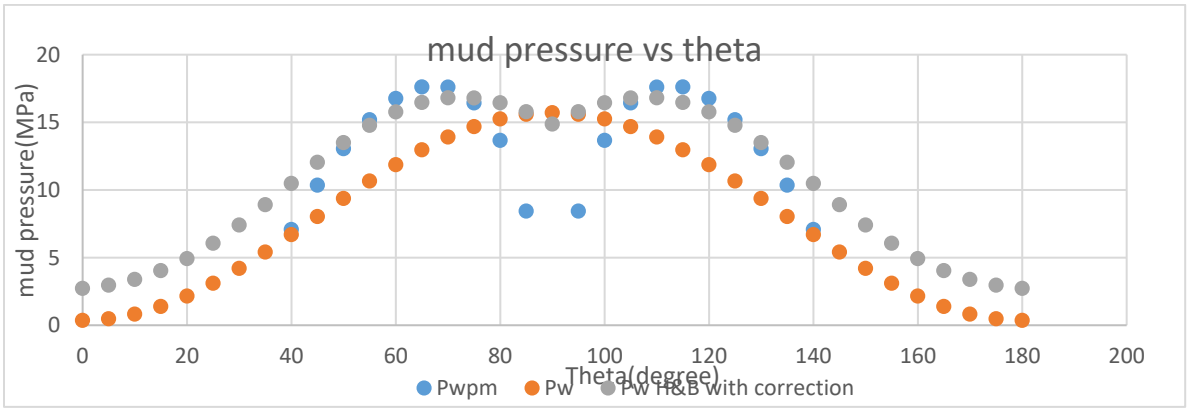

Figure 61 Pmud vs theta, with correction, δ=0, σ_{max}=36MPa

The highest mud pressure is around 17MPa. The risk region is around the peak so around θ=60 and θ=120°, because the highest mud pressure exists, so the closer we are to the pressure to avoid the tensile fracturing and the narrower is the mud weight window.

For the weakness plane model: The peak near theta=60° and 120° occur because the wellbore is less likely to be stable at these inclinations. When δ=0°, β is around 60° which is aligned parallel to the bedding plane, so higher mud pressure should be used in order to maintain the stability of the wellbore. When the bedding plane are aligned parallel to the drilling direction (θ=0 or 180°), the mud requires the lowest pressure.

The weakness plane model matches Hoek and brown for all the inclination θ especially when it fails along the weakness plane in the range [40-85] and [95-140].

For δ=45°:

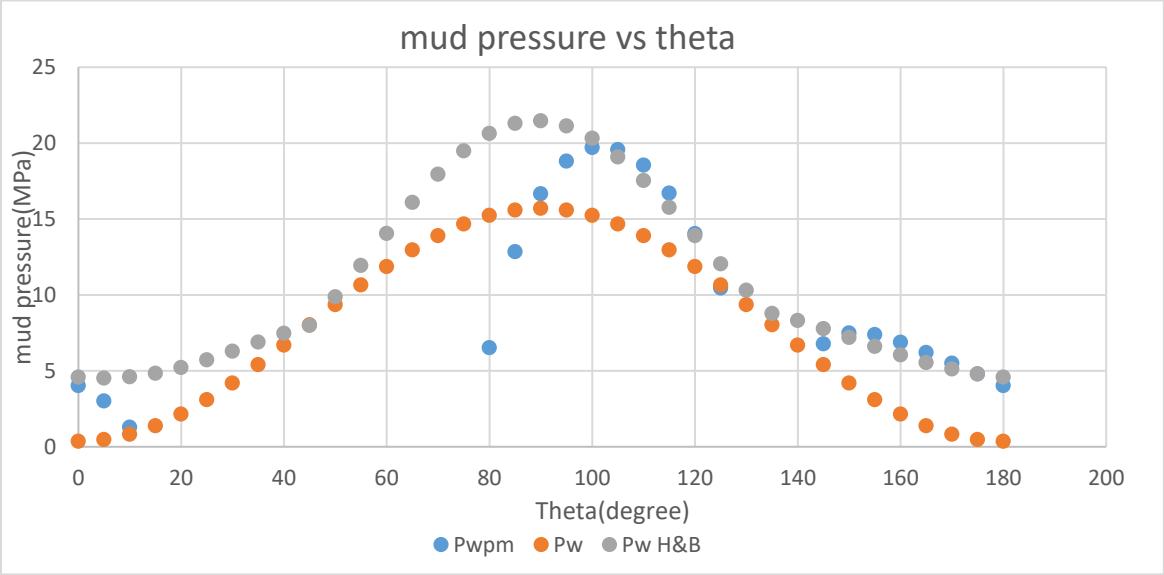

Figure 62 Pmud vs theta, with correction, δ=45, σ_{max}=36MPa

The highest mud pressure is around 21.5MPa. The risk region is around the peak so around θ=90°, because the highest mud pressure exists, so the closer we are to the pressure to avoid the tensile fracturing and the narrower is the mud weight window.

The peak near theta=90° occurs in the weakness plane model because the wellbore is less likely to be stable at the inclination. The wellbore is aligned along the inclination of the bedding plane (plane of weakness), so higher mud pressure should be used in order to maintain the stability of the wellbore. When the bedding plane are aligned parallel to the drilling direction (θ=0 or 180°), the mud requires the lowest pressure.

The weakness plane model matches Hoek and brown for all the inclination θ especially when it fails along the weakness plane in the range [0-10], [80-110] and [140-180].

For δ=90°:

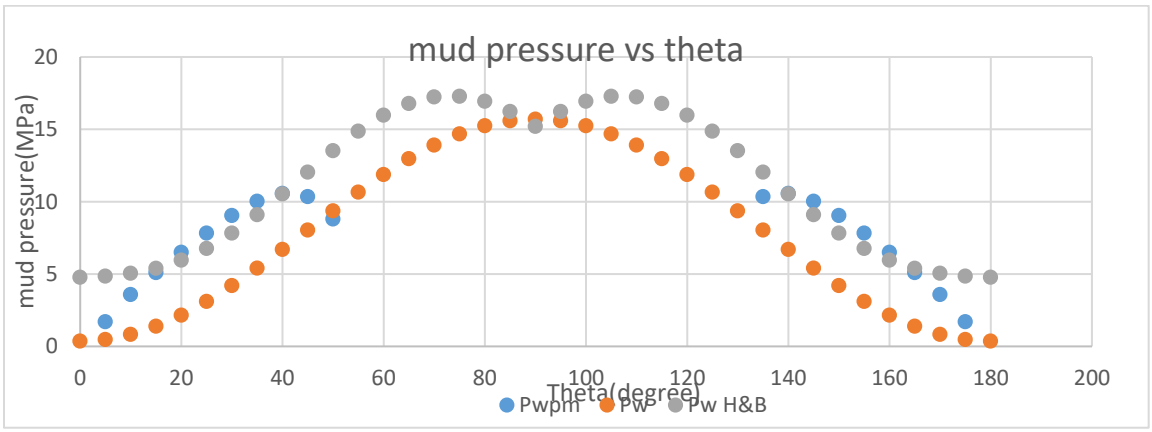

Figure 63 Pmud vs theta, with correction, δ=90, σ_{max}=36MPa

The highest mud pressure is around 17.3MPa. The risk region is around the peak so around θ=70 and θ=110°, because the highest mud pressure exists, so the closer we are to the pressure to avoid the tensile fracturing and the narrower is the mud weight window.

For the weakness plane model: The peak near theta=45° and 135° occur because the wellbore is less likely to be stable at these inclinations. When δ=90°, β is around 45 which is aligned parallel to the bedding plane, so higher mud pressure should be used in order to maintain the stability of the wellbore. When the bedding plane are aligned parallel to the drilling direction (θ=0 or 180°), the mud requires the lowest pressure.

The weakness plane model matches Hoek and brown for all the inclination θ especially when it fails along the weakness plane in the range [0-50] and [135-180]. There is an average fitting between the two methods

2.6.1.2 without correction

For δ=0°:

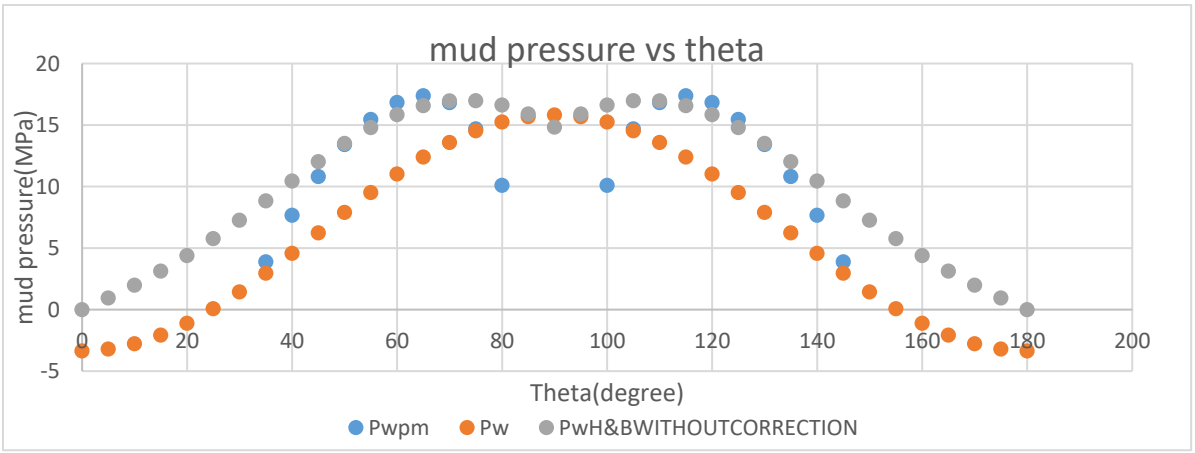

Figure 64 Pmud vs theta, without correction, δ=0, σ_{max}=36MPa

The highest mud pressure is around 17MPa.The risk region is around the peak so around θ=70 and θ=110°, because the highest mud pressure exists, so the closer we are to the pressure to avoid the tensile fracturing and the narrower is the mud weight window.

For the weakness plane model: The peak near theta=60° and 120° occur because the wellbore is less likely to be stable at these inclinations. When δ=0°, β is around 60 which is aligned parallel to the bedding plane, so higher mud pressure should be used in order to maintain the stability of the wellbore. When the bedding plane are aligned parallel to the drilling direction (θ=0 or 180°), the mud requires the lowest pressure.

There is a poor fitting between the weakness plane model and Hoek and brown.

For δ=45°:

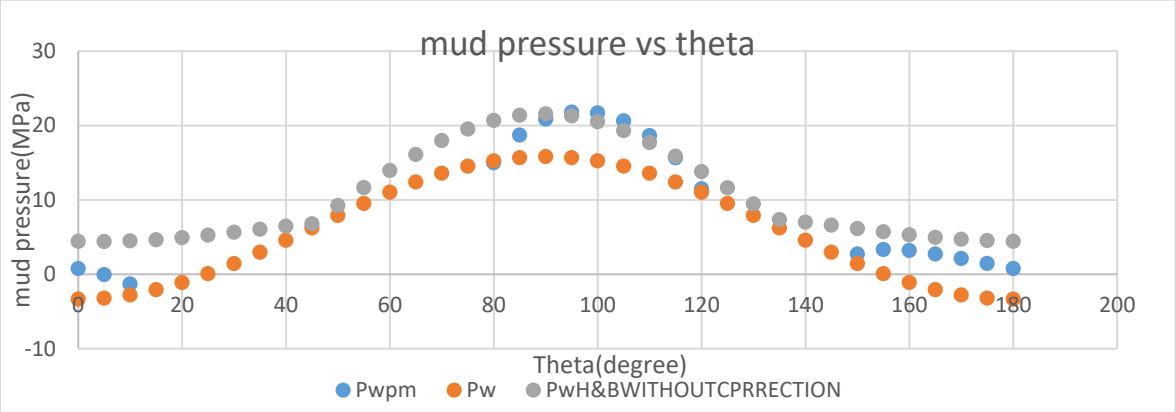

Figure 65 Pmud vs theta, without correction, δ=45, σ_{max}=36MPa

The highest mud pressure is around 21.5MPa. The risk region is around the peak so around θ=90°, because the highest mud pressure exists, so the closer we are to the pressure to avoid the tensile fracturing and the narrower is the mud weight window.

The peak near theta=90° occurs in the weakness plane model because the wellbore is less likely to be stable at the inclination. The wellbore is aligned along the inclination of the bedding plane (plane of weakness), so higher mud pressure should be used in order to maintain the stability of the wellbore. When the bedding plane are aligned parallel to the drilling direction (θ=0 or 180°), the mud requires the lowest pressure.

There is a poor fitting between the weakness plane model and Hoek and brown for all the inclination angle theta.

For δ=90°:

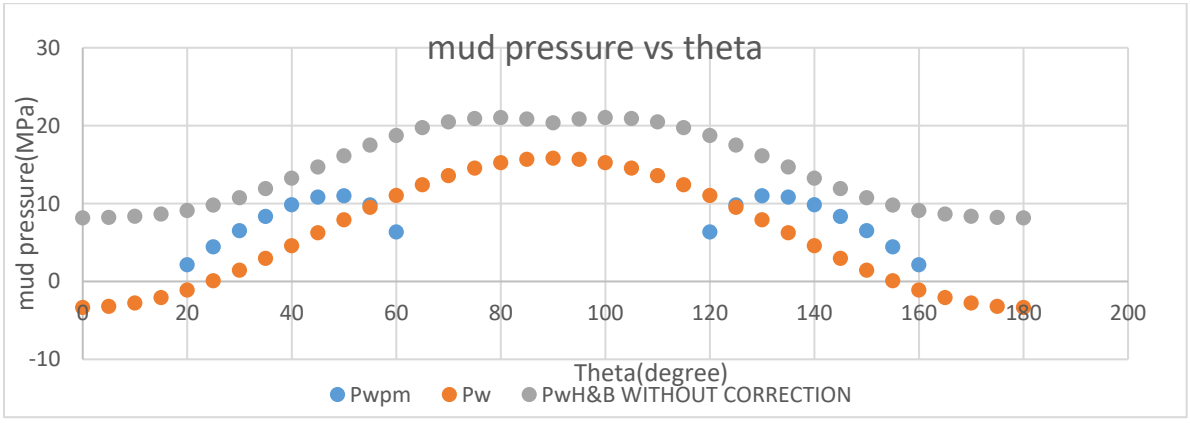

Figure 66 Pmud vs theta, without correction, δ=90, σ_{max}=36MPa

The highest mud pressure is around 21MPa. The risk region is around the peak so around θ=80 and θ=110°, because the highest mud pressure exists, so the closer we are to the pressure to avoid the tensile fracturing and the narrower is the mud weight window.

For the weakness plane model: The peak near theta=50° and 130° occur because the wellbore is less likely to be stable at these inclinations. When δ=90°, β is around 45 which is aligned parallel to the bedding plane, so higher mud pressure should be used in order to maintain the stability of the wellbore. When the bedding plane are aligned parallel to the drilling direction (θ=0 or 180°), the mud requires the lowest pressure.

There is no fitting between the two methods in general for all the inclination angle theta.

2.6.2 for σmax =23MPa, σ_{min}=20MPa, k=1.15

2.6.2.1 with correction

For δ=0°:

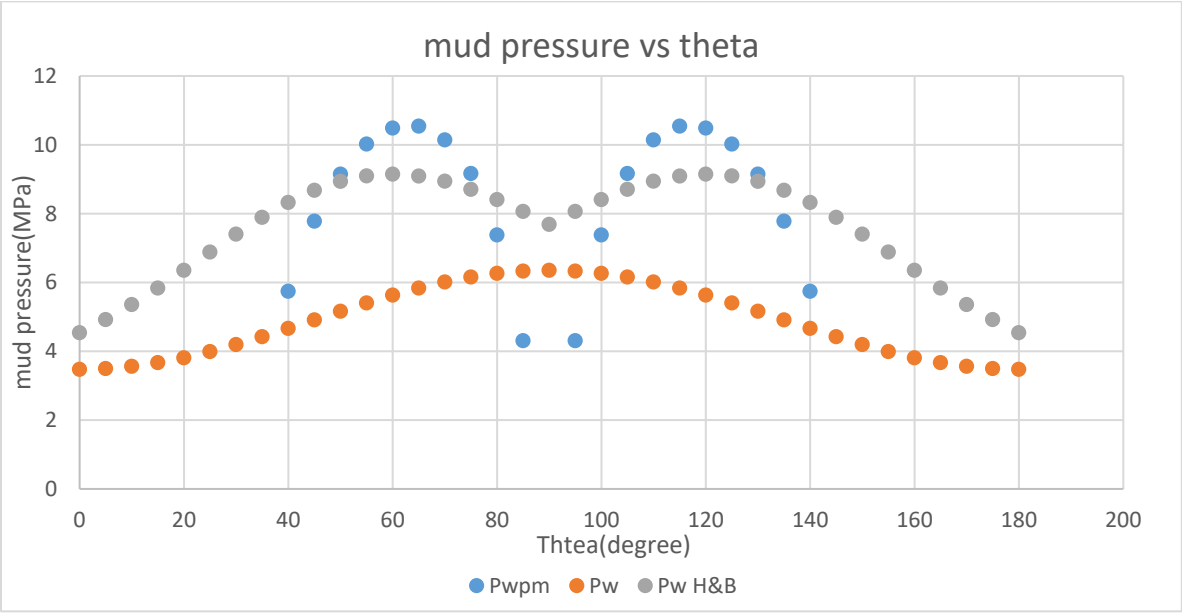

Figure 67 Pmud vs theta, with correction, δ=0, σ_{max}=23MPa

The highest mud pressure is around 9.2MPa. The risk region is around the peak so around θ=60 and θ=120°, because the highest mud pressure exists, so the closer we are to the pressure to avoid the tensile fracturing and the narrower is the mud weight window.

For the weakness plane model: The peak near theta=60° and 120° occur because the wellbore is less likely to be stable at these inclinations. When δ=0°, β is around 60 which is aligned parallel to the bedding plane, so higher mud pressure should be used in order to maintain the stability of the wellbore. When the bedding plane are aligned parallel to the drilling direction (θ=0 or 180°), the mud requires the lowest pressure.

The weakness plane model matches Hoek and brown for all the inclination θ especially when it fails along the weakness plane in the range [40-85] and [95-140]. There is an average fitting between the two methods

For δ=45°:

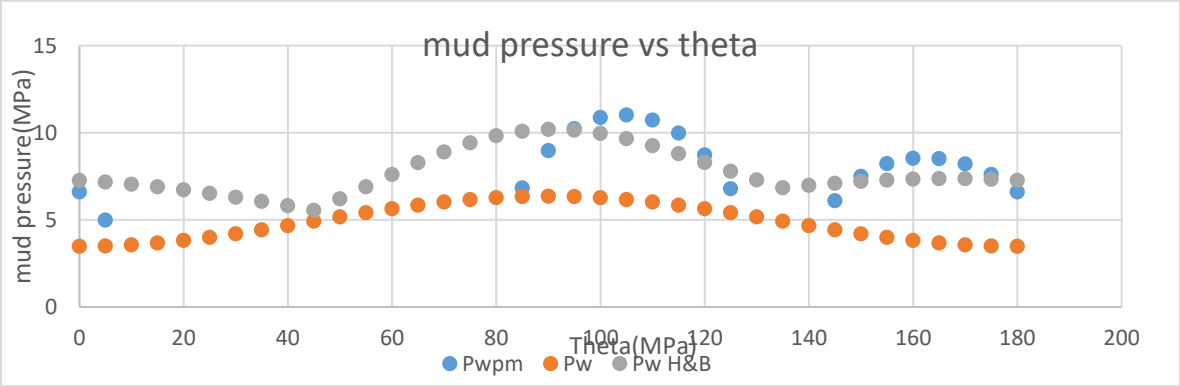

Figure 68 Pmud vs theta, with correction, δ=45, σ_{max}=23MPa

The risk region is around the peak so around θ=90°, because the highest mud pressure exists, so the closer we are to the pressure to avoid the tensile fracturing and the narrower is the mud weight window.

The peak near theta=90° occurs in the weakness plane model because the wellbore is less likely to be stable at the inclination. The wellbore is aligned along the inclination of the bedding plane (plane of weakness), so higher mud pressure should be used in order to maintain the stability of the wellbore. When the bedding plane are aligned parallel to the drilling direction (θ=0 or 180°), the mud requires the lowest pressure.

The weakness plane model matches Hoek and brown for all the inclination θ especially when it fails along the weakness plane in the range [0-10], [80-110] and [140-180]. There is an average fitting between the two methods

For δ=90°:

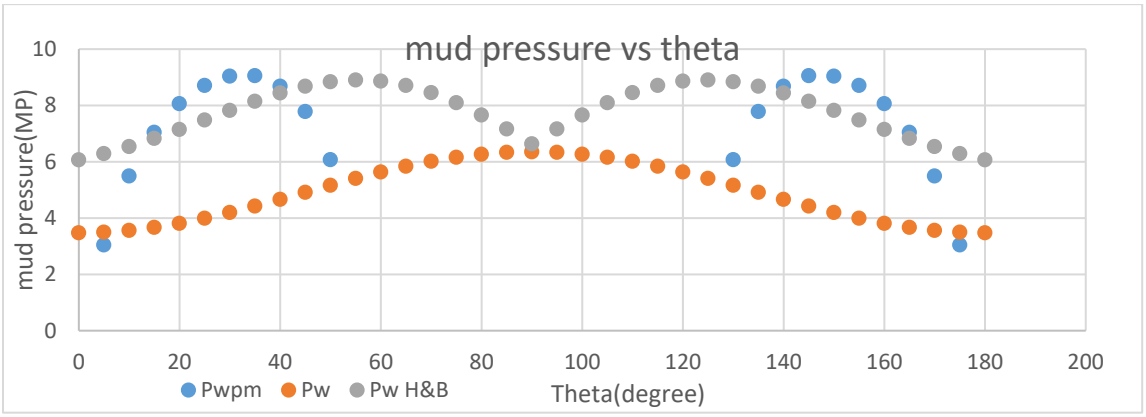

Figure 69 Pmud vs theta, with correction, δ=90, σ_{max}=23MPa

The highest mud pressure is around 9MPa.The risk region is around the peak so around θ=60 and θ=120°, because the highest mud pressure exists, so the closer we are to the pressure to avoid the tensile fracturing and the narrower is the mud weight window.

For the weakness plane model: The peak near theta 30° and 150° occur because the wellbore is less likely to be stable at these inclinations. When δ=90°, β is around 60 which is aligned parallel to the bedding plane,

so higher mud pressure should be used in order to maintain the stability of the wellbore. When the bedding plane are aligned parallel to the drilling direction (θ=0 or 180°), the mud requires the lowest pressure.

We don't have a good matching between Hoek and Brown and the weakness plane in general for almost all the inclination angle.

2.6.2.2 without correction

For δ=0°:

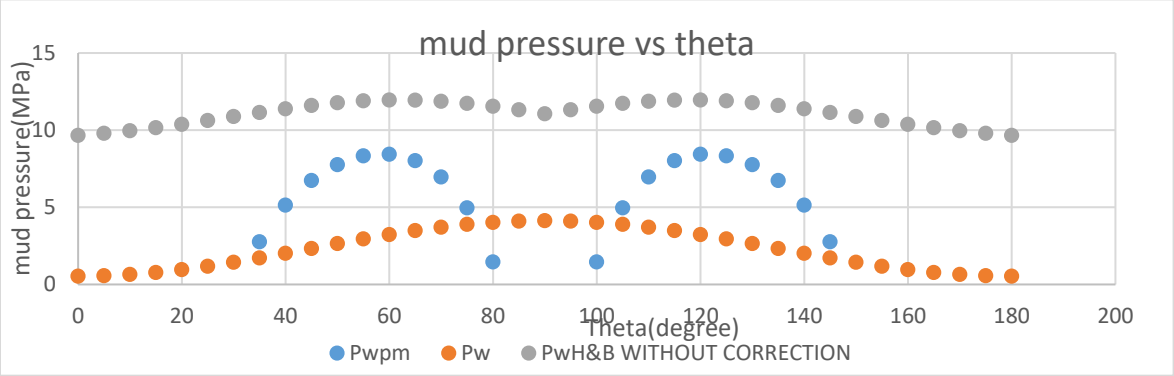

Figure 70 Pmud vs theta, without correction, δ=0, σ_{max}=23MPa

The highest mud pressure is around 12MPa.The risk region is around the peak so around θ=70 and θ=110°, because the highest mud pressure exists, so the closer we are to the pressure to avoid the tensile fracturing and the narrower is the mud weight window.

For the weakness plane model: The peak near theta=60° and 120° occur because the wellbore is less likely to be stable at these inclinations. When δ=0°, β is around 60 which require the highest mud pressure. Higher mud pressure should be used in order to maintain the stability of the wellbore. When the bedding plane are aligned parallel to the drilling direction (θ=0 or 180°), the mud requires the lowest pressure.

We don't have a good matching between Hoek and Brown and the weakness plane in general for almost all the inclination angle.

For δ=45°:

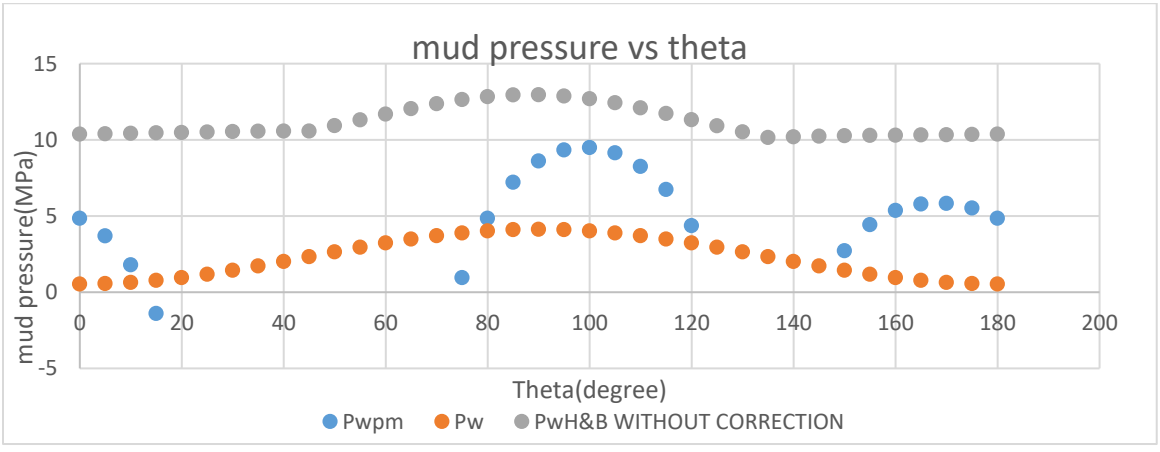

Figure 71 Pmud vs theta, without correction, δ=45, σ_{max}=23MPa

risk region is around the peak so around θ=90°, because the highest mud pressure exists, so the closer we are to the pressure to avoid the tensile fracturing and the narrower is the mud weight window.

The peak near theta=90° occurs in the weakness plane model because the wellbore is less likely to be stable at the inclination. The wellbore is aligned along the inclination of the bedding plane (plane of weakness), so higher mud pressure should be used in order to maintain the stability of the wellbore. When the bedding plane are aligned parallel to the drilling direction (θ=0 or 180°), the mud requires the lowest pressure.

We don't have a good matching between Hoek and Brown and the weakness plane in general for almost all the inclination angle.

For δ=90°:

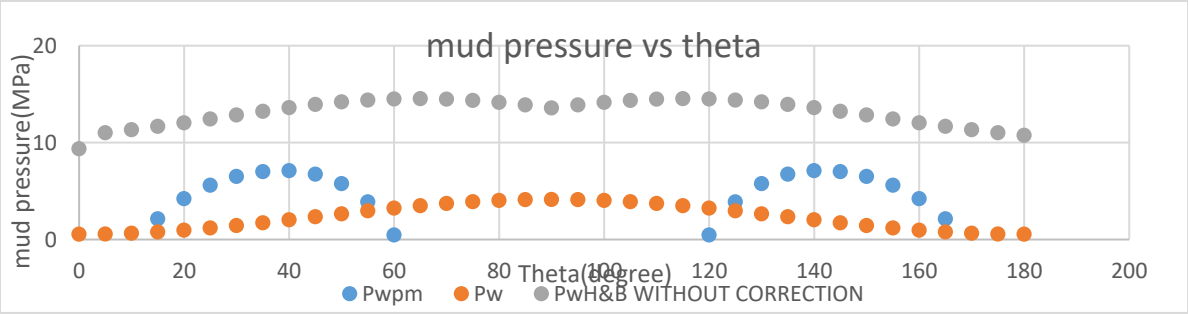

Figure 72 Pmud vs theta, without correction, δ=90, σ_{max}=23MPa

The highest mud pressure is around 9MPa.The risk region is around the peak so around θ=60 and θ=120°, because the highest mud pressure exists, so the closer we are to the pressure to avoid the tensile fracturing and the narrower is the mud weight window.

For the weakness plane model: The peak near theta=40° and 140° occur because the wellbore is less likely to be stable at these inclinations. When δ=90°, β is around 45 which is aligned parallel to the bedding plane, so higher mud pressure should be used in order to maintain the stability of the wellbore. When the bedding plane are aligned parallel to the drilling direction (θ=0 or 180°), the mud requires the lowest pressure.

We don't have a good matching between Hoek and Brown and the weakness plane in general for almost all the inclination angle.

2.6.3 for σmax =σmin=20MPa, k=1

2.6.3.1 with correction

For δ=0°:

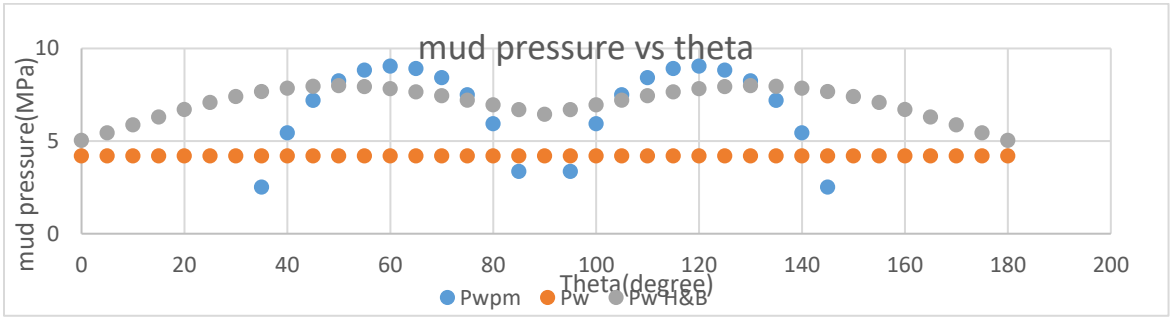

Figure 73 Pmud vs theta, with correction, δ=0, σ_{max}=20MPa

The highest mud pressure is around 8MPa.The risk region is around the peak so around θ=50 and θ=130°, because the highest mud pressure exists, so the closer we are to the pressure to avoid the tensile fracturing and the narrower is the mud weight window.

For the weakness plane model: The peak near theta=60° and 120° occur because the wellbore is less likely to be stable at these inclinations. When δ=0°, β is around 60 which is aligned parallel to the bedding plane, so higher mud pressure should be used in order to maintain the stability of the wellbore. When the bedding plane are aligned parallel to the drilling direction (θ=0 or 180°), the mud requires the lowest pressure.

We don't have a good matching between Hoek and Brown and the weakness plane in general for almost all the inclination angle.

For δ=45°:

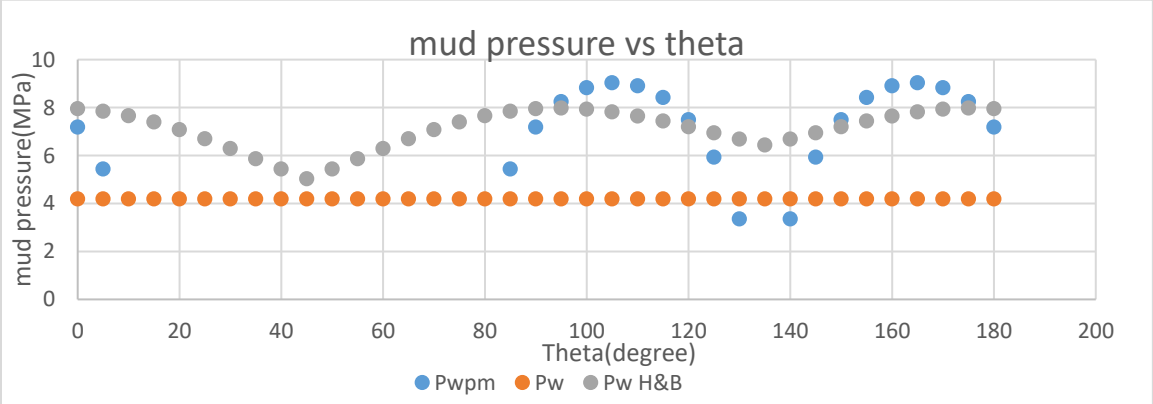

Figure 74 Pmud vs theta, with correction, δ=45, σ_{max}=20MPa

The risk region is around the peak so around θ=90°, because the highest mud pressure exists, so the closer we are to the pressure to avoid the tensile fracturing and the narrower is the mud weight window.

The peak near theta=90° occurs in the weakness plane model because the wellbore is less likely to be stable at the inclination. The wellbore is aligned along the inclination of the bedding plane (plane of weakness), so higher mud pressure should be used in order to maintain the stability of the wellbore. When the bedding plane are aligned parallel to the drilling direction (θ=0 or 180°), the mud requires the lowest pressure.

We don't have a good matching between Hoek and Brown and the weakness plane in general for almost all the inclination angle.

For δ=90°:

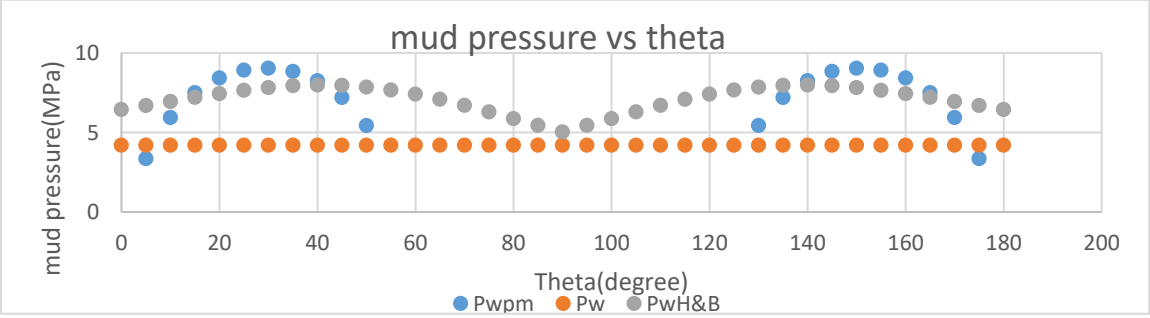

Figure 75 Pmud vs theta, with correction, δ=90, σ_{max}=20MPa

The highest mud pressure is around 8MPa.The risk region is around the peak so around θ=40 and θ=140°, because the highest mud pressure exists, so the closer we are to the pressure to avoid the tensile fracturing and the narrower is the mud weight window.

For the weakness plane model: The peak near theta=30° and 150° occur because the wellbore is less likely to be stable at these inclinations. When δ=90°, β is around 60 which is aligned parallel to the bedding plane, so higher mud pressure should be used in order to maintain the stability of the wellbore. When the bedding plane are aligned parallel to the drilling direction (θ=0 or 180°), the mud requires the lowest pressure.

We don't have a good matching between Hoek and Brown and the weakness plane in general for almost all the inclination angle.

2.6.3.2 without correction

For δ=0°:

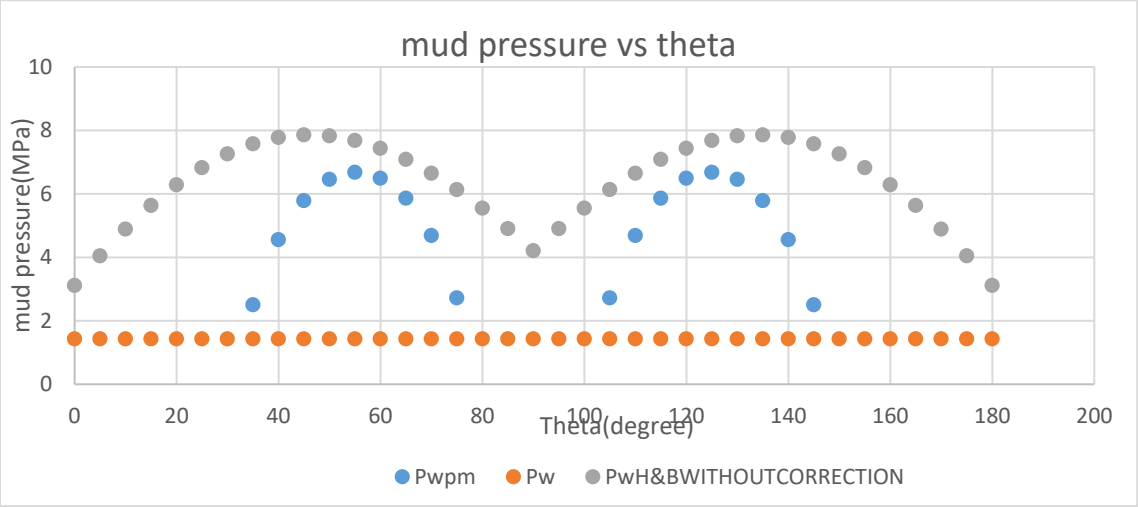

Figure 76 Pmud vs theta, without correction, δ=0, σ_{max}=20MPa

The highest mud pressure is around 8MPa.The risk region is around the peak so around θ=45 and θ=135°, because the highest mud pressure exists, so the closer we are to the pressure to avoid the tensile fracturing and the narrower is the mud weight window.

For the weakness plane model: The peak near theta=55° and 125° occur because the wellbore is less likely to be stable at these inclinations. When δ=0°, β is around 50 which is aligned parallel to the bedding plane, so higher mud pressure should be used in order to maintain the stability of the wellbore. When the bedding plane are aligned parallel to the drilling direction (θ=0 or 180°), the mud requires the lowest pressure.

We don't have a good matching between Hoek and Brown and the weakness plane in general for almost all the inclination angle.

For δ=45°:

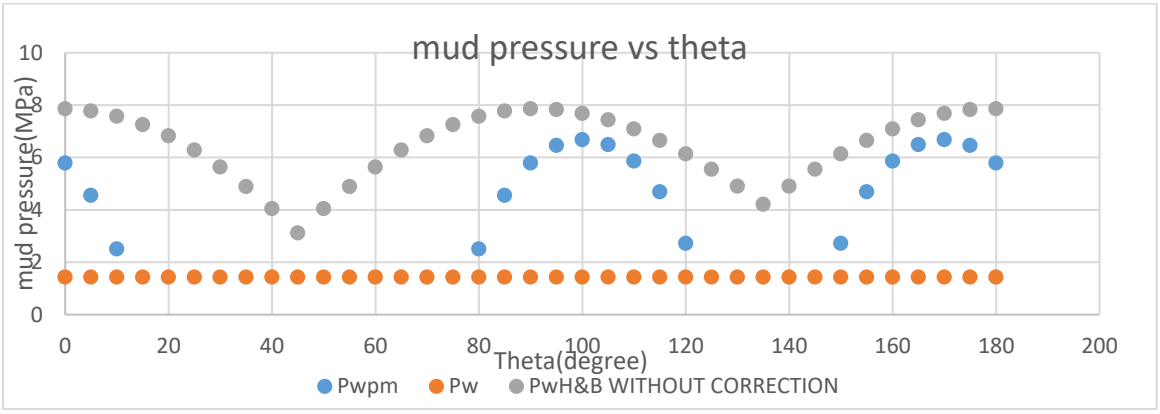

Figure 77 Pmud vs theta, without correction, δ=45, σ_{max}=20MPa

The risk region is around the peak so around θ=0,90 and 180° because the highest mud pressure exists, so the closer we are to the pressure to avoid the tensile fracturing and the narrower is the mud weight window.

The peak near theta=90° occurs in the weakness plane model because the wellbore is less likely to be stable at the inclination. The wellbore is aligned along the inclination of the bedding plane (plane of weakness), so higher mud pressure should be used in order to maintain the stability of the wellbore. When the bedding plane are aligned parallel to the drilling direction (θ=0 or 180°), the mud requires the lowest pressure.

We don't have a good matching between Hoek and Brown and the weakness plane in general for almost all the inclination angle.

For δ=90°:

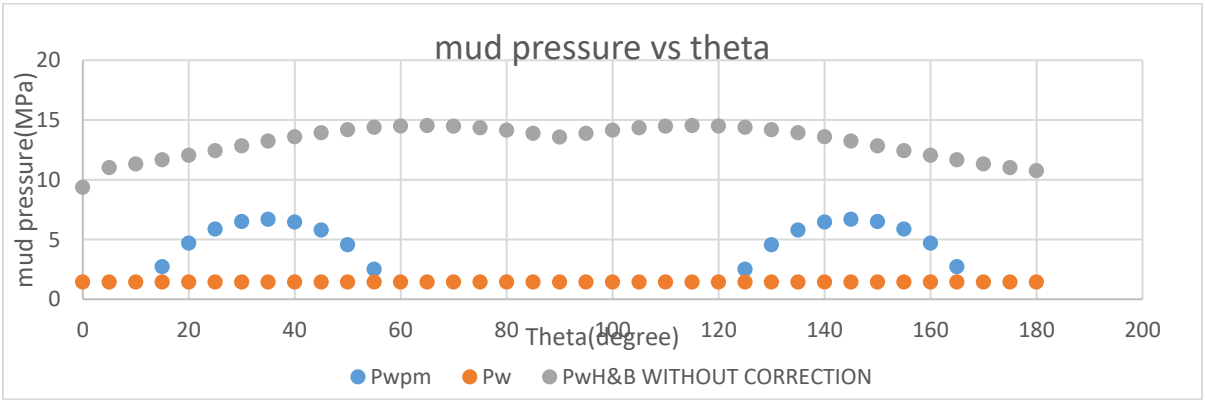

Figure 78 Pmud vs theta, without correction, δ=90, σ_{max}=20MPa

The risk region is around the peak so around θ=65 and θ=125°, because the highest mud pressure exists, so the closer we are to the pressure to avoid the tensile fracturing and the narrower is the mud weight window.

For the weakness plane model: The peak near theta=40° and 140° occur because the wellbore is less likely to be stable at these inclinations. When δ=90°, β is around 50 which is aligned parallel to the bedding plane,

so higher mud pressure should be used in order to maintain the stability of the wellbore. When the bedding plane are aligned parallel to the drilling direction (θ=0 or 180°), the mud requires the lowest pressure.

We don't have a good matching between Hoek and Brown and the weakness plane in general for almost all the inclination angle.

2.7For the second author (Abdi)

2.7.1 for σmax =36MPa, σ_{min}=20MPa, k=1.8

For δ=0°:

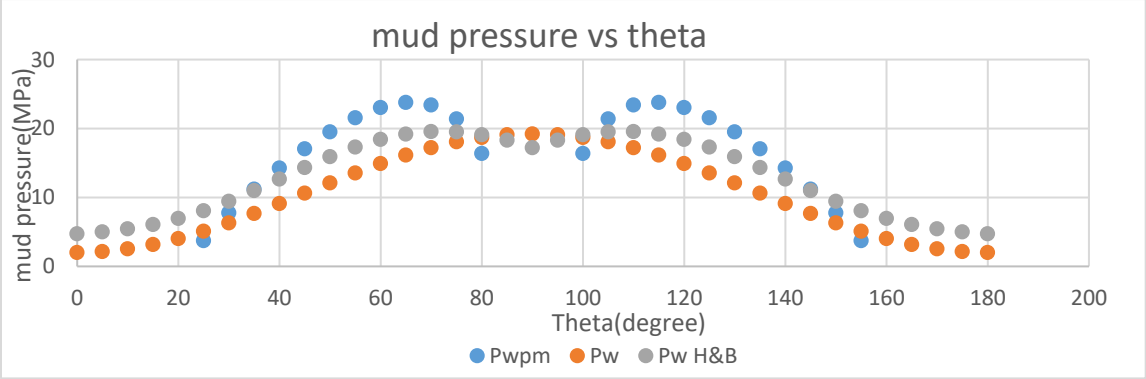

Figure 79 Pmud vs theta, second author, δ=0, σ_{max}=36MPa

The highest mud pressure is around 20MPa.The risk region is around the peak so around θ=70 and θ=110°, because the highest mud pressure exists, so the closer we are to the pressure to avoid the tensile fracturing and the narrower is the mud weight window.

For the weakness plane model: The peak near theta=60° and 120° occur because the wellbore is less likely to be stable at these inclinations. When δ=0°, β is around 30 which is aligned parallel to the bedding plane, so higher mud pressure should be used in order to maintain the stability of the wellbore. When the bedding plane are aligned parallel to the drilling direction (θ=0 or 180°), the mud requires the lowest pressure.

The weakness plane model matches Hoek and brown for all the inclination θ especially when it fails along the weakness plane in the range [30-80] and [100-145].

For δ=45°:

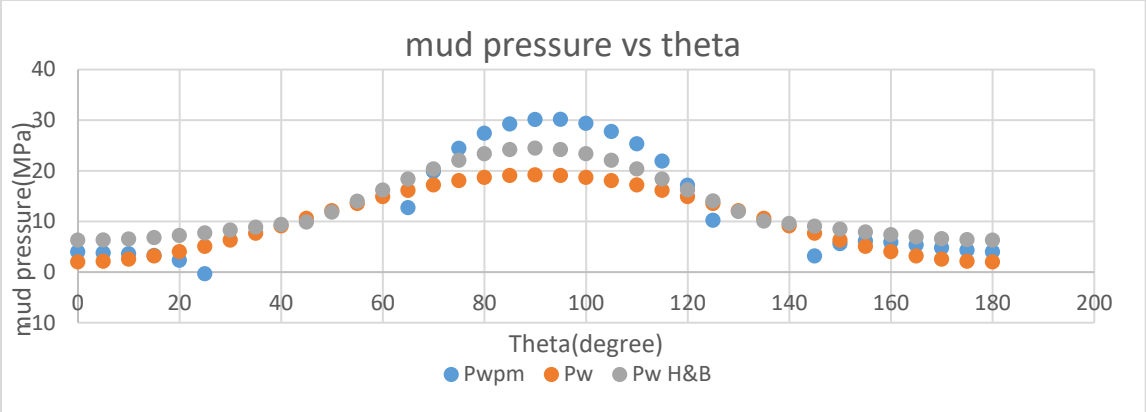

Figure 80 Pmud vs theta, second author, δ=45, σ_{max}=36MPa

The highest mud pressure is around 24.5MPa. The risk region is around the peak so around θ=90°, because the highest mud pressure exists, so the closer we are to the pressure to avoid the tensile fracturing and the narrower is the mud weight window.

The peak near theta=90° occurs in the weakness plane model because the wellbore is less likely to be stable at the inclination. The wellbore is aligned along the inclination of the bedding plane (plane of weakness), so higher mud pressure should be used in order to maintain the stability of the wellbore. When the bedding plane are aligned parallel to the drilling direction (θ=0 or 180°), the mud requires the lowest pressure.

The weakness plane model matches Hoek and brown for all the inclination θ especially when it fails along the weakness plane in the range [0-20], [65-125] and [145-180].

For δ=90°:

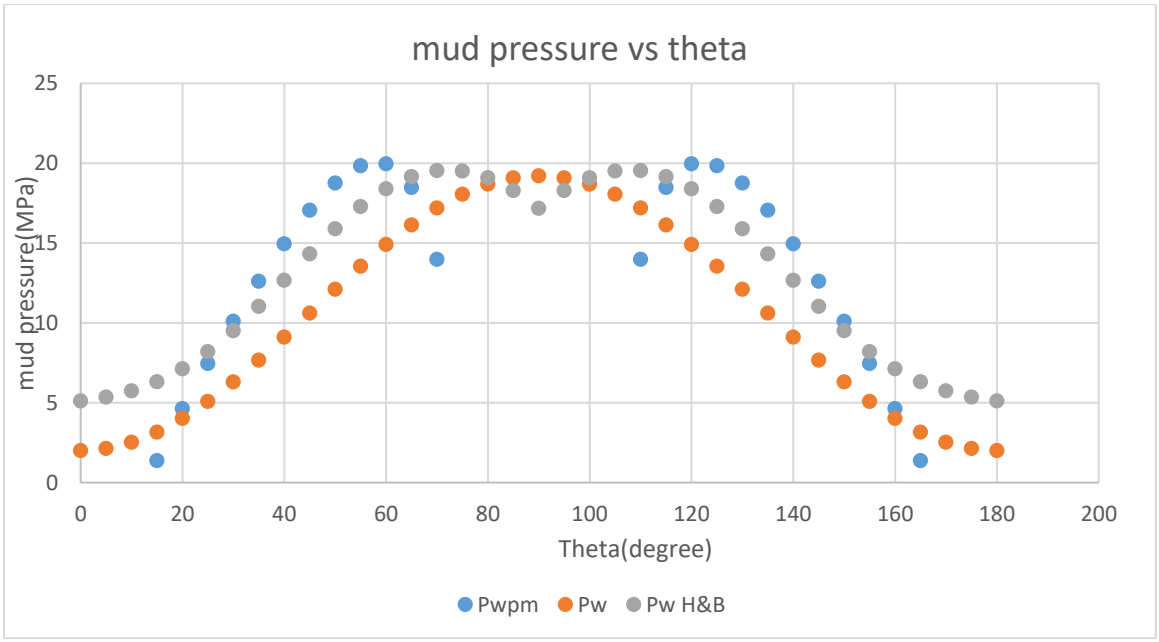

Figure 81 Pmud vs theta, second author, δ=90, σ_{max}=36MPa

The highest mud pressure is around 20MPa.The risk region is around the peak so around θ=70 and θ=110°, because the highest mud pressure exists, so the closer we are to the pressure to avoid the tensile fracturing and the narrower is the mud weight window.

For the weakness plane model: The peak near theta=60° and 120° occur because the wellbore is less likely to be stable at these inclinations. When δ=90°, β is around 30 which is aligned parallel to the bedding plane, so higher mud pressure should be used in order to maintain the stability of the wellbore. When the bedding plane are aligned parallel to the drilling direction (θ=0 or 180°), the mud requires the lowest pressure.

We have an average matching between Hoek and Brown and the weakness plane in general for almost all the inclination angle.

2.7.2 for σmax =23MPa, σ_{min}=20MPa, k=1.15

For δ=0°:

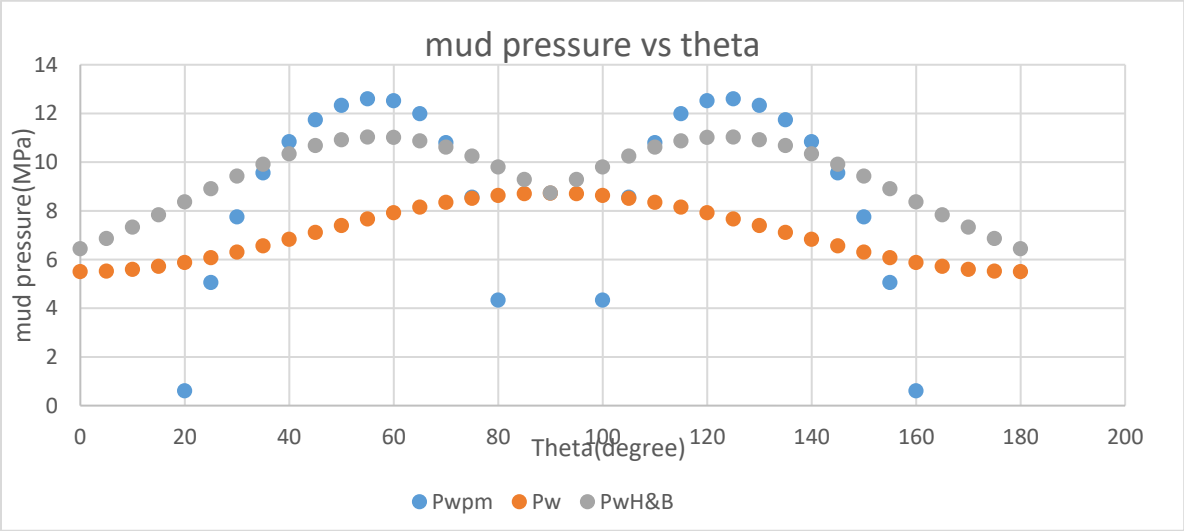

Figure 82 Pmud vs theta, second author, δ=0, σ_{max}=23MPa

The risk region is around the peak so around θ=60 and θ=120°, because the highest mud pressure exists, so the closer we are to the pressure to avoid the tensile fracturing and the narrower is the mud weight window.

For the weakness plane model: The peak near theta=60° and 120° occur because the wellbore is less likely to be stable at these inclinations. When δ=0°, β is around 30 which is aligned parallel to the bedding plane, so higher mud pressure should be used in order to maintain the stability of the wellbore. When the bedding plane are aligned parallel to the drilling direction (θ=0 or 180°), the mud requires the lowest pressure.

The weakness plane model matches Hoek and brown for all the inclination θ especially when it fails in the weakness plane in the range [35-80] and [95-140]. There is an average fitting between the two methods

For δ=45°:

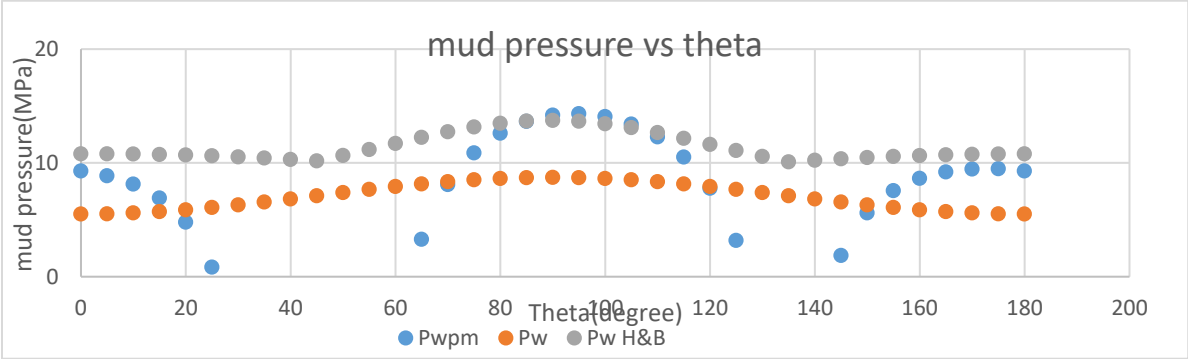

Figure 83 Pmud vs theta, second author, δ=45, σ_{max}=23MPa

The risk region is around the peak so around θ=90°because the highest mud pressure exists, so the closer we are to the pressure to avoid the tensile fracturing and the narrower is the mud weight window.

The peak near theta=90° occurs in the weakness plane model because the wellbore is less likely to be stable at the inclination. The wellbore is aligned along the inclination of the bedding plane (plane of weakness), so higher mud pressure should be used in order to maintain the stability of the wellbore. When the bedding plane are aligned parallel to the drilling direction (θ=0 or 180°), the mud requires the lowest pressure.

The weakness plane model matches Hoek and brown for all the inclination θ especially when it fails along the weakness plane in the range [0-10], [70-110] and [150-180]. There is an average fitting between the two methods.

For δ=90°:

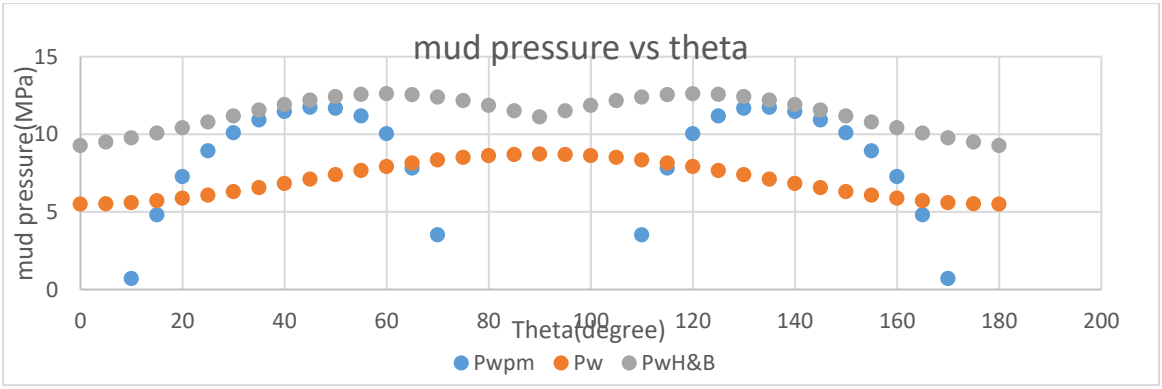

Figure 84 Pmud vs theta, second author, δ=90, σ_{max}=23MPa

The risk region is around the peak so around θ=60 and θ=120°, because the highest mud pressure exists, so the closer we are to the pressure to avoid the tensile fracturing and the narrower is the mud weight window.

For the weakness plane model: The peak near theta=45° and 135° occur because the wellbore is less likely to be stable at these inclinations. When δ=90°, β is around 45 which is aligned parallel to the bedding plane, so higher mud pressure should be used in order to maintain the stability of the wellbore. When the bedding plane are aligned parallel to the drilling direction (θ=0 or 180°), the mud requires the lowest pressure.

We don't have a good matching between Hoek and Brown and the weakness plane in general for almost all the inclination angle.

2.7.3 for σ_{max} =σ_{min}20MPa, k=1

For δ=0°:

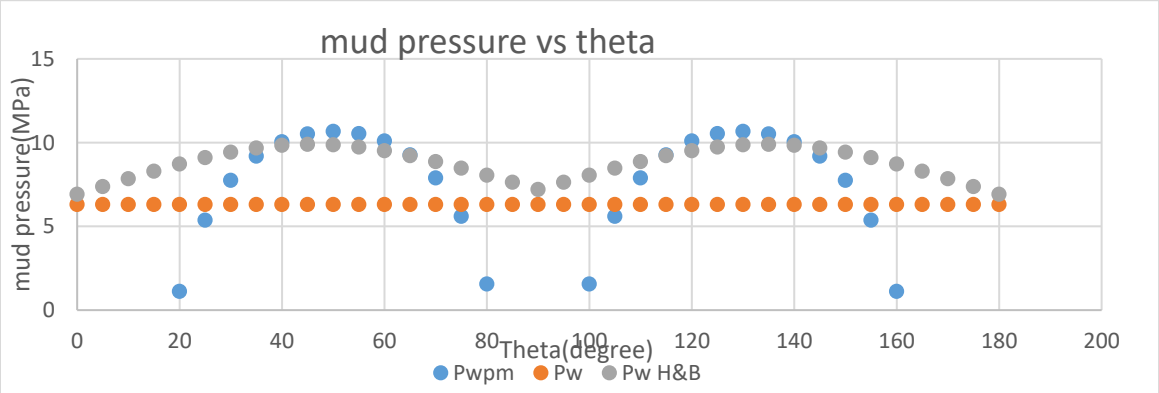

Figure 85 Pmud vs theta, second author, δ=0, σ_{max}=20MPa

The highest mud pressure is around 10MPa.The risk region is around the peak so around θ=50 and θ=130°, because the highest mud pressure exists, so the closer we are to the pressure to avoid the tensile fracturing and the narrower is the mud weight window.

For the weakness plane model: The peak near theta=50° and 130° occur because the wellbore is less likely to be stable at these inclinations. When δ=0°, β is around 45 which is aligned parallel to the bedding plane, so higher mud pressure should be used in order to maintain the stability of the wellbore. When the bedding plane are aligned parallel to the drilling direction (θ=0 or 180°), the mud requires the lowest pressure.

We don't have a good matching between Hoek and Brown and the weakness plane in general for almost all the inclination angle.

For δ=45°:

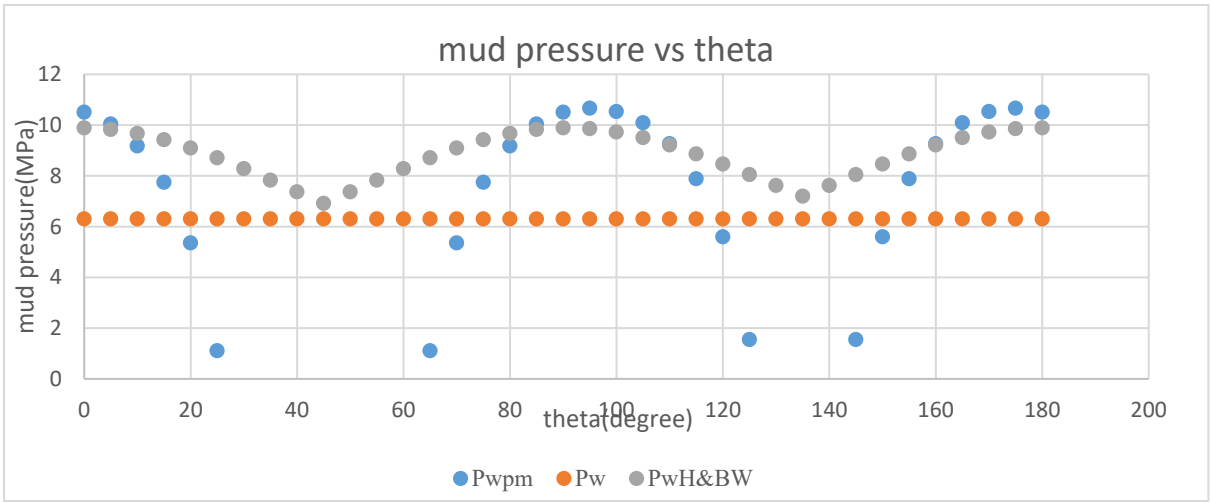

Figure 86 Pmud vs theta, second author, δ=45, σ_{max}=20MPa

The risk region is around the peak so around θ=90° because the highest mud pressure exists, so the closer we are to the pressure to avoid the tensile fracturing and the narrower is the mud weight window.

The peak near theta=90° occurs in the weakness plane model because the wellbore is less likely to be stable at the inclination. The wellbore is aligned along the inclination of the bedding plane (plane of weakness), so higher mud pressure should be used in order to maintain the stability of the wellbore. When the bedding plane are aligned parallel to the drilling direction (θ=0 or 180°), the mud requires the lowest pressure.

The weakness plane model matches Hoek and brown for all the inclination θ especially when it fails along the weakness plane in the range [0-10], [80-110] and [140-180].

We don't have a good matching between Hoek and Brown and the weakness plane in general for almost all the inclination angle.

For δ=90°:

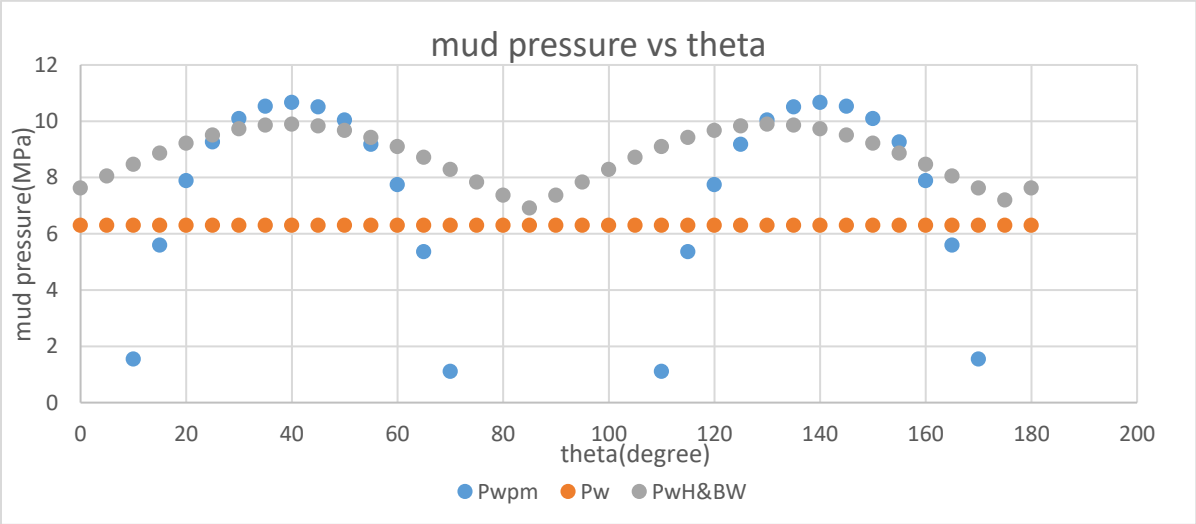

Figure 87 Pmud vs theta, second author, δ=90, σ_{max}=20MPa

The risk region is around the peak so around θ=40 and θ=130°, because the highest mud pressure exists, so the closer we are to the pressure to avoid the tensile fracturing and the narrower is the mud weight window.

For the weakness plane model: The peak near theta=40° and 140° occur because the wellbore is less likely to be stable at these inclinations. When δ=90°, β is around 45 which is aligned parallel to the bedding plane, so higher mud pressure should be used in order to maintain the stability of the wellbore. When the bedding plane are aligned parallel to the drilling direction (θ=0 or 180°), the mud requires the lowest pressure.

We don't have a good matching between Hoek and Brown and the weakness plane in general for almost all the inclination angle.

2.8 Results Analysis

2.8.1 for k=1.8

For both author Niandou and Abdi, we have the highest mud pressure at δ=45° compared to δ=0° and δ=90°. The region of risk changes with the change of δ. It is at θ=90° for δ=45°, while we have two regions of risk for δ=0 and δ=90° which are near 75 and 105°.

2.8.2 for k=1.15

For both author Niandou and Abdi, we have the highest mud pressure at δ=45° compared to δ=0° and δ=90°.The region of risk changes with the change of δ. It is at θ=90° for δ=45°, while we have two regions of risk for δ=0 and δ=90° which are near 60 and 120°.

2.8.3 for k=1

For both author Niandou and Abdi, we have the highest mud pressure at δ=45° compared to δ=0° and δ=90°. The region of risk changes with the change of δ. It is at θ=90° for δ=45°, while we have two regions of risk for δ=0 and δ=90° which are near 50 and 130°.

2.8.4 for δ=0°

The highest mud pressure changes with the change of σ_{max}. It shows a maximum for k=1.8 and a minimum mud pressure for k=1. When the degree of anisotropy decrease, the first maximum mud pressure calculated with Hoek and Brown which take place for theta less than 90° occur for a lower value of theta, while the second maximum mud pressure which take place for theta higher than 90°, occur for a higher theta.

3.8.5 for δ=45°

The highest mud pressure changes with the change of σ_{max}. It shows a maximum for k=1.8 and a minimum mud pressure for k=1. The maximum mud pressure occurs at θ=90°.

2.8.6 for δ=90°

The highest mud pressure changes with the change of σ_{max}. It shows a maximum for k=1.8 and a minimum mud pressure for k=1. When the degree of anisotropy decrease, the first maximum mud pressure calculated with Hoek and Brown which take place for theta less than 90° occur for a lower value of theta, while the second maximum mud pressure which take place for theta higher than 90°, occur for a higher theta.

Chapter 3 Conclusion

After the mud pressure calculation using H&B and WPM in the section 3 with different degrees of anisotropy and different values of δ. My results show the following conclusions:

- ✓ The highest mud pressure is at delta=45°, so it is the most dangerous situation because the MWW has a closer maximum and minimum and it is easier to have tensile fracturing.
- ✓ We don't have any matching between the weakness plane model and Hoek and brown in case the data is not corrected with different values of delta and with different degree of anisotropy, so the fitting is a crucial factor in order to have a true value of mud pressure with both methods.
- ✓ Without a well-fitting of the experimental data with Mohr coulomb or Hoek and Brown modified, we have a higher value of the mud pressure. So we obtain a higher value of the minimum value of mud pressure to avoid shear failure and thus the wellbore is more likely to fail.
- ✓ When the degree of anisotropy decrease, the mud pressure decrease (peak) and our wellbore is more likely to be stable compared when we have a certain degree of anisotropy (high or low)
- ✓ We have a good agreement between WPM and H&B for δ=0 and 45° for k= 1.8, but it's not the case for δ=90°.
- ✓ We have a good fitting between WPM and H&B for k=1.15 for δ=0 and 45° and a poor fitting for δ=90°.
- ✓ For k=1, there is no agreement at all between the WPM and H&B for different values of δ
- ✓ When the degree of anisotropy decrease, the fitting between WPM and H&B decrease
- ✓ The WPM cannot capture the real behavior of the strength for the "tournemire shale "because the plateau assumes a constant value of strength along a range of inclination angles.
- ✓ We have an agreement between Niandou and Abdi with mud pressure calculation.

Outlook

This thesis utilizes experimental data obtained from laboratory tests, which are considered the most reliable method. However, conducting these tests can be prohibitively expensive. On the other hand, indirect measurements such as log data are not highly reliable for estimating the mechanical properties of shale or determining the weakness plane. To address this, mud pressure calculations can be performed using experimental data from indirect tests, considering the various cases that have already been investigated. By finding a compromise between cost-effectiveness and reliability, it is possible to achieve mud pressure estimates that are both economical and as accurate as possible.

References

[1] Chen, X.; Tan, C.P.; Detournay, C. A study on wellbore stability in fractured rock masses with impact of mud infiltration. J. Pet. Sci. Eng. **2003**, 38, 145–154. [CrossRef]
[2] Younessi, A.; Rasouli, V. A fracture sliding potential index for wellbore stability analysis. Int. J. Rock Mech.Min. Sci. **2010**, 47, 927–939. [CrossRef]
[3] Last, N.C.; McLean, M.R. Assessing the impact of trajectory on wells drilled in an overthrust region. J. Pet. Tech. **1996**, 48, 620–626. [CrossRef]
[4] Twynam, A.J.; Shaw, D.; Heard, M.; Wilson, K.J. Successful use of a synthetic drilling fluid in eastern Venezuela. In Proceedings of the International Conference on Health, Safety, and Environment in Oil and Gas Exploration and Production, Caracas, Venezuela, 7–10 June 1998.
[5] Willson, S.M.; Last, N.C.; Zoback, M.D.; Moos, D. Drilling in South America: A wellbore stability approach for complex geologic conditions. In Proceedings of the Latin American and Caribbean Petroleum Engineering Conference, Caracas, Venezuela, 21–23 April 1999.
[6] https://link.springer.com/article/10.1007/s13202-015-0198-2
[7] Økland, D.; Cook, J.M. Bedding-related borehole instability in high-angle wells. In Proceedings of the Eurock'98-Rock Mechanics in Petroleum Engineering, Trondheim, Norway, 8–10 July 1998.
[8] Brehm, A.;Ward, C.D.; Bradford, D.W.; Riddle, D.E. Optimizing a deepwater subsalt drilling program byevaluating anisotropic rock strength effects on wellbore stability and near wellbore stress effects on thefracture gradient. In Proceedings of the Drilling Conference Society of Petroleum Engineers, Miami, FL,USA, 21–23 February 2006.
[9]https://asmedigitalcollection.asme.org/energyresources/article-abstract/140/9/092903/368222/A-Comprehensive-Wellbore-Stability-Model
[10]https://www.sciencedirect.com/science/article/abs/pii/S1365160912001554#preview-section-references
[11]https://www.researchgate.net/publication/269138505_Stability_Analysis_of_Deviated_Boreholes_Using_the_Mogi-Coulomb_Failure_Criterion_With_Applications_to_Some_Oil_and_Gas_Reservoirs
[12] Wu, B.; Tan, C.P. Effect of shale bedding plane failure on wellbore stability-example from analyzing stuck-pipe wells. In Proceedings of the 44th US Rock Mechanics Symposium and 5th US-Canada Rock Mechanics Symposium, Salt Lake City, UT, USA, 27–30 June 2010.
[13] Narayanasamy, R.; Barr, D.; Mine, A. Wellbore-instability predictions within the cretaceous mudstones, clair field,West of Shetlands. SPE Drill. Complet. **2010**, 25, 518–529. [CrossRef]
[14] Jaeger, J.C. Shear failure of anisotropic rocks. Geol. Mag. **1960**, 97, 65–72. [CrossRef]
[15] Aadnoy, B.S.M.E. Stability of highly inclined boreholes. SPE Drill. Eng. **1988**, 3, 259–268. [CrossRef]
[16] Lee, H.; Ong, S.H.; Azeemuddin, M.; Goodman, H. A wellbore stability model for formations with anisotropic rock strengths. J. Pet. Sci. Eng. **2012**, 6, 109–119. [CrossRef]
[17] Li, Y.; Fu, Y.; Tang, G.; She, C.; Guo, J.; Zhang, J. Effect of weak bedding planes on wellbore stability for shale gas wells. In Proceedings of the Asia Pacific Drilling Technology Conference and Exhibition, Tianjin, China, 9–11 July 2012.
[18] Zhang, J. Borehole stability analysis accounting for anisotropies in drilling to weak bedding planes. Int. J.Rock Mech. Min. Sci. **2013**, 60, 160–170. [CrossRef]

[19] Lee, H.; Chang, C.; Ong, S.H.; Song, I. Effect of anisotropic borehole wall failures when estimating in situ stresses: A case study in the Nankai accretionary wedge. Mar. Pet. Geol. **2013**, 48, 411–422. [CrossRef]
[20] Yan, G.; Karpfinger, F.; Prioul, R.; Tang, H.; Jiang, Y.; Liu, C. Anisotropic wellbore stability model and its application for drilling through challenging shale gas wells. In Proceedings of the International Petroleum Technology Conference, Kuala Lumpur, Malaysia, 9–11 December 2014.
[21] He, S.;Wang,W.; Zhou, J.; Huang, Z.; Tang, M. A model for analysis of wellbore stability considering the effects of weak bedding planes. J. Nat. Gas Sci. Eng. **2015**, 27, 1050–1062. [CrossRef]
[22] Kanfar, M.F.; Chen, Z.; Rahman, S.S. Risk-controlled wellbore stability analysis in anisotropic formations.J. Pet. Sci. Eng. **2015**, 134, 214–222. [CrossRef]
[23] Fekete, P.; Dosunmu, A.; Anyanwu, C.; Odagme, S.B.; Ekeinde, E.Wellbore stability management in weak bedding planes and angle of attack in well planing. In Proceedings of the SPE Nigeria Annual International Conference and Exhibition, Lagos, Nigeria, 5–7 August 2014.
[24] Konstantinovskaya, E.; Laskin, P.; Eremeev, D.; Pashkov, A.; Semkin, A.; Karpfinger, F.; Trubienko, O. Shale stability when drilling deviated wells: Geomechanical modeling of bedding plane weakness, field X, Russian platform. In Proceedings of the SPE Russian Petroleum Technology Conference and Exhibition, Moscow,Russia, 24–26 October 2016.
[25] Brady, B.H.; Brown, E.T. Rock Mechanics: For Underground Mining, 3rd ed.; Kluwer Academic Publishers:Norwell, MA, USA, 2005.
[26]http://www.hydrofrac.com/hfb_home.html
[27]https://petrowiki.spe.org/Borehole_instability#:~:text=Borehole%20collapse%20occurs%20when%20the,and%20possible%20loss%20of%20well.
[28] https://www.trenchlesspedia.com/definition/3570/borehole-collapse
[29] https://onepetro.org/JPT/article-abstract/36/06/889/73274/Wellbore-Stability
[30]Detournay, E., and Cheng, A. H.-D. (1993). “Fundamentals of Poroelasticity,” in Analysis and Design Methods (Pergamon), 113–171. doi:10.1016/b978-0-08- 040615-2.50011-3
[31]Hoek, E., and Brown, E. T. (2019). The Hoek-Brown Failure Criterion and GSI - 2018 Edition. J. Rock Mech. Geotechnical Eng. 11 (3), 445–463. doi:10.1016/j. jrmge.2018.08.001
[32] https://en.wikipedia.org/wiki/Terzaghi%27s_principle
[33]http://www.scielo.org.co/scielo.php?script=sci_arttext&pid=S0122-53832019000200005#:~:text=Compaction%20is%20the%20main%20cause,by%20correlations%20in%20conventional%20reservoirs.
[34]Crawford, B.R.; De Dontney, N.L.; Alramahi, B.; Ottesen, S. Shear strength anisotropy in fine-grained rocks. In Proceedings of the 46th US Rock Mechanics/Geomechanics Symposium, Chicago, IL, USA, 24–27 June 2012.
[35]Tien, Y.M.; Kuo, M.C.; Juang, C.H. An experimental investigation of the failure mechanism of simulated transversely isotropic rocks. Int. J. Rock Mech. Min. Sci. 2006, 43, 1163–1181.
[36] https://www.hindawi.com/journals/amse/2019/1340934/
[37] https://www.sciencedirect.com/topics/engineering/confining-pressure
[38] https://link.springer.com/article/10.1007/s11771-022-4991-z
[39] https://www.lyellcollection.org/doi/10.1144/SP443.20
[40]Hoek, E.; Brown, E.T. Empirical strength criterion for rock masses. J. Geotech. Geoenviron. Eng. 1980, 106, 1013–1035.
[41]Tien, Y.M.; Kuo, M.C. A failure criterion for transversely isotropic rocks. Int. J. Rock Mech. Min. Sci. 2001, 38, 399–412. [CrossRef]

[42]Colak, K.; Unlu, T. Effect of transverse anisotropy on the Hoek–Brown strength parameter ‘mi’ for intact rocks. Int. J. Rock Mech. Min. Sci. 2004, 41, 1045–1052.
[43]https://link.springer.com/article/10.1007/s00603-012-0281-7
[44]chromeextension://efaidnbmnnnibpcajpcglclefindmkaj/https://www.pisante.com/corsi/documenti/documenti/muratura/lagomarsino/muratura/criteri%20di%20resistenza.PDF
[45] https://www.rocscience.com/help/rsdata/documentation/materials/strength-criterion/mohr-coulomb
[46]chromeextension://efaidnbmnnnibpcajpcglclefindmkaj/https://www.rcet.org.in/uploads/academics/rohini_87560265463.pdf
[47] https://resources.wolframcloud.com/FormulaRepository/resources/MohrCoulomb-Failure-Criterion
[48] Labuz, J.F.; Zang, A. Mohr-Coulomb failure criterion. Rock Mech. Rock Eng. 2012, 45, 975–979.
[49] https://www.frontiersin.org/articles/10.3389/feart.2022.860818/full
[50]Carter, B. J., Scott Duncan, E. J., and Lajtai, E. Z. (1991). Fitting Strength Criteria to Intact Rock. Geotech Geol. Eng. 9 (1), 73–81. doi:10.1007/bf00880985
[51]Alber, M., and Heiland, J. (2001). Investigation of a limestone Pillar Failure Part 1: Geology, Laboratory Testing and Numerical Modeling. Rock Mech. Rock Eng. 34 (3), 167–186. doi:10.1007/s006030170007 Ambati, V., Mahadasu, N. B., and Nair, R. R. (2021)
[52]Cai, M. (2010). Practical Estimates of Tensile Strength and Hoek-Brown Strength Parameter M I of Brittle Rocks. Rock Mech. Rock Eng. 43 (2), 167–184. doi:10. 1007/s00603-009-0053-1
[53]Coviello, A., Lagioia, R., and Nova, R. (2005). On the Measurement of the Tensile Strength of Soft Rocks. Rock Mech. Rock Engng. 38, 251–273. doi:10.1007/ s00603-005-0054-7
[54]Perras, M. A., and Diederichs, M. S. (2014). A Review of the Tensile Strength of Rock: Concepts and Testing. Geotech Geol. Eng. 32 (2), 525–546. doi:10.1007/ s10706-014-9732-0
[55]https://www.sciencedirect.com/topics/engineering/kirsch-solution
[56] https://dnicolasespinoza.github.io/node44.html
[57]chrome-extension://efaidnbmnnnibpcajpcglclefindmkaj/https://isrm.net/download/media.file.8add23a5af653626.313330133323137323233 5f645f626f7265686f6c655f73746162696c69742e706466.pdf
[58] Kirsch, G. Die theorie der elastizitaet und die beduerfnisse der festigkeitslehre. VDI Z. 1898, 29, 797–807.
[59]chromeextension://efaidnbmnnnibpcajpcglclefindmkaj/https://core.ac.uk/download/pdf/82971408.pf
[60] https://www.scirp.org/journal/paperinformation.aspx?paperid=79970
[61]https://www.nature.com/articles/s41598-022-12527-4#:~:text=Overbalanced%20drilling%20technique%20is%20one,of%20formation%20fluid14%2C15.
[62]https://www.sciencedirect.com/topics/engineering/underbalanced-drilling#:~:text=Underbalanced%20drilling%20is%20a%20practice,to%20flow%20while%20drilling%20proceeds.
[63] https://dnicolasespinoza.github.io/node47.html
[64]Zhang, J. Borehole stability analysis accounting for anisotropies in drilling to weak bedding planes. Int. J. Rock Mech. Min. Sci. 2013, 60, 160–170.
[65]Willson, S.M.; Last, N.C.; Zoback, M.D.; Moos, D. Drilling in South America: A wellbore stability approach for complex geologic conditions. In Proceedings of the Latin American and Caribbean Petroleum Engineering Conference, Caracas, Venezuela, 21–23 April 1999.
[66]Brehm, A.; Ward, C.D.; Bradford, D.W.; Riddle, D.E. Optimizing a deepwater subsalt drilling program by evaluating anisotropic rock strength effects on wellbore stability and near wellbore stress effects on the

fracture gradient. In Proceedings of the Drilling Conference Society of Petroleum Engineers, Miami, FL, USA, 21–23 February 2006.

[67] Jaeger, J.C.: Shear failure of anisotropic rocks. Geol. Mag. **97**(01), 65
Kirsch, : Die Theorie der Elastizität und die Bedürfnisse der Festigkeitslehre. Zeitschrift des Vereines deutscher Ingenieure **42**, 797–807 (1898)

[68] Tien, Y.M., Kuo, M.C.: A failure criterion for transversely isotropic rocks. Int. J. Rock Mech. Min. Sci. **38**(3), 399–412 (2001)

[69] Colak, K., Unlu, T.: Effect of transverse anisotropy on the Hoek-Brown strength parameter 'm i' for intact rocks. Int. J. Rock Mech. Min. Sci. **41**(6), 1045–1052 (2004)

[70] Deangeli, C., Omwanghe, O.: Prediction of mud pressures for the stability of wellbores drilled in transversely isotropic rocks. Energies **11**(8), 1944 (2018)